Study of the resistance to Cucumber mosaic virus aggressive strains in the melon (Cucumis melon L.) accession PI 161375

Jinqiang Yan

UNIVERSITAT AUTÒNOMA DE BARCELONA

Facultat de Biociències

Dept. Biologia Animal, Biologia Vegetal i Ecologia

Study of the resistance to *Cucumber mosaic virus* aggressive strains in the melon (*Cucumis melon* L.) accession PI 161375

Dissertation presented by Jinqiang Yan for the degree of Doctor in Plant Biology and Biotechnology by the Universitat Autònoma de Barcelona (UAB).

This work was performed in the Centre for Research in Agricultural Genomics (CRAG).

Thesis directors		Tutor	PhD candidate
Dra. Ana Montserrat Martín Hernández	Dra. Marta Pujol Abajo	Dra. Ana Montserrat Martín Hernández	Jinqiang Yan

Barcelona, October 2018

Index

Index of contents

Results

Part I QTL analysis for resistance to the aggressive train CMV-FNY

Index of Figures

Introduction

Results

Part I QTL analysis for resistance to the aggressive CMV-FNY strain

Part IV Virulence determinants responsible for overcoming the resistance mediated by *cmv1*, *cmvqw3.1* and *cmvqw10.1*

Discussion

Index of Tables

Introduction

Material and Methods

Results

Part I QTL analysis for resistance to the aggressive CMV-FNY strain

List of digital supplementary materials

Figure S1 Genotyping of F2 made from the cross DHL142 x DHL1046 with CAPS marker PS-15-H02

Figure S2 Genotyping of F2 made from the cross DHL142 x DHL1046 with CAPS marker PS-40-E11

Figure S3 Genotyping of F_2 made from the cross DHL142 x DHL1046 with microsatellite marker ECM116

Table S1 Table S1 Genotype of F2 population made from cross DHL142 x DHL2012

Table S2 Table S2 Genotype of F2 population made from cross DHL142 x 20-91-15

Table S3 Genotype of F2 population made from cross DHL69 x DHL2012

Table S4 Genotype of F2 population made from cross DHL142 x DHL1046

Table S5 CMV-FNY infection phenotypes of F2 population made from cross DHL142 x DHL2012

Table S6 CMV-FNY infection phenotypes of F2 population made from cross DHL142 x 20-91-15

Table S7 CMV-FNY infection phenotypes of F2 population made from cross DHL69 x DHL2012

Table S8 CMV-FNY infection phenotypes of F2 population made from cross DHL142 x DHL1046

Table S9 Re-sequencing genotyping of IL 20-28-62

Table S10 List of SNP markers used in F2 populations genotyping

Abbreviations

5'CAP	$m^7G(5')ppp(5')N$
AFLP	Amplified Fragment Length Polymorphism
AUSPC	Area Under the Symptom Progress Curve
BRP1	RNA binding protein
BS	Bundle Sheath Cells
BYDV	*Barley Yellow Dwarf Virus*
CARNA5	CMV-Associated RNA5
CC	Companion Cells
CMV	*Cucumber Mosaic Virus*
CP	Coat Protein
DAS-ELISA	Double Antibody Sandwich Enzyme-Linked Immunosorbent Assay
DHLs	Double Haploid Lines
DPI	Days Post Inoculation
dsDNA	double-stranded DNA
dsRNA	double-stranded RNA
ESTs	Expressed Sequence Tags
GBS	Genotyping-By-Sequencing
IM	Interval Mapping
KDa	Kilodaltons
KW	Kruskall Wallis
LG	Linkage Group
MP	Movement Protein
NILs	Near Isogenic Lines
PDs	Plasmodesmata
PPU	Pore Plasmodesmata Units
PS	Piel de Sapo
PTGS	Post-Transcriptional Gene Silencing
qRT-PCR	Real Time Quantitative Reverse Transcription PCR
QTL	Quantitative Trait Loci

RAPD	Random Amplified Polymorphic DNA
RFLP	Restriction Fragment Length Polymorphism
RILs	Recombinant inbred lines
RNAi	RNA interference
RNPs	Ribonucleoproteins
SA	Salicylic Acid
SC	Songwhan Charmi
SE	Sieve Elements
SNP	Single Nucleotide Polymorphism
ssDNA	single-stranded DNA
SSR	Simple Sequence Repeat
ssRNA	single- stranded RNA
TAV	*Tomato Aspermy Virus*
TIPs	Tonoplast Intrinsic Proteins
TMV	*Tobacco Mosaic Virus*
UTR	Untranslated Region
VP	Vascular Parenchyma
VPS41	Vacuolar Protein Sorting 41
VRC	Viral Replication Complex
WMV	*Watermelon mosaic virus*
ZYMV	*Zucchini Yellow Mosaic Virus*

Summary

The exotic melon accession PI 161375 cultivar Songwhan Charmi (SC) shows resistance to most of *Cucumber mosaic virus* (CMV) strains. The resistance to CMV subgroup II strains was reported as recessive, controlled by the gene *cmv1* which is able to prevent the phloem entry of the virus by restricting it in the bundle sheath cells. This restriction depends on the movement protein (MP), the determinant of virulence. Two more QTLs, *cmvqw3.1* and *cmvqw10.1* are required, working together with *cmv1*, for the resistance to the subgroup I strain CMV-M6. However, CMV-FNY, a more aggressive strain from subgroup I, was able to overcome the resistance conferred by *cmv1/cmvqw3.1/cmvqw10.1*. In this thesis we aim to (i) identify the additional QTLs responsible for the resistance to CMV-FNY, (ii) characterize the resistance conferred by the QTLs *cmv1/cmvqw3.1/cmvqw10.1* and (iii) identify the virulence factors involved with these QTLs.

QTL analysis was addressed developing several F_2 populations made between the CMV-FNY-resistant lines DHL142, DHL69 and several CMV-FNY-susceptible melon lines. Several putative minor QTLs were detected in LG II, LG IX, LG X and LG XII. However, none of these QTLs were reproducibly detected neither in several F_2 populations nor using different methods of phenotyping. The evaluation of our QTL detecting system indicated that it is not appropriate for detecting minor QTL, being the most probable limiting factor the correct phenotyping of the infection for QTL detection in a F_2 population.

The study of the resistance conferred by combinations of two or the three QTLs showed that, although the plants were susceptible to CMV-FNY, there was a delay in the infection, indicating that the resistance involves a restriction of the viral movement. Further analysis showed that the restriction worked at the level of phloem entry, rather than at the level of movement within the phloem. Therefore, this indicates that *cmvqw3.1* and *cmvqw10.1* are impairing CMV-FNY movement at the same step of the viral infection where *cmv1* restricts CMV-LS.

Pseudorecombinants generated between CMV-FNY / CMV-M6 and between CMV-FNY / CMV-LS demonstrated that the determinant of virulence was not mapped in RNA3.

Taken together, our results suggest that the resistance to CMV in SC accession is built by a series of resistance layers, being *cmv1* the first layer, against subgroup II strains; the second layer, *cmvqw3.1* and *cmvqw10.1*, that provide efficient resistance to CMV-M6; and the third layer being the unknown QTL, necessary for efficient resistance to CMV-FNY. At present, we

know that the first two layers of resistance would be working in the restriction of CMV entry to the phloem.

Resumen

La accesión de melón exótico PI 161375, cultivar Songwhan Charmi (SC) es resistente a la mayoría de las cepas de *Cucumber mosaic virus* (CMV). La resistencia a las cepas del subgrupo II de CMV es recesiva y controlada por el gen *cmv1*, que es capaz de prevenir la entrada del virus en el floema deteniéndolo en las células de la vaina que rodean la vena. Esta restricción depende de la proteína de movimiento (MP), el determinante de la virulencia frente a este gen. Para resistir a la cepa CMV-M6, del subgrupo I, se requieren dos QTL más, *cmvqw3.1* y *cmvqw10.1*, funcionando en colaboración con *cmv1*. Sin embargo, CMV-FNY, una cepa más agresiva del subgrupo I, es capaz de superar la resistencia conferida por *cmv1/cmvqw3.1/cmvqw10.1*. En esta tesis, nuestro objetivo es (i) identificar los QTL adicionales responsables de la resistencia a CMV-FNY, (ii) caracterizar la resistencia conferida por los QTL *cmv1/cmvqw3.1/cmvqw10.1* e (iii) identificar los factores de virulencia involucrados con estos QTL.

El análisis de QTL se abordó desarrollando varias poblaciones F_2 entre las líneas DHL142 o DHL69, resistentes a CMV-FNY, y varias líneas de melón susceptibles a CMV-FNY, donde se detectaron varios QTL menores en LG II, LG IX, LG X y LG XII. Sin embargo, ninguno de estos QTLs fue detectado reproduciblemente en varias poblaciones F_2, ni utilizando diferentes métodos de fenotipado, lo que indicó que nuestro sistema de detección de QTL no es apropiado para detectar QTLs menores. El factor limitante más probable puede ser la dificultad del fenotipado de la infección para la detección de QTLs en una población F2.

El estudio de la resistencia conferida por combinaciones de dos o los tres QTL mostró que, aunque las plantas eran susceptibles a CMV-FNY, hubo un retraso en la infección, lo que indica que la resistencia implica una restricción del movimiento viral. Un análisis posterior mostró que la restricción funcionaba al nivel de la entrada al floema, más que al nivel del movimiento dentro del floema. Por lo tanto, esto indica que *cmvqw3.1* y *cmvqw10.1* están dificultando el movimiento de CMV-FNY en el mismo paso de la infección viral donde cmv1 restringe CMV-LS.

Los pseudorecombinantes generados entre CMV-FNY / CMV-M6 y entre CMV-FNY / CMV-LS demostraron que el determinante de virulencia no mapeaba en el RNA3.

Tomados en conjunto, nuestros resultados sugieren que la resistencia al CMV en la accesión SC está formada por una serie de niveles de resistencia, siendo *cmv1* el primer nivel, efectivo

contra las cepas del subgrupo II; el segundo nivel, formado por *cmvqw3.1* y *cmvqw10.1*, que cooperarían con *cmv1* para proporcionar resistencia frente a CMV-M6; y el tercer nivel sería el QTL no identificado aún, necesario para la resistencia frente a CMV-FNY. En la actualidad, sabemos que los dos primeros niveles de resistencia estarían participando en la restricción de la entrada de CMV al floema.

Resum

L'accessió exòtica de meló PI 161375 cultivar Songwhan Charmi (SC) presenta resistència a la major part de soques de *Cucumber mosaic virus* (CMV). S'ha descrit que la resistència a soques del subgrup II de CMV és recessiva i que està controlada pel gen *cmv1*, que és capaç d'evitar l'entrada del virus al floema mitjançant una restricció a nivell de les cèl·lules de la beina. Aquesta restricció depèn de la proteïna de moviment (MP) viral, que és el determinant de la virulència. Per tenir resistència a la soca CMV-M6, pertanyent al subgrup I, a part de *cmv1*, també es requereixen dos altres QTLs: *cmvqw3.1* i *cmvqw10.1*. No obstant, una soca més agressiva del subgrup I, CMV-FNY, és capaç de superar la resistència conferida per *cmv1/cmvqw3.1/cmvqw10.1*. Aquesta tesis té com objectius (i) identificar altres QTLs responsables de la resistència a CMV-FNY, (ii) caracteritzar la resistència conferida pels QTLs *cmv1/cmvqw3.1/cmvqw10.1*, i (iii) identificar els factors de virulència implicats en aquests tres QTLs.

L'anàlisi de QTLs es va dur a terme mitjançant diverses poblacions F_2 obtingudes del creuament entre les línies resistents a CMV-FNY, DHL142 i DHL69, i línies susceptibles. Es van detectar alguns possibles QTLs d'efecte menor als LG II, LG IX, LG X i LG XII. No obstant, cap d'aquests QTLs va ser reproduïble a les diferents poblacions avaluades, ni pels diferents mètodes de fenotipat utilitzats. Un cop avaluat el sistema d'anàlisi de QTLs emprat es va demostrar que aquest no havia estat l'apropiat per QTLs d'efecte menor. Probablement el factor limitant hauria estat la robustesa de l'avaluació fenotípica de la infecció en poblacions F_2.

L'estudi de la resistència, conferida per combinacions de dos o tres QTLs, va mostrar que malgrat les plantes s'acabaven infectant per CMV-FNY, hi havia un retard en la infecció, indicant que la resistència intervé restringint el moviment viral. Més endavant es va demostrar que la restricció actua a nivell de l'entrada al floema, enlloc d'intervenir a nivell del moviment del virus un cop dins del floema. Així doncs, *cmvqw3.1* i *cmvqw10.1* actuen dificultant el moviment de CMV-FNY al mateix punt de la infecció viral on ho fa *cmv1* amb CMV-LS.

La generació de pseudorecombinants entre CMV-FNY / CMV-M6 i CMV-FNY / CMV-LS va demostrar que el determinant de la virulència no es troba al RNA3.

Aquests resultats suggereixen que la resistència a CMV de l'accessió SC es construeix mitjançant diferents nivells, essent *cmv1* el primer nivell conferint resistència envers el subgrup II; el segon nivell *cmvqw3.1* i *cmvqw10.1* conferint una resistència eficient envers CMV-M6; i

un tercer nivell on altres QTLs encara per determinar serien necessaris per conferir una resistència eficient a CMV-FNY. Actualment, sabem que els dos primers nivells de resistència estarien actuant restringint l'entrada de CMV al floema.

Introduction

1. Plant Viruses

Plant pathogens can cause severe economic losses in agricultural production and a huge impact on the quality of the final product. Plant pathogens include fungi, bacteria, viruses, mycoplasmas, spiroplasmas and viroids (Anderson and Morales, 1994). Among all the plant pathogens, viruses are generally considered to rank second threat to plant production losses, after fungi. The first study of viruses was reported in 1898, when Beijerinck described for the first time *Tobacco mosaic virus* (TMV).

Viruses are submicroscopic agents that cause infections in plants, animals, fungi and bacteria. As they can reproduce only in the host cells, they are considered obligate intracellular parasites. Viruses have relatively simple characteristics, with a nucleocapsid formed by the coat protein (CP) that protects the genomic nucleic acid. Some viruses have an additional envelop covering the capsid. The whole structure of virus is called virion.

The viral genome can be double-stranded DNA (dsDNA), single-stranded DNA (ssDNA), double-stranded RNA (dsRNA), or single-stranded RNA (ssRNA). Most plant viruses are ssRNA virus (Waterhouse et al., 2001).Viruses replicate in the host cells by using their metabolism and assemble themselves in these host cells. Generally, life cycle of plant viruses includes transmission either by their insect vectors or by mechanical means, cell entrance, virion uncoating, genome replication and translation, movement cell-to-cell and long distance movement through the phloem (Hipper et al., 2013).

2. Cucumber mosaic virus (CMV)

Cucumber mosaic virus (CMV) belongs to the *Bromoviridae* family and *Cucumovirus* genus. CMV was firstly described in 1916 as the causal agent of a disease developed in melon in Michigan (Jagger, 1916) and in cucumber in New York (Doolittle, 1916). Since then, CMV has been described worldwide from temperate to tropical zones.

2.1 Genome organization

Like all the other members of family *Bromoviridae,* CMV is composed of three positive-stranded genomic RNAs, RNA1, RNA2, RNA3 and two subgenomic RNAs, RNA4 and RNA4A.The genome structure of CMV is presented in Figure I-1. Each genomic segment has a

3' tRNA-like structure (Ahlquist et al., 1981; Rietveld et al., 1983) and a 5'cap structure (Symons, 1975). The length of the different RNAs differs between virus strains. The length of RNA1 ranges from 3357 to 3391 nucleotides (nt). The length of RNA2 differs from 3036 to 3060 nt while the length of RNA3 goes from 2197 to 2220 nt. RNA1 encodes the 111 kilodaltons (KDa) protein 1a, containing a putative methyltransferase and helicase motifs and is involved in viral replication (Habili and Symons, 1989). RNA2 encodes the 97 KDa replicase (or 2a protein), and a 11 KDa 2b protein, which is translated from a subgenomic RNA, RNA4A (630-702 nt) in a different frame and encodes a suppressor of RNA silencing. RNA3 encodes the 30 KDa protein 3a, the viral movement protein (MP), involved in the cell-to-cell movement, and also the 3b or coat protein (CP), involved in coating the genomic RNA to form the virion. RNA1 and RNA2 together were reported essential for virus replication (Nitta et al., 1988). Apart from the function in replication, RNA1 was shown to be related with viral cell-to-cell and long-distance movement (Gal-On et al., 1994). Is also related with the severity of symptoms and has a potential role in the induction of pathogenicity (Roossinck and Palukaitis, 1990). The 2a protein is a virus RNA polymerase that carries out the viral replication. This protein must interact with the 1a protein for a proper replication, because when N-terminal 126 amino acid region of 2a is phosphorylated, the 2a protein cannot interact with 1a protein and the replication is inhibited (Kim et al., 2002). Moreover, 2a was related to virus cell-to-cell movement and efficiency of symptom development (Choi et al., 2005). The 2b protein was recognized as a suppressor of post-transcriptional gene silencing (PTGS) preventing initiation of gene silencing (Lucy et al., 2000). The 2b protein was also related with the salicylic acid (SA) mediated anti-viral resistance (Ji and Ding, 2001). The protein 3a, encoded by RNA3, is the viral movement protein (MP), involved in the cell-to-cell movement through plasmodesmata (PDs) by modification of their size exclusion limit (Vaquero et al., 1994). The virus moves through PDs as a ribonucleoprotein complex (Ding et al., 1995). A 3a mutated virus could not infect normal tobacco plants, while the CMV 3a transgenic tobacco plants could complement the 3a mutated virus for its cell-to-cell movement but also for long distance movement, indicating that the MP has also a role in long distance movement (Kaplan et al., 1995). The CP is a 24KDa protein encoded by the subgenomic RNA4 and was proved essential for both, cell to cell and long distance viral movement. A small satellite-like linear RNA named CARNA5, dependent on the helper RNA for the replication, was identified decades ago (Kaper and Tousignant, 1977). CARNA5 (CMV-associated RNA5) is a 300-400 nt long

heterogeneous mixture of cleavage of CMV RNAs1, 2 and 3. RNA5 is produced in subgroup II strains of CMV, but not in subgroup I strains (Thompson et al., 2008) and has a role in CMV recombination (De Wispelaere and Rao, 2009). CMV satellite RNAs, on the other hand, are small non-coding RNAs with no sequence similarity to the viral genome, but dependent on the viral genome (the helper virus). They modify the pathogenesis, accumulation and transmission of CMV depending on the strain of helper virus and satellite RNA and on the host plant species (Palukaitis and Garcia-Arenal, 2003).

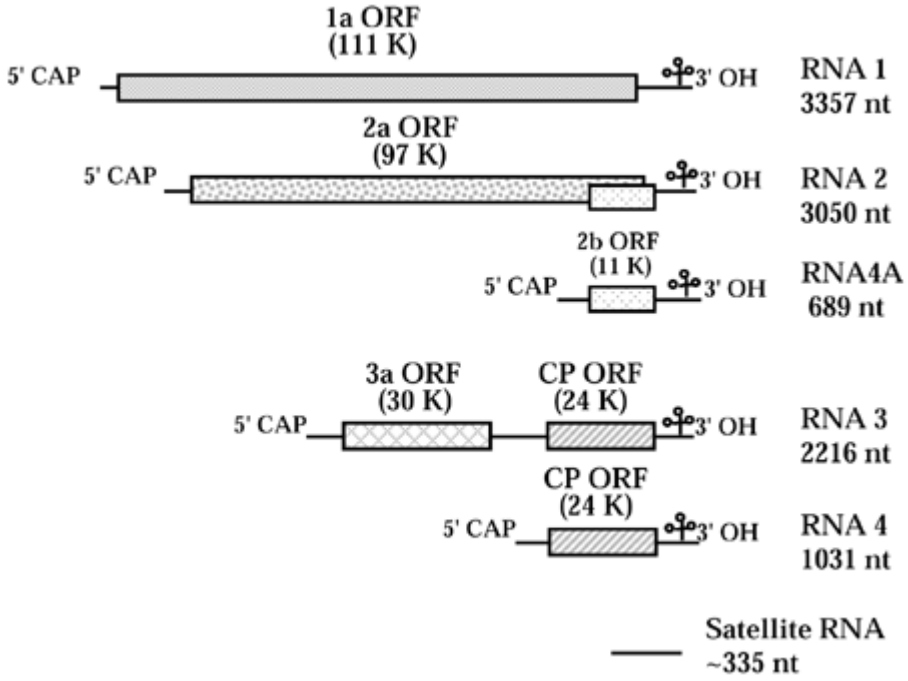

Figure I-1. Genome organization of CMV. The lengths of each genomic RNA are indicated in nucleotides (nt) and the mass of proteins are indicated in kilodaltons (K). The open reading frames (ORF) are indicated in boxes (adopted from (Roossinck, 2001)).

2.2 Taxonomy and classification

CMV was firstly classified into two subgroups, subgroup I and subgroup II, based on the serological data, peptide mapping of the CP, nucleic acid hybridization and sequence analysis (Palukaitis et al., 1992). CMV subgroup I was further divided into subgroups IA and IB according to the alignment of the 5′ non-translated regions of RNA 3 for 26 strains of CMV and the classification was also confirmed analyzing the CP genes of 53 CMV strains (Roossinck et al., 1999). Subgroup II and subgroup IA strains have a worldwide distribution, whereas subgroup

IB strains were described to originate only from Asia. The subgroup II includes strains like CMV-LS, CMV-Q and CMV-Ly. Strains CMV-Ix, CMV-Sd and CMV-C72 belong to subgroup IB while strains CMV-FNY, CMV-Y and CMV-O belong to subgroup IA. Subgroups I and II have about 70% sequence homology between them, whereas subgroups IA and IB are 92-94% identical. The phylogenetic analysis indicated that subgroup II strains had the least divergence while subgroup IB strains have the highest divergence (Roossinck et al., 1999).

2.3 CMV viral cycle

In nature, CMV is transmitted by aphids in a non-persistent manner. CMV could also be transmitted plant to plant mechanically by sap inoculation. First, after transmission, CMV enters into plant epidermal or mesophyll cells. Then, start the virion disassembly and viral translation and replication. Thereafter, the newly assembled viral complexes start cell-to-cell movement, long-distance movement and the replication in newly infected cells (Garcıa-Arenal and Palukaitis, 2008). A general view of virus cell-to-cell and long-distance movement in plant tissues is represented in Figure I.2.

2.3.1 Viral replication

As depicted in Figure I-2, once the genomic RNAs are released in the host cell, they are directly used as templates for translation producing the viral replication proteins1a and 2a, but some unknown host proteins are also needed. Protein 1a co-localize with protein 2a in tonoplast where CMV replication takes place (Cillo et al., 2002). The replication proteins, together with genomic RNAs, form the viral replication complex (VRC). Arabidopsis Tonoplast Intrinsic Proteins (TIPs) family members TIP1 and TIP2 interact with the1a protein and affect the replication of CMV (Kim et al., 2006). Additionally, some host proteins like RNA binding protein (BRP1), Glyceraldehyde 3-phosphate dehydrogenase (GAPDH) and 30S ribosomal subunit protein S11 (RPS11) were also found in the VRCs (Hayes and Buck, 1990; Chaturvedi et al., 2016; Wang et al., 2017). Then, the complementary negative strand RNAs are synthesized using the positive genomic RNAs as templates. Thereafter, a great amount of positive stranded progeny genomic RNAs are synthesized using the negative RNAs as templates and then released in tonoplast. The sub-genomic RNA4 and RNA4A are synthesized from the negative complementary strand RNA3 and RNA2, respectively, through recognition of the corresponding sub-genomic promoters. Satellite RNAs are synthesized by the viral replicase using the genomic

RNAs as templates. The progeny positive strand RNAs can undergo translation, replication and movement to adjacent cells as ribonucleoproteins or encapsulated into virions.

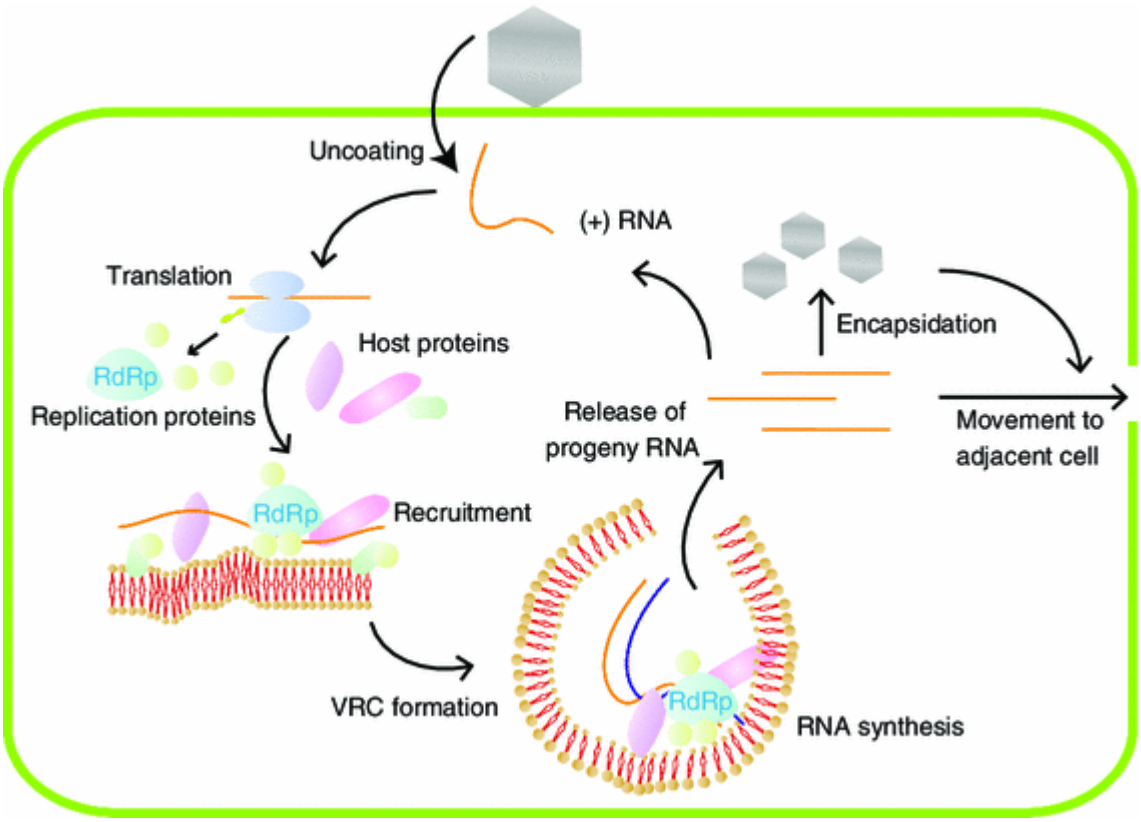

Figure I-2. Schematic representation of a general cycle of positive-strand RNA viruses. VRC: viral replication complexes; RdRp: RNA-dependent RNA polymerase (adopted from (Hyodo and Okuno, 2014)).

2.3.2 Cell-to-cell movement

CMV moves cell-to-cell from epidermal or mesophyll cells to bundle sheath cells, towards vascular parenchyma until companion cells before it reaches sieve elements (Figure I-3).Virus spread from infected cell to adjacent cells via plasmodesmata (Kumar et al., 2015). Plasmodesmata act as intercellular channels during the interaction with the surrounding environment. During this cell-to-cell movement process, the MP is reported as the main viral protein involved. It binds the viral RNA to form ribonucleoprotein complexes that interact with host proteins to modify the PD structure and function (Andreev et al., 2004). MP helps the virus movement by changing and increasing the gating capacity of PDs to allow viral pass (Ding et al., 1995; Su et al., 2010). The MP has been involved in the ability of CMV to systemically infect

soybean (Hong et al., 2007) and melon (Guiu-Aragonés et al., 2015). In melon, it allows subgroup II strains, like CMV-LS to infect systemically melon plants. However, CMV-LS is unable to infect the melon line carrying the resistance gene *cmv1* (Guiu‐Aragonés et al., 2016). Reassembled CMV-LS, carrying the MP from CMV-FNY, from subgroup I, could break *cmv1* conferred resistance, pass through bundle sheath cell PDs and systemically infect melon plants (Guiu‐Aragonés et al., 2015). Apart from the MP, CP also reported affects the cell-to-cell movement efficiency (Canto et al., 1997; Wong et al., 1999). Studies combining RNA3 of CMV and TAV showed that efficient movement requires compatibility between the 29 C-terminal amino acids of the MP and the C-terminal two-thirds of the CP (Salanki et al., 2004).

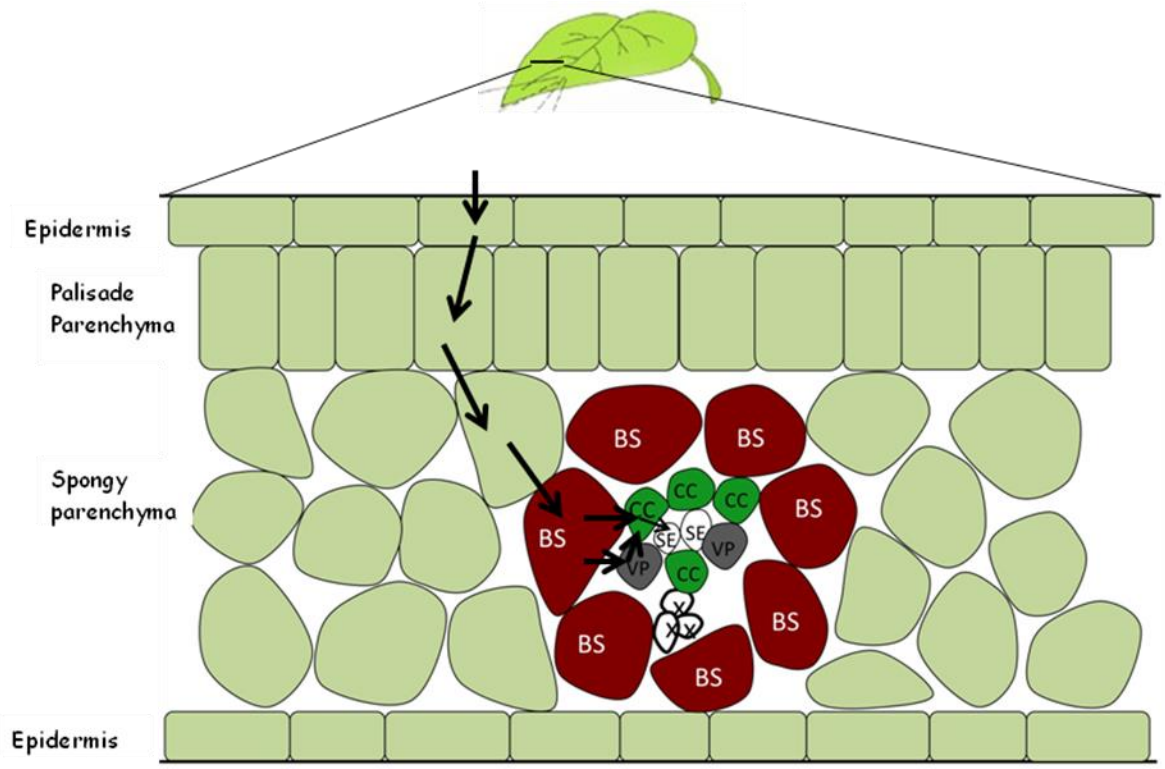

Figure I-3. Viral infection movement through the different cells in the leaf. BS: Bundle sheath cells; CC: Companion cells; VP: Vascular parenchyma cells; SE: Sieve elements; X: Xyleme (Drawing adopted from C. Guiu).

2.3.3 Long-distance movement

Long-distance movement in the phloem starts after virus entry into sieve elements (SE) following the pathway: bundle sheath cells to vascular parenchyma to companion cells to SE (Figure I-3). SE are enucleated cells connected with companion cells, which have high metabolic

activity. The SE are interconnected by wide pores and form a low-resistance cellular connections for the flux of elaborated sap. Although some macromolecules can pass through SE without specific regulation, the virions or viral complexes are still difficult to move freely in the phloem. Thus, both viral and host proteins are involved in movement through the phloem. Different viral proteins were reported to affect CMV long-distance movement. Three amino acids of the βB-βC loop of CP were found essential but not the only factor for viral long-distance movement (Salánki et al., 2011). CMV 2a protein was found not only involved in the replication but also affect viral systemic infection via inhibiting long-distance movement (Carr et al., 1994). CMV 1a, previously considered only involved in the replication, showed a function in regulating the long-distance movement rate (Gal-On et al., 1994). The CP is especially important, as observed in different hosts, including cucurbits, maize or *Tetragonia expansa* (Kobori et al., 2002; Palukaitis and Garcia-Arenal, 2003; Salánki et al., 2011). It is postulated that CMV disassembles in the cytoplasm of companion cells before entering the SE and move through the Pore Plasmodesmata Units (PPU). PPUs are specialized, branched PDs, with larger size exclusion limit than other PDs that communicate companion cells with SE (Roberts and Oparka, 2003). The virus moves through PPUs as a ribonualeoprotein complex with the aid of the MP and CP to reassemble in the SE as virions. Therefore, the CP has an essential role in the movement through the phloem (Blackman et al, 1998). Some host factors also partially affect CMV long-distance movement in crop plants like pepper, however the resistance mechanism is still not clear (Nono‐Womdim et al., 1993; Caranta et al., 2002). In cucumber, a phloem exudate protein, homologous to the protein PP1 from pumpkin, participates in translocating RNPs or virions within the phloem stream (Requena et al., 2006). In *N.benthamiana* plants, the host methyltransferase Tcoi1 interacts with CMV 1a leading to methylation of the viral protein, finally promoting the long-distance movement of CMV (Kim et al., 2008).

Viral complexes start the unloading process and exit from the SE through the major veins when it reaches the sink tissues. Finally, the virus disseminates throughout the whole plant.

2.4 Plant host

CMV has the widest host range among plant viruses. The virus infects more than 1200 plant species of both monocots and dicots, including many important vegetables like most of horticultural crops in *Cucurbitaceae* and *Solananceae* families, ornamentals, woody and semi-woody plants (Edwardson and Christie, 1991). The severity of infection varies from the plant

species infected and the age of the plants while the infection occurred. The infection symptoms vary from typical mosaic, severely stunted, malformed leaves, wrinkled, curled or small leaves or necrosis in leaves. CMV can also induce ring-spotting, roughness and deformation in fruits (Figure I-4)

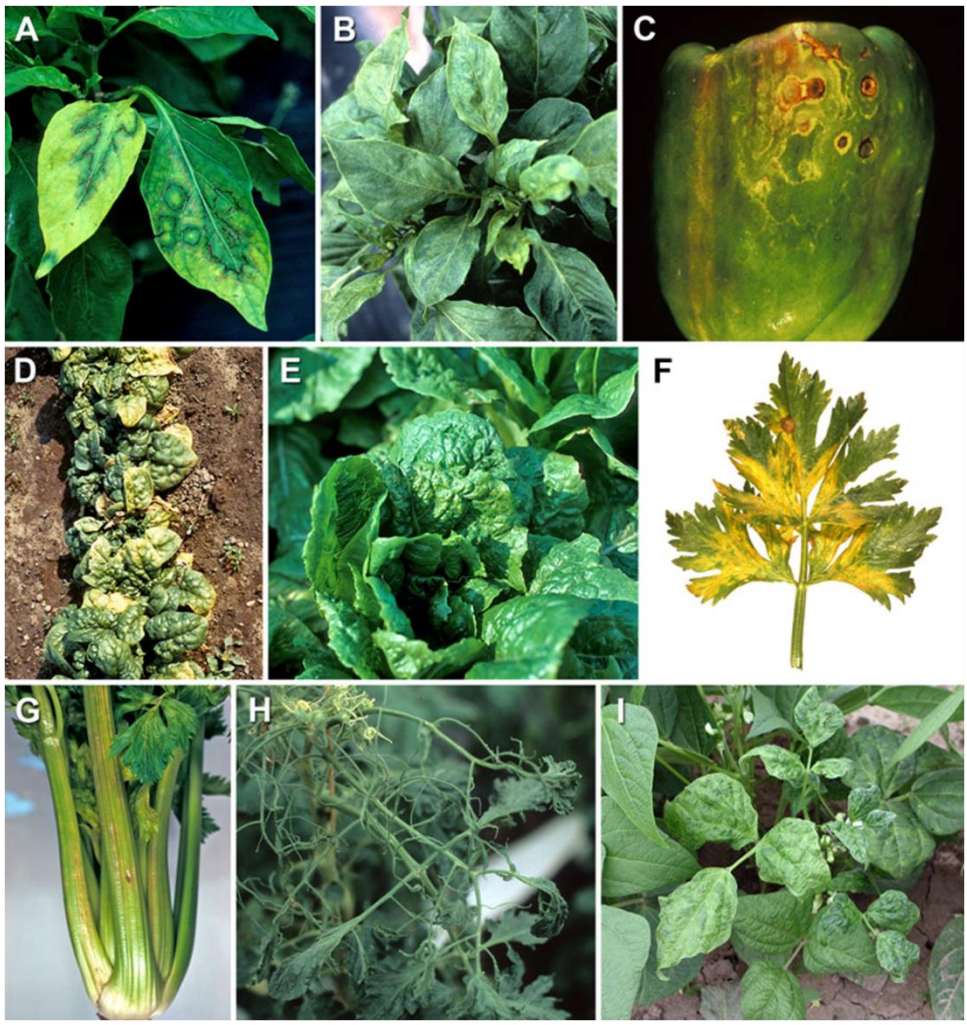

Figure I-4. CMV infection symptoms in pepper, spinach, lettuce, celery, tomato and beans (Figure taken from American Phytopathological Society, https://www.apsnet.org/Pages/default.aspx).

2.5 Virus transmission and management

CMV could be transmitted mechanically by humans through cultivating, grafting or even simply touching healthy plants after touching infected plants. CMV was also reported to be transmitted by seeds in pepper (Ali and Kobayashi, 2010), chickweed (Tomlinson and CARTER,

1970), bean (Bos and Maat, 1974) and spinach (Yang et al., 1997). In natural conditions, CMV is transmitted by more than 60 aphid species in a non-persistent manner. The transmission efficiency depends on the aphid species (Raccah et al., 1985), host plants (Hobbs et al., 2000) as well as virus strains (Gera et al., 1979).

The use of pesticides against viral infections is limited, therefore, the most efficient way to protect plants from CMV infection should be searching for natural resistant resources in different plant species, and study the resistance mechanism to transfer it to breeding programs.

3. Resistance to CMV

3.1 Natural resistance

A few natural resistant plants have been reported in different species (Table I-1). Some of them were reported to be monogenic and dominant, but mostly are recessive and polygenic, showing a complex quantitative resistance with major and minor quantitative trait (QTLs) regulating together the resistance.

Table I-1. CMV resistance mediated by dominant, recessive genes or polygenic control in different plant species

Type of resistance	Plant species	Resistance gene / QTLs	Reference
Dominant	Arabidopsis	*RCY1*	(Takahashi et al., 2002)
	Pepper	*Cmr1*	(Kang et al., 2010)
Recessive	Arabidopsis	*cum1, cum2*	(Yoshii et al., 2004)
	Pepper	*cmr2*	(Choi et al., 2018)
	Melon	*cmv*1	(Essafi et al., 2009)
Quantitative	Pepper	*qCmr2.1* and *qCmr11.1*	(Guo et al., 2017)
		cmvP1-5.1 and *cmvP1-10.1*	*(Eun et al., 2016)*
	Cucumber	*cmv6.1*	*(Shi et al., 2018)*
	Melon	*cmv1, cmvqw3.1* and *cmvqw10.1*	(Guiu-Aragonés et al., 2014)

In the model plant Arabidopsis thaliana, the ecotype C24 showed resistance to the yellow strain CMY-Y, accompanied by a hypersensitive response (HR), characterized by the

development of necrotic local lesions (NLL). This resistance is controlled by the dominant locus *RCY1*, encoding a CC-NBS-LRR-type protein, a RPP8/HRT family resistant gene. When the *RCY1* from C24 was expressed in a susceptible line, it showed a restriction in virus systemic spread (Takahashi et al., 2002). Another example was *cum1* and *cum2* mediated recessive CMV resistance. *CUM1* and *CUM2* encode, respectively, the translation factors eIF4E and eIF4G and the Arabidopsis *cum1* and *cum2* mutants specifically prevent the efficient translation of CMV 3a protein, leading to impairment of cell-to-cell CMV movement (Yoshii et al, 2004).

In pepper, several resistant resources have been identified in China and Korea. In China, the inbred line 'PBC688' showed resistance to CMV-FNY controlled by two loci, *qCmr2.1* on chromosome 2 and *qCmr11.1* on chromosome 11. For *qCmr2.1*, a N-like protein homologous to the N protein associated with TMV-resistance in *Solanum* crops was described as a candidate gene (Guo et al., 2017). The Korean *Capsicum annuum* cultivar 'Bukang', resistant to CMV-FNY and CMV-Korean strains, showed a dominant resistance controlled by *Cmr1* gene, mapping at the centromeric region of LG2 (Kang et al., 2010). However, 20 years after deploying this resistant material in the Korean breeding program, a new isolate CMV-P1 overcame the resistance conferred by *Cmr1*. Recently, an Indian *C. annuum* cultivar 'Lam32' and a Korean line'A1' were found to display resistance to CMV-P1 strain. The resistance of 'Lam32' was controlled by a single recessive resistant gene, *cmr2*, mapping on chromosome 8 (Choi et al., 2018). The resistance present in the line 'A1' was recessive and controlled by two QTLs *cmvP1-5.1* and *cmvP1-10.1*, located on chromosomes 5 and 10, respectively (Eun et al., 2016).

In cucumber, several resources have been reported as resistant to CMV strains but few molecular mechanisms were investigated. The cucumber inbred line '02245' shows resistance to CMV (without reporting which strain), with a QTL, *cmv6.1* on chromosome 6, explaining the majority of the phenotypic variation. Furthermore, the gene *Csa6M133680* was reported as a candidate gene for the resistance by genetic and expression analysis (Shi et al., 2018). In melon, the gene *cmv1* encoding a *Vacuolar protein sorting 41* (*CmVPS41*), confers resistance to CMV subgroup II strains (Giner et al., 2017), but not to subgroup I strains. For resistance to these strains, two other QTLs, *cmvqw3.1* and *cmvqw10.1*, together with *cmv1* were necessary (Guiu-Aragonés et al, 2014).

Until now, only few CMV resistance genes like *RCY1* (Takahashi et al., 2001), *cum1* and *cum2* (Yoshii et al., 2004) and *VPS41* (Giner et al., 2017) were cloned.

The natural resistance to CMV in monocot crops has been also reported. In maize, after analyzing 82 landraces in Japan, 12 out of them showed resistance to CMV-Y. Aso-3 showed necrotic local lesions and kept resistant to CMV-Y. The resistance was controlled by a single dominant gene but further molecular mechanism has not been reported. This maize-CMV resistant system was proposed to be a model to study the HR-mediated resistance in monocot crops (Takahashi et al., 2018).

3.2 Transgenic plants

3.2.1 Pathogen-derived resistance

Plants transformed with some of CMV related sequences (CP, replicase or satellite RNA) showed an increase of virus resistance. CMV CP is the most used viral factor in the plant transformation. However, the resistance degree and efficiency differed in the donor strains as well as plant species. Transgenic tobacco plants expressing the CP could protect plants from CMV infection, independently of the viral load of the inoculum, however transgenic plants expressing antisense CP could protect plants only under low virus concentration (Cuozzo et al., 1988). It was also reported that tobacco plants transformed with CP from CMV-O showed more resistance to CMV-O than to CMV-Y and also showed resistance to another *cucumovirus* member *chrysanthemum mild mottle virus* (Nakajima et al., 1993). In squash, the resistance of transgenic plants expressing CMV CP varied between transgenic lines, some showing absolute resistance while others infected with mild mosaic symptom or even totally susceptible. The squash transformed with the CP genes from CMV and *Watermelon mosaic virus* (WMV) 2 conferred total resistance to both CMV and WMV viruses (Tricoll et al., 1995). RNAi (RNA interference) mediated resistance based on CMV CP resulted in varied CMV resistance among transgenic lines (Ntui et al., 2014). Replicase-related transgenic plants were also developed. Truncated CMV 2a replicase protein transformed plants suppressed CMV viral replication and long-distance movement (Carr et al., 1994). Transforming an altered form of CMV replicase inhibited CMV viral replication and restricted CMV from entering into the minor veins in tobacco plants (Wintermantel et al., 1997). Transforming a defective replicase gene of CMV in *Lilium* plants showed increase resistance level with no virus detectable in newly developed

leaves (Azadi et al., 2011). Tobacco plants transformed with CP of the subgroup I strain CMV-*Gladiolus* resulted in a broad resistance to most CMV strains tested (Dubey et al., 2015). Apart from the CP and replicase related resistance, some microsatellite RNA were also used to obtain CMV resistant transgenic plants. Transforming a DNA copy of CMV satellite RNA resulted in the decrease of CMV replication as well as suppressed CMV symptom development in different plant species like tobacco (Harrison et al., 1987), tomato (Saito et al., 1992) and hot pepper (Kim et al., 1997).

3.2.2 Non-pathogen-derived resistance strategies

Extracellular ribonucleases were also proved to participate in defense against viruses with RNA genomes. Transgenic tobacco plants expressing bovine pancreatic ribonuclease (RNase A) showed increased resistance to CMV (Sugawara et al., 2016). Using yeast-two-hybrid system, the 30S ribosomal subunit protein S11 (RPS11) was found to interact with CMV 2b protein, its suppressor of gene silencing. NbRPS11 knockdown *Nicotiana benthamiana* plants showed the ability to inhibit CMV replication and accumulation (Wang et al., 2017). Some vitamins and plant hormones were also found to protect plants from CMV infection. Vitamin B_x could increase fruit yield and protect pepper plants from CMV infection (Song et al., 2013). Tomato plants over-expressing prosystermin, the systemin precursor**,** showed increasing resistance to CMV infection (Bubici et al., 2017). Some plant growth-promoting rhizobacteria (PGPR) were also able to protect tomato plants from CMV infection (Dashti et al., 2012; Elsharkawy et al., 2012). Some other factors like *Trichoderma asperellum* SKT-1 could also function in defending CMV infection (Elsharkawy et al., 2013).

4. Melon

Melon (*Cucumis melo* L.) (2n = 2 × 12= 24) belongs to the *Cucurbitaceae* family, genus *Cucumis*. In *Cucurbitaceae* family, there are many agronomical important crops such as cucumber (*Cucumis sativus* L.), watermelon [*Citrullus lanatus*, zucchini squash (Cucurbita pepo L.) and pumpkin (*Cucurbita moschata* Duch.exPoir.).

Melon is a worldwide important fruit crop. According to the data collected by Food and Agriculture Organization of the United Nations (http://www.fao.org/faostat/en/#data/QC), the melon production worldwide has increased over the past decades from 6.9 million tons in year 1961 to 31 million tons in year 2016 (Figure I-5). China is the leading production country with

16 million tons production per year, more than half of the total production in the world. Spain is a melon exporting country, being the 7th in production. It showed an increase until 2009, and a sharp decrease since then. In year 2016, the melon production in Spain was 0.66 million tons.

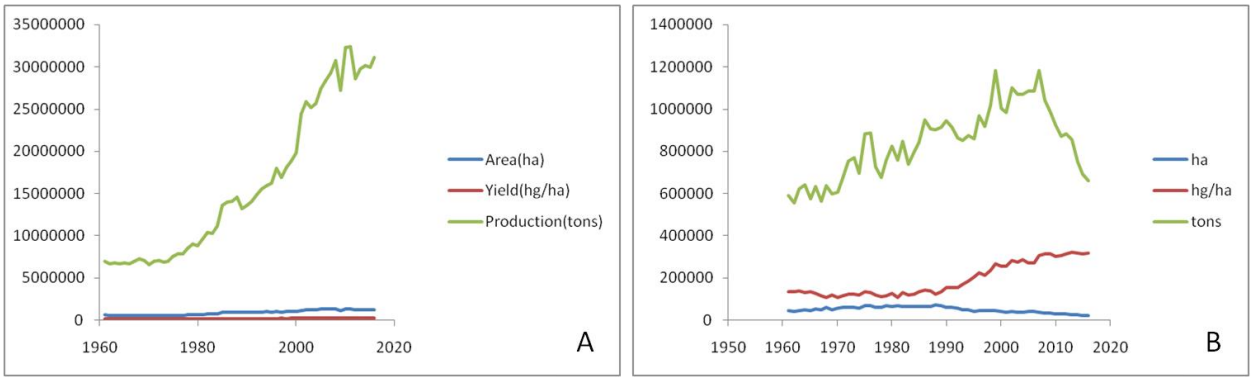

Figure I-5. Melon production A) worldwide and B) in Spain from 1961 to 2016. Green line, blue line and red line in the figure indicate the amount of melon production (tons), the melon planted areas (ha) and the melon yield (hg/ha) across years, respectively. (Data applied from http://www.fao.org/faostat/en/#data/QC))

4.1 Melon taxonomy and diversity

Cucumis melo is divided into two subspecies, *C. melo* ssp. *melo* and *C. melo ssp. agrestis (*Jeffrey, 1980). The subspecies *C. melo* ssp. *melo* has pilose or lanate ovaries covered with spreading, long hair while *C. melo ssp. agrestis* has sericeous ovaries covered with appressed, short hair (Stepansky et al., 1999). Using high density SNP molecular markers distributed across the 12 melon chromosomes, the classical classification of genus *Cucumis melo* into *C. melo* ssp. *melo* and *C. melo ssp. agrestis* (Blanca et al., 2012; Esteras et al., 2013) was confirmed. To have more detailed knowledge about each subspecies, there has been different classifications performed according to their botanical morphological characters (flowering time, aroma, taste…) and DNA polymorphisms. Combining morphological traits like vegetative and flowering stages, mature fruit morphology and fruit quality parameters, together with DNA fingerprinting as Inter-SSR (Simple Sequence Repeat)-PCR and RAPD (Random Amplified Polymorphic DNA), a worldwide collection of *Cucumis melo* varieties were classified into two groups, the first group *C. melo* ssp. *melo* including *cantalupensis* and *inodorus* types, and the second group *C. melo ssp. agrestis* including *conomon, chito, dudaim, agrestis and momordic*a (Stepansky *et al.*,

1999). More recently, another classification system was proposed to divide *C. melo* ssp. *melo* into ten groups (*Cantalupensis, Reticulatus, Adana, Chandalak, Ameri, Inodorus, Chate, Flexuosus, Dudaim* and *Tibish*) and *C. melo ssp. agrestis* into five groups (*Momordica, Conomon, Chinensis, Makuwa,* and *Acidulus) (Pitrat, 2008)*.

The melon consumed daily is mostly from *C. melo* ssp. *melo*. Apart from the general classification between subgroup species, some studies were also performed to investigate *C. melo* ssp. *melo* intraspecific genetic diversity (Monforte et al, 2003). The morphology and molecular diversity of more than one hundred Spanish accessions in the Spanish germplasm collection, together with other reference accession were studied. It was found that Spanish accessions were genetically distinct from other accessions with USA or European origins, hence Spanish melons could be used as sources to broaden genetic diversity of USA and other European melon germplasm. (López-Sesé et al., 2003). In China, melon accessions collected across nearly the whole country were analyzed together with reference accessions. It was found that Chinese accessions, no matter if they were netted or non-netted, thin-skinned or thick-skinned, they clustered together and separated from melon accessions from other regions such as Spain, Japan or USA (Luan et al., 2008). Genetic differences were also observed among African accessions (Mliki et al., 2001) and Japanese accessions (Nakata et al., 2005). Hence, introducing germplasm from other regions could improve the genetic diversity.

Nearly all the disease resistant melon varieties were found in *C. melo* ssp. *agrestis* but most of these varieties have unfavorable fruit traits. The diversity analysis of 17 *C. melo* ssp. *agrestis* genotypes in southern Caspian sea region using AFLP (Amplified Fragment Length Polymorphism) markers revealed a high genetic diversity among the genotypes (Shamasbi et al., 2014). In the diversity analysis combining cultivated and wild melons, *C. melo* ssp. *agrestis* was clearly separated from *C. melo* ssp. *Melo*; and the subgroup *agrestis* was structured according to their geographical origins (Serres-Giardi and Dogimont, 2012).

4.2 Genetic and genomic resources in melon

The big diversity observed in melon offers the opportunity to perform genetic studies to understand the basis of important agronomical traits such as plant development, fruit quality or disease resistance.

To decipher the genetic mechanism of interesting traits, different mapping populations have been developed, such as F_2, backcross (BC) populations, recombinant inbred lines (RILs), near isogenic lines (NILs) or double haploid lines (DHLs).

F_2 or F_2-derived F_3 populations have been frequently used, since they can be easily developed. Based on the F_2 population made between PI 414723 and the cultivar cv. Top Mark, a genetic map was constructed using RAPD, ISSR, SSR, and Restriction Fragment Length Polymorphism (RFLP) markers to clone the disease resistant homologous gene Pto-receptor-kinase family and the leucine-rich repeat R-genes family in melon (Brotman et al., 2000). For cloning the *Melon necrotic spot virus* (MNSV) resistance gene *nsv* from the melon accession PI 161375, F_2 and BC1populations as well as the offspring derived were used (Morales et al., 2005). Based on the F_2 population developed by crossing the multi-resistant genotype TGR-1551 and the susceptible Spanish cultivar 'Bola de Oro', a genetic map was constructed and one major QTL, *Pm-R,* was identified to confer resistance to some strains of powdery mildew (Yuste-Lisbona et al., 2011). F_2 populations produced between Indian wild melon "Trigonus" and Spanish cultivar "Piel de Sapo" was also successfully used to analyze QTLs related with domestication-related traits, such as fruit morphology, fruit size and pulp content (Díaz et al., 2017).

RILs were also used as a powerful tool for the primary QTL analysis. Based on 81 melon (*Cucumis melo* L.) RILs derived from a cross between USDA 846-1 and "Top Mark.", a few QTLs related with soluble solids and other fruit quality QTL were identified (Paris et al. 2008). Ninety-nine RI lines were developed from PI 414723 (subspecies *agrestis*) and 'Dulce' (subspecies *melo*) and used to construct a genetic map using SSR, SNP, INDEL and AFLP makers. Finally, 44 melon fruit QTLs, including sugar content, fruit flesh color and carotenoid content, were identified (Harel-Beja et al., 2010). In order to identify the QTL responsible for the resistance to powdery mildew in the highly resistant melon line AR5, a population of 93 RILs derived from crosses between melon line AR5 and the susceptible line 'Earl's Favourite' were produced. The resistance was controlled by two loci (Fukino et al., 2008). A RIL population developed from a cross between PI 414723 (*C. melo* var. momordica) and 'Dulce' was used to analyze the genetic factors controlling fruit quality traits. More than 200 QTLs and some specific genes like Thiol acyltransferase (*CmThAT1*) gene were detected affecting flesh color, taste and aroma (Galpaz et al., 2018).

BC populations have been also easily produced and commonly used as a great tool for genetic analysis. Combining RAPD, microsatellite and AFLP markers, a linkage map was constructed based on 66 backcross progenies produced between 'AnanasYokneum' and'MR-1'. This map allowed to identify markers related to disease resistance genes (Fusarium wilt, downy, powdery mildew) (Wang et al., 1997). BC populations were also used combined with other populations in QTL analysis for powdery mildew resistance (Kim et al., 2016), virus resistance (Sáez et al., 2017) and domestication related traits (Díaz et al., 2017).

NILs are lines with small introgressions of the donor parental line in the background of the recurrent parental genome, so that the whole genome is covered within the entire NIL collection. NILs have been developed in many plant species and used frequently as a powerful tool for QTL analysis related with developmental traits (Keurentjes et al., 2006; Zhang et al., 2006; Melchinger et al., 2007; Clark et al., 2008), fruit quality (Bernacchi et. al, 1998), crop production (Xie et al., 2006), and biotic and abiotic resistance (Martin et al., 1991; Brouwer and Clair, 2004; Niones, 2004). In melon, a NIL population was developed using the Spanish cultivar Piel de Sapo (PS) as recurrent parental line and the exotic Korean accession PI 161375, cultivar Songwhan Charmi (SC), as donor parent (Eduardo et al., 2005) (Figure I-6). SC has a relatively high genetic distance with PS (Garcia-Mas et al., 2000; Monforte et al., 2003). The collection was composed of 57 lines covering almost the whole genome of SC. As the fruit of PS differs from that of SC, these NILs were used for QTL analysis related with fruit quality traits, like fruit length, fruit shape, ovary shape, external color, flesh color (Eduardo et al., 2007; Obando et al., 2008; Fernandez-Silva et al., 2010). The NILs were also used to investigate the QTLs related to fruit ripening and softening (Moreno et al., 2008; Vegas et al., 2013; Ríos et al., 2017), aroma volatile profile (Obando-Ulloa et al., 2010) or sugar and acid composition (Obando-Ulloa et al., 2009). As the exotic accession SC was described to have multiple disease resistances, the NILs were also used to analyze the resistance to CMV (Essafi et al., 2009).

Figure I-6. Spanish cultivar PS (on the left) and exotic Korean accession SC (on the right) used as parental lines to develop the melon NILs population (images from http://bulletin.upct.es/index.php/melon)

DHL populations are a collection of completely homozygous lines that contain half of the genome of each parental line, representing a mosaic of both parental genomes. These lines have been developed and widely used for multi-trait analysis in many crop species as rice (Jiang et al., 2004; Cha-um et al., 2009), cucumber (Claveria et al., 2005) as well as melon (Lotfi et al., 2003; Monforte et al., 2004). In melon a DHL collection was developed using PS and SC as parental lines for the identification of QTLs related to fruit quality (Monforte et al., 2004) and CMV resistance (Guiu-Aragonés et al., 2014). Later on, the DHL92 derived from this collection was used to generate the melon reference genome sequence (Garcia-Mas et al., 2012).

The mapping populations have been genotyped using different molecular markers to allow the construction of genetic maps used for QTL analysis.

4.3 Melon reference genome

In 2012, the melon reference genome sequence was published using the homozygous DHL92 line applying the whole-genome shotgun strategy based on 454 pyrosequencing technology. Finally, a 375 Mb assembled genome containing 1,594 scaffolds and 29,865 contigs was obtained. After the transposon annotation and masking the repetitive regions, 27,427 predicted genes were annotated (Garcia-Mas et al., 2012). Recently, the scaffold anchoring (Argyris et al., 2015), assembly and annotation (Ruggieri et al., 2018) have also been improved to get a better melon reference genome.

Apart from the genomic sequence, the melon cytoplasmic genome sequence was also determined. The chloroplast genome had156 Kb, while the mitochondrial genome size was 2.74 Mb (Rodríguez-Moreno et al., 2011).

Based on the melon reference genome, whole genome re-sequencing or genotyping-by-sequencing (GBS) have been also performed. These new cost-effective technology allowed the dissection of the genetics behind disease resistance (Natarajan et al., 2016; Hu et al., 2017), fruit traits (Nimmakayala et al., 2016; Chang et al., 2017) or for genetic variation and genetic structure analysis (Pavan et al., 2017).

4.4 Melon diseases and resistance

Not only melon production but melon fruit quality could be heavily affected by plant pathogens. The plant pathogens that could infect melon plants varied from insects, bacteria, fungi to viruses, being the most important the diseases caused by viruses and fungi.

4.4.1 Insects

The burst of insects always resulted in great losses in melon production. One of the most destructive insect diseases is melon fruit fly, distributed worldwide from Asia, South America, Africa and Australia. Melon fruit fly feeds inside the fruit, sometimes on flower or stems and could cause fruit distortion and also introduce other pathogens which facilitate fruit decomposition. Aphids were also described as another destructive pest, after sap-sucking by aphids, the yield of host plants will be reduced and the nutritional components will be also affected (Hales et al., 1997). Viruses like *Watermelon mosaic virus* and *Cucumber mosaic virus* (Raccah et al., 1985) are transmitted by aphids. Hence, it's of great importance to identify the resistant genes. The *Vat* gene confers resistance to aphid infection in different melon lines, and has been widely used in plant breeding programs (Chen et al., 1997; Klingler et al., 2001; Boissot et al., 2010).

4.4.2 Fungi and bacteria

Melon diseases such as fusarium wilt, powdery mildew and downy mildew caused by fungi and bacteria could also produce severe infections. Fusarium wilt is one of the most devasting diseases in melon production. This disease is difficult to control because *Fusarium oxysporum* f.sp. *melonis* is a soil-borne pathogen and can keep its viability for a few years. Four *F. oxysporum* f.sp. *melonis* races (race 0, 1, 2, and 1.2) were reported to cause melon wilt

symptoms. Several resistance genes have been found conferring resistance to different races. The dominant resistant gene *Fom-1* confers resistance to race 0 and race 2 (Risser, 1973; Brotman et al., 2013). *Fom-2* confers resistance to race 0 and race1 (Risser et al., 1976; Joobeur et al., 2004). More recently, some minor QTLs, together with a major QTL that correlated with *Fom-2*, were found contributing to the resistance to race 1 (Branham et al., 2018). The aggressive strain race 1.2 can overcome the resistance conferred by *Fom-1* and *Fom-2*. Some melon lines showed partial resistance to some strains of race 1.2, with polygenic control of the resistance (Perchepied and Pitrat, 2004; Perchepied et al., 2005) and some epistatic effects functioning in the resistance (Chikh-Rouhou et al., 2011). The genetics and mechanism of resistance to powdery mildew and downy mildew was also described in different melon lines (McCreight et al., 1987; Epinat et al., 1992; Perchepied et al., 2005; Fukino et al., 2008; Zhang et al., 2013; Ning et al., 2014; KT, 2016).

4.4.3 Virus

Several virus species like *Watermelon mosaic virus* (WMV), *Zucchini yellow mosaic virus* (ZYMV), and CMV can infect melon plants. Until now, all the resistant materials found in melon belong to subspecies *agrestis*. The Indian melon line PI 414723 was resistant to some viruses including ZYMV. The resistance to ZYMV was described to be controlled by the dominant gene *Zym* (Pitrat and Lecoq, 1984). Melon genotype TGR-1551 restricts WMV infection and this resistance was controlled by one major QTL in LG XI and some other minor QTLs (Palomares-Rius et al., 2011). Among all the plant viruses, CMV was found to cause 50% production losses when melon plants are infected in the early stage, before flowering (Alonso-Prados et al., 1997). However, only few resistant melon lines were described as resistant to CMV (Diaz et al., 2003).

Five oriental cultivars, Yamatouri, Miyamauri, Mawatauri, Sanuki-shirouri, and Shinjong, confer resistance to the Indonesian isolate CMV-B2 (Daryono et al., 2003). Some other melon genotypes, like SC, and Freeman's cucumber were resistant to some CMV pathotypes. Among these reported resistant melon lines, the genetic control and molecular mechanism of Korean accession SC has been studied deeply.

4.4.4 Resistance to CMV in the melon line PI 161375

The Korean accession SC is resistant to most of CMV strains except those of type CMV-Song, which overcome all known resistances (Pitrat and Lecoq, 1980; Diaz et al., 2003). Using a RIL population made between the susceptible genotype ‘Védrantais’ and SC, a major QTL in

LG XII was detected explaining most of phenotypic variation for the resistance to all the CMV strains tested in the experiment. Some minor QTLs were also detected but were strain specific (Dogimont et al., 2000). In a collection of NILs with SC introgressions into PS background, a major QTL in LG XII, named *cmv1*, was mapped within a 5.78 Mb interval and conferred resistance to strains CMV-P9 and P104.82, but not to the strain TL (Essafi et al., 2009). Finally, it was determined to confer resistance to all subgroup II strains, but not to those of subgroup I (Guiu-Aragonés et al., 2015). The *cmv1* acts as a gatekeeper preventing the virus cell-to-cell movement specifically from bundle sheath cells to vascular parenchyma or intermediary cells so that the virus cannot reach the phloem. In susceptible lines, the virus can pass through this barrier to systemically infect melon plants (Guiu‐Aragonés et al., 2016). *Cmv1* was fine mapped to a 132 Kb interval containing three annotated genes. Among them, the Vacuolar protein sorting-associated protein 41 (VPS41) was further validated as the gene conferring resistance to CMV subgroup II strains by using a VPS41 TILLING mutant and VPS41 transgenic melon lines. A deleterious *CmVPS41* mutation among TILLING "Charentais" susceptible plants showed a decrease of susceptibility upon CMV-LS infection. The resistant SC plants transformed with susceptible PS *CmVPS41* were susceptible to CMV (Giner et al., 2017). Furthermore, the movement protein of CMV was found to be the virulence determinant against *cmv1*. When the viruses harbored CMV-LS MP, melon plants containing *cmv1* showed resistance to CMV infection, while they were infected if the virus carried a CMV-FNY MP (Guiu‐Aragonés et al., 2015). Further analysis revealed that four amino acid positions were the only changes between both MPs necessary to overcome the resistance conferred by *cmv1* (Guiu-Aragonés et al, 2015). The subgroup I strain CMV-M6 can overcome *cmv1*-mediated resistance. In a screening inoculating the DHL collection with CMV-M6, Guiu-Aragonés et al, 2014 found two QTLs, *cmvqw3.1* and *cmvqw10.1*, which must work together with *cmv1* to confer resistance against CMV-M6 (Guiu-Aragonés et al., 2014). However, the strain CMV-FNY can still break the resistance conferred together by these three QTLs while SC still shows resistance. Hence, we hypothesize the existence of additional QTL(s) in SC responsible for the resistance to CMV-FNY.

Objectives

The main objective of this PhD thesis is to study the complex resistance mechanism of the melon accession PI 161375 to different CMV stains. To achieve this goal, three specific objectives are addressed:

1. Identification of minor QTL(s) responsible for the resistance to the CMV-FNY strain by using different F_2 populations.

2. Characterization of the resistance mediated by *cmv1*, *cmvqw3.1*, *cmvqw10.1* and additional QTL(s).

3. Identification of the viral factor that determines the virulence of CMV-FNY against the resistance conferred together by *cmv1*, *cmvqw3.1* and *cmvqw10.1*.

Materials and Methods

1 Plant materials

1.1 Melon lines

The Spanish cultivar Piel de Sapo (PS), susceptible to all the CMV (*Cucumber mosaic virus*) strains tested in our experiments, was used as positive control in all the infection experiments. The exotic Korean melon accession PI 161375, cultivar "SongwhanCharmi" (SC), resistant to all the CMV strains tested in our experiments, was used as negative control.

Double haploid lines DHL142, DHL69, DHL2012, DHL1046 (Gonzalo et al., 2005), the introgression line (IL) 20-91-15, and SC were used to produce the different F_2 populations.

ILs 20-91-15 (containing QTLs *cmvqw3.1*, *cmvqw10.1* and *cmv1*), 20-28-62 (containing *cmvqw10.1*and *cmv1*) and 5-123 (containing *cmvqw3.1* and *cmv1*) were used to characterize the resistance mechanisms of different QTLs and for the identification of the determinants of virulence.

All the melon seeds used were treated with 3 g/L captan for 5 min, rinsed thoroughly and soaked in water overnight. Seeds were pre-germinated around 3 days in plates at 28 ℃ with photoperiod of 12 h under light and 12 h in the dark.

For the infection experiments, the seedlings were planted either in a versatile environmental test chamber (MLR-350H, SANYO) or in a horizontal chamber (Fitotronic Version2, Inkoa) under long day condition consisting of 22 ℃ for 16 h with light and 18 ℃ for 8 h in dark throughout the whole infection.

To produce the F_2 generation for the identification of the additional QTL(s), first the seedlings were grown in the greenhouse at CRAG under long day conditions, with 22-24 ºC for 16 h and 20 ºC for 8h until five-leaf-stage and then transferred to the greenhouse in Torre Marimon (Caldes de Montbui, Barcelona). Then, the lines DHL142, DHL69 and SC were crossed with DHL2012, DHL1046 or 20-91-15. Forty-five days after pollination (dap), the melons were harvested to get F_1 seeds. F_1 seeds were germinated and seedlings were transferred to greenhouses at Torre Marimon and self-pollinated to get enough F_2 seeds from each cross for QTL analysis.

1.2 *Nicotiana benthanimana* and zucchini squash

Nicotiana benthamiana plants and zucchini squash (Cu*curbita pepo* L.) Chapin F1 (Semillas Fitó SA, Barcelona, Spain) were grown under long day conditions as described for melon plants at CRAG greenhouses facilities.

2 Viruses

2.1 Viral strains

The CMV strains used in this study were CMV-M6 (Diaz et al. 2003), CMV-FNY (Rizzo and Palukaitis, 1990) and CMV-LS (Rizzo and Palukaitis, 1990). Strains CMV-M6 and CMV-FNY belong to subgroup IA while CMV-LS belongs to subgroup II.

2.2 Viral clones for in vitro transcription and agro-infiltration

Infectious clones suitable for in vitro transcription pLS-CMV1, pLS-CMV2 and pLS-CMV3 of the strain CMV-LS and pFny1, pFny2 and pFny3 of the strain CMV-FNY were provided by Prof. P.Palukaitis (Zhang et al, 1994). Infectious clones pCR1(+), pCR2(+) and pCR3(+), suitable for Agrobacterium-mediated transformation, were provided by Dr. Kim Kook-Hyung, from Seoul National University (Seo et al., 2009). For the strain CMV-M6, M6.1 and M6.2 are cloned into pGEM®-T, for in vitro transcription, and M6.3 is cloned in the binary vector pGREEN II (Guiu-Aragonés, 2014).

Clones pLS-CMV1, pLS-CMV2, pLS-CMV3, pFny2, pFny3and M6.2 were transformed in competent cell DH5□. Clones M6.1 and pFny1 were transformed in competent SURE cells. The binary constructs pCR1(+), pCR2(+), pCR3(+) and M6.3 were transformed in Agrobacterium GV3101 for agroinfiltration.

3 Bacterial strains

The *E.coli* strains and the genotype of each strain are listed in Table M-1. The *A.tumefaciens* strains used were GV3101/pSOUP and C58C1, both resistant to tetracycline and rifampicin.

Table M-1. *E. coli* strains and their genotypes

E. coli Strain	Genotype
DH5α	F– Φ80lacZΔM15 Δ(lacZYA-argF) U169 recA1 endA1 hsdR17 (rK–, mK+) phoA supE44 λ– thi-1 gyrA96 relA1
JM109	endA1recA1gyrA96 thi hsdR17 (rk–, mk+) relA1 supE44 Δ(lac-proAB) [F´ traD36, proAB, laqIqZΔM15]
10β	Δ(ara-leu) 7697 araD139 fhuA ΔlacX74 galK16 galE15 e14- Φ80dlacZΔM15 recA1 relA1 endA1 nupG rpsL (StrR) rph spoT1 Δ(mrr-hsdRMS-mcrBC)
Stbl4	mcrA Δ(mcrBC-hsdRMS-mrr) recA1 endA1 gyrA96 gal-thi-1 supE44 λ- relA1 Δ(lac-proAB)/F' proAB+lacIqZΔM15 Tn10 (TetR)
SURE	e14– (McrA–) Δ(mcrCB-hsdSMR-mrr)171 endA1 supE44 thi-1 gyrA96 relA1 lac recBrecJsbcCumuC::Tn5 (Kanr) uvrC [F' proAB lacIqZΔM15 Tn10 (Tetr)]

4 Virus Inoculations

4.1 Sap inoculation

Viral inocula were freshly prepared by grinding the new leaves of infected either zucchini squash or *N. benthamiana* in 0.2% diethyl dithiocaremate of sodium (DIECA) buffer in the presence of active carbon, to disrupt more efficiently the cells. The sap was then rub inoculated on the cotyledons of 7 to 10 day old melon plants previously sprayed with silicon carbide (Carborundum). When necessary, the virus was inoculated to fully expanded first new leaves of 14 to 16 day old melon plants. For this, around 1 g of infected tissue from infected zucchini squash was homogenized in 10 ml 0.2% DIECA buffer. Then, 50 µl of homogenized sap was mechanically inoculated on the first leaves previously sprayed with Carborundum.

4.2 Agro-infiltration and viral RNA inoculation

To generate pseudo-recombinant viruses by using binary vectors or in vitro transcription clones, mixed inoculations were applied on 3-leaves-stage *N. benthamiana* plants. Agrobacteria were first induced for 1 to 2 h in the induction buffer and then agroinfiltration was performed in the underneath of the leaves. When combining agroinfiltration and in vitro transcription for a particular combination, forty-five minutes after the agroinfiltration, in vitro transcribed RNAs were inoculated on the same infiltrated leaves. When *N. benthamiana* plants showed systemic infection symptoms, the newly infected leaves were used to produce sap to inoculate the cotyledons of 7 to10 day old melon plants.

5 DNA isolation

5.1 Genomic DNA extraction

100 mg of young leaves were harvested and grinded to fine powder in liquid N_2 in 1.5 ml eppendorf and then 500 µl of pre-heated Doyle buffer (65 ºC) was added. The samples were kept at 65 ºC for 30 min after vortex. Then 500 µl of chloroform: isoamilalcohol (24:1) was added, mixed and centrifuged at 11,000 rpm for 10 min. The aqueous layer was transferred to a new eppendorf where 500 µl of pre-chilled isopropanol were added, mixed gently and centrifuged at 11,000 rpm for 5 min. The supernatant was removed and the pellet was cleaned by adding 200 µl of 75% ethanol, and centrifuged at 11,000 rpm for 3 min. The supernatant was removed and the pellet was air dried at room temperature. The pellet was re-suspended in 50 µl of milli-Q H_2O. Finally, 1 µl of RNase was added to remove RNA contamination. An agarose gel was run to confirm the quality and quantity of extracted DNA. All the DNAs were stored at -20 ºC for further use.

5.2 Genomic DNA extraction for re-sequencing melon lines

One to three grams of melon young leaves were collected and grinded to fine powder in liquid N_2 and homogenized in 7.5 ml/g pre-warmed CTAB buffer. Equal volume of chloroform-isoamylalcohol (24: 1) were added, mixed and centrifuged for 20 min at 3,000 rpm. Upper layer was taken and mixed with 2/3 of the volume of pre-chilled isopropanol, followed by 5 min centrifuge at 2,000 rpm. After removing the isopropanol, the pellet was cleaned with 10 ml washing buffer and dissolved in 1 ml TE buffer. Later, DNA was treated with 50 µg/ml RNase for 1 h at 37 ºC and purified with phenol-chloroform-isoamylalcohol method and dissolved in

200 ml TE buffer. The integrity was assessed by gel electrophoresis and the quantity was checked using Qubit fluorometric quantification system (Thermo Fisher Scientific, Inc.). Five µg of DNA were used for re-sequencing.

5.3 Plasmid DNA extraction

E. coli strains were cultured at 37 ºC in L medium in the presence of the appropriate antibiotic. Agrobacterium was grown at 28 ºC in the same medium. Then the plasmid extraction was performed with the GeneJET Plasmid Miniprep Kit (Thermo Fisher Scientific, Inc.) according to manufacturer's instructions. The quality and quantity of plasmid was assessed using Nanodrop and agarose gel electrophoresis.

6 RNA isolation

6.1 Total RNA extraction using Tri-Reagent

The plant tissues were collected and grinded to fine powder in liquid N_2 in 1.5 ml eppendorf. Then, the powder was homogenized in the presence of 1 ml TRI Reagent (TRI Reagent® RNA Isolation Reagent, Sigma), followed by adding 200 µl of chloroform and vortexed for 15 s. After leaving the mixture at room temperature for 2 to 15 min, samples were centrifuged 15 min at 14,000 rpm at 4 ºC. Then, the supernatant was transferred to an RNase free tube, precipitated with 500 µl isopropanol and washed with 500 µl of 75% ethanol. The pellet was dissolved in 50 µl RNase free H_2O. Finally, DNA contamination was eliminated using TURBO DNA-free™ Kit (Thermo Fisher Scientific, Inc.) according to manufacturer's instructions. All the RNAs were stored at -80 ºC for further use.

6.2 Total RNA extraction using Plant mini kit

To get high quality RNA for qRT- PCR, RNeasy Plant Mini Kit (Qiagen) was used. This method was used for RNA extraction from melon petioles. Around 100 mg petioles were collected and grinded in liquid N_2. RNA was extracted following manufacturer's instructions. After the extraction, the quality and quantity of RNA was checked using Nanodrop and agarose gel.

7 Introgression lines re-sequencing

Re-sequencing of the ILs 20-91-15, 20-28-62 and 5-123 was performed using HiSeq2000 Illumina paired-end sequencing (2 × 125). The bioinformatic analysis was done in collaboration

with Dr. Kostantinos Alexiou, the bioinformatician of the Genetics and Genomics Vegetable Crops group at CRAG. The pipeline used for re-sequencing analysis was SUPER pipeline as described by Sanseverino *et al.* (2013).

The resulting sequences were mapped to the newer version of the melon genome v3.6.1 (https://www.melonomics.net/melonomics.html). General filtering was performed by fulfilling the criteria with bi-allelic sites, SNPs only. Minimum depth was set to 6, minimum genotype quality to 30, minimum SNP quality to 30, minimum count for alternative allele to 2. A chromosome 0 was also defined for sequences not belonging to any chromosome. The re-sequencing data of each IL was then compared with the genome of PS and SC to determine the genotype origin of ILs.

8 In vitro transcription

Infectious clones pLS-CMV1, pLS-CMV2 were linearized with *Not*I and *Hind*III, respectively. Infectious clones pLS-CMV3, M6.1 and pFny1 were linearized with *Pst*I. RNAs were generated from 1 µg of linearized plasmid by using T7 mMESSAGEmMACHINE® in vitro transcription kit (Ambion, Thermo Fisher Scientific, Austin, USA).

9 Plasmid construction

RNA1 and RNA2 from CMV-M6 were cloned in the binary vector pSNU1. M6-RNA1 was amplified from the construct pGEM-6.1 (Guiu-Aragonés, 2014) using Phusion Green High-Fidelity DNA Polymerase, with primer pair M6_1&2_Gibson-1F (gttcatttcatttggagagggGTTTATTTACAAGAGCGTACG) and M6_1_Gibson-3'R (gcgtgagctcggtaccgTGGTCTCCTTTTAGAGACC). M6-RNA2 was amplified, using the same DNA polymerase, with primer pair M6_1&2_Gibson-1F and M6_2_Gibson-3'R (gcgtgagctcggtaccgTGGTCTCCTTTTGGAGG). As vector, the construct pCR3(+), which contains the RNA3 from CMV-FNY cloned into pSNU1, was digested with EcoRI and BamHI to release the viral sequence. The digested fragment and PCR amplicons were then gel-purified by using High Pure PCR Product Purification Kit (Roche, Germany). DNA assembly was performed by using NEBuilder® HiFi DNA Assembly Cloning Kit according to the manufacturer's instructions. The assembled products of M6.1 were transformed in E. coli strains 10β and Stbl4, the late one, optimized for transformation of unstable fragments. The assembled

products of M6.2 were transformed in *E. coli* strains DH5α and JM109. The colonies were confirmed by colony PCR using primer pair M6.1-2650F (GATGTTGTACCGCTTGTGCGTT) and pCR3V-R (CGGCAACAGGATTCAATCTTA) for RNA1, and primer pair M6.2-2500F (GTATGGTGGAGGCGAAGAACG) and pCR3V-R for RNA2. Plasmids from positive colonies were extracted as described above. For analysis of the clones, triple enzyme digestion with *PstI*, *SalI* (TAKARA) and *XmaI* (Biolab) was applied for M6.2 constructions. Double enzyme digestion with *XbaI* and *SacI* (TAKARA) was performed for M6.1 constructions. After confirmation by enzymatic digestion, the constructs were sequenced. The correct constructs were then transformed into Agrobacterium strain C58C1 and stored at -80 ℃ for further use.

10 Virus detection

10.1 ELISA (Enzyme-Linked Immuno Sorbent Assay)

To confirm virus infection, young leaves (around 100 mg) of infected and non-infected melon plants were harvested and homogenized in the extraction buffer and then the homogenized solution was tested using DAS-ELISA (double antibody sandwich enzyme-linked immunosorbent assay). DAS-ELISA was performed as described by Essafi et al. (2009) using the polyclonal antiserum (Loewe Biochemica GmbH, Otterfing, Germany) which recognizes the coat protein (CP) of CMV-LS, CMV-M6 and CMV-FNY. The sample will be considered as infected if the value of ELISA is two times greater than that of non-inoculated samples.

10.2 Visual phenotyping

To identify minor QTLs, viral infection symptoms were recorded every day from 6-7 dpi until 19-26 dpi with different methods:

a) The infection scale was classified into 6 degrees varying from 0 to 5 according to the severity of symptoms (Guiu-Aragonés et al., 2014).

b) The infection was recorded as a qualitative trait, where 1 was assigned for infected plants (any severity degree from 1 to 5), and 0 for the plants that do not show any symptom.

c) In order to have a estimation of the progress of the infection, the Area Under the Symptom Progress Curve (AUSPC) (Shaner and Finney, 1977) was applied with the following formula:

$$\mathrm{AUSPC} = \sum_{i=1}^{n} [(S_i + S_{i+1})/2](t_{i+1} - t_i)$$

Where S_i is the symptom intensity at the date t_i, in days.

10.3 Reverse transcription-polymerase chain reaction (RT-PCR)

To detect virus infection, around 100 mg of leaf samples were used for total RNA extraction. Reverse Transcription was performed after RNA extraction with TRI REAGENT and DNase treatment. First, hybridization of primer-RNA was done with around 1 µg RNA in the presence of 1.54 µM oligo $(dT)_{20}$ in 13 µl final volume at 70 ℃ for 10 min and then in ice for 5 min. Then, cDNA synthesis was carried out in the presence of 200 U PrimeScript Reverse Transcriptase (TAKARA, Japan), 40 U RNaseOUT™ Recombinant Ribonuclease Inhibitor (Invitrogen), 454.5 µM dNTPs , 4 µl of 5× PrimerScript buffer in a final volume of 22 µl and incubated at 50℃ for 1 h to synthesize the cDNA. The PCR reaction was performed in 20 µl final volume containing 1x NH_4 reaction buffer, 0.2 mM dNTPs, 2.5 mM $MgCl_2$, 0.5 µM forward primer, 0.5µM reverse primer, 1.5 U BIOTAQDNA polymerase (Bioline) and 2 µl cDNA. The reaction was performed on S1000 thermal cycler (Bio-Rad) with a denaturation cycle at 94 ℃ for 2 min, followed by 35 cycles of 94 ℃ for 30 s, annealing for 1 min, and 72 ℃ for 2 min and a final extension at 72 ℃ for 5 min was followed. The annealing temperature was calculated with the formula $Tm = 4\times N_{(G+C)}+2\times N_{(A+T)}-5$. The primer pair used to detect CMV-FNY was F109-400F (CCTTCATCAGGTCTGCGG) and F109-1400R (TTTCCAAGTTGTTCGTACTTC) or primer pair F109-900F (TTCATCAACGAGTCTACTATG) and F109-2000R (GGATCAACGGTAAAGTACG). The primer pair to detect CMV-LS was LS1-1F (GTTTTATTTACAAGAGCGTACG) and LS1-1400R (GAAGCATTCCACATATCGTAC). The primer pair used to detect ZYMV-AGII was pAG68F (GACAAAGAAGATGACAAAGGG) and pAG68R (GCATTGTATTCACACCTAGCA).

10.4 Real time quantitative RT-PCR (qRT-PCR)

The CMV-FNY accumulation in the petioles of inoculated leaves from different melon lines was measured by using qRT-PCR. For each melon line, at least 3 biological replicates were processed. The petioles were collected and grinded in liquid N_2 for RNA extraction as indicated before. Reverse transcription was performed as described above, except for the RNA quantity that was decreased to 300 ng. Real-time PCR was done on LightCycler® 480 Instrument by

using SYBR Green I Master (Roche, Germany). The reaction system was as follows: 1× SYBR Green I Master, 0.5 µM forward primer, 0.5µM reverse primer, 2 µL cDNA and PCR-grade H_2O to 20 µL final volume. The amplification protocol consisted of an initial step at 95 °C for 10 min, and 45 cycles of 95 °C for 10 s and 60 °C for 30s. The primers to detect virus accumulation were designed with Primer3, version 4.1.0 (http://primer3.ut.ee/) based on the movement protein region of CMV-FNY (Table M-2). The presence of secondary structure was checked with Oligo Calculator version 3.27 (http://biotools.nubic.northwestern.edu/OligoCalc.html).

Table M-2. Primers designed for qRT-PCR

Primer name	Sequence 5'-3'	nt
MP_M6FNYqPCR_1F	CATATCGCAGCTGGGAAGAC	20
MP-M6FNYqPCR-1R	CAAATATTGCGAAGATTCAATGT	23

The primer specificity was tested by PCR amplification and agarose gel electrophoresis. Intra-assay variation was evaluated by performing technical triplicates with all the amplifications. Cp values were calculated using LightCycler® 480 (Roche Life Science) software. A five point standard curve, using different cDNA dilutions from 1:1, 1:5, 1:25, 1:125 to 1: 625, was performed to check amplification efficiency of different primer pairs. The efficiency was calculated as reported by (Saladié et al., 2015). The relative amount of viral specific expression was determined using cyclophilin (CmCYP7) (Saladié et al., 2015) as reference housekeeping gene and then normalized to mock inoculated PS expression.

11 Data analysis

All the statistical analysis and figures of qRT-PCR were performed using R software (R version 3.4.1). ΔΔCt values, representing relative virus accumulation of each biological replicate of all the analyzed melon lines were visualized in boxplots or one dimensional scatter plots by using "Boxplot" function or "stripchart" function. To calculate the significance between each two variables among several individuals, "shapiro.test" function was first applied analyzing whether the data had a normal distribution or not. If the data was normally distributed, one-way ANOVA was applied to assess if significant differences exists between group means. If so, the

significance value of each comparison was determined using Tukey's honestly significant difference (HSD) post hoc test. If the data was not normally distributed, Kruskal-Wallis test was applied to check if significant differences exist between group means. If so, Dunn test post hoc test was applied to obtain the significance value of each comparison. To check whether the differences between relative virus accumulation in proximal and distal petioles in the same line were significant, two-tailed t-test was applied as normality was assumed for our biological replicates.

12 Genotyping

12.1 SNP genotyping (single-nucleotide polymorphism)

SNP primers were designed by using PrimerPicker (KBioscience 2009) based on the SNPs validated by Illumina Assay Design Tool (ADT) (Argyris et al., 2015). Flanking sequences, including SNPs, were submitted to the software obtaining two forward allele-specific primers and one reverse common primer. Finally, a 48×48 SNP assay was run on the Fluidigm platform at the Genomics service at CRAG. The genotype data were obtained by using Fluidigm SNP Genotyping Analysis Software. The detailed information of SNP markers used is listed in Table S10.

12.2 SSR (Simple Sequence Repeat)

According to the genotypes of resistant and susceptible parental lines, polymorphic SSR maker ECM116 (Fernandez-Silva et al., 2008) was selected to fill the gap in LG X where the SNPs were not polymorphic or did not work well. SSRs were amplified by primers flanking the repetitive sequences, being one of the primers labeled with IRD-800(MWG Biotech AG, Ebersberg, Germany). The amplification product was then visualized by LICOR IR2 sequencer (Li-cor Inc, Lincoln, New England, USA).

12.3 CAPS (Cleaved Amplified Polymorphic Sequences)

CAPS makers PS-15-H02 and PS-40-E11 (Deleu et al., 2009) were also selected in linkage group X. For marker PS-15-H02, PCR amplification was firstly performed including 1x NH_4 reaction buffer, 0.5 mM dNTPs, 2 mM $MgCl_2$, 0.4 μM primer Ce307-F (TGAGTACAAGTTCGTCATTCGACA), 0.4 μM primer Ce307-R (CATTTGATGCAGAGTTGATCACAG), 1.5 U BIOTAQDNA polymerase (Bioline), 2 ng/μl genomic DNA in 25 μl final volume. The reaction was performed on S1000 thermal cycler (Bio-

Rad) with a denaturation step at 96 ℃ for 2 min, followed by 35 cycles of 96 ℃ for 30 s, 56 ℃ for 30 s, and 72 ℃ for 1.5 min. A final extension at 72 ℃ for 5 min was followed. After amplification, PCR products were digested with the enzyme *Alu*I (TAKARA). In the case of marker PS-40-E11, PCR amplification was performed with the reaction system including 1x NH_4 reaction buffer, 0.1 mM dNTPs, 2.9 mM $MgCl_2$, 0.4 μM primer w331 (TATCACGTGCCAGACGACAT), 0.4 μM primer w332 (TTGACCTCCCCGTCACTAAC), 2.5 U BIOTAQDNA polymerase (Bioline), 2 ng/μl genomic DNA, 0.5 μl DMSO to a final volume of 25 μl. The reaction was performed on S1000 thermal cycler (Bio-Rad) with a denaturation at 94 ℃ for 2 min, followed by 35 cycles of 94 ℃ for 20 s, 58 ℃ for 20 s, and 72 ℃ for 30 s, followed with a final extension at 72 ℃ for 5 min. The PCR products were also digested with the enzyme *Alu*I (TAKARA).

To differentiate RNA1, RNA2 and RNA3 between CMV-FNY and CMV-M6, CAPS markers were also developed based on the sequence of the two viral strains. For RNA1, PCR amplification was done by using primer pair F109-3'R (TGGTCTCCTTTTAGAGACCC) and F109-3000F (GTACTGTGGTGTATTGAACG) and plasmids pGEM-M6.1 for CMV-M6 and pFny1 for CMV-FNY. For RNA2, PCR amplification was done by using primer pair F209-3'R (TGGTCTCCTTTTGGAGGC) and F209-2200F (GAATGTCTCAGTCGTGTATC) and plasmids pCR-M6.2 for CMV-M6 and pCR2(+) for CMV-FNY. For RNA3, PCR amplification was done by using primer pair F309-3'R (TGGTCTCCTTTTGGAGGCC) and F309-1600F (TTCGAGTTAATCCTTTGCCG), and plasmids pGREEN-M6.3 for CMV-M6 and pCR3(+) for CMV-FNY. PCR amplification was performed with the reaction system including 1x NH_4 reaction buffer, 0.2 mM dNTPs, 1.5 mM $MgCl_2$, 0.5 μM forward primer, 0.5 μM reverse primer, 1.5 U BIOTAQDNA polymerase (Bioline) and 0.4 ng/μl plasmid or H_2O. The PCR reaction was performed on S1000 thermal cycler (Bio-Rad) with a denaturation step at 94 ℃ for 2 min, followed by 35 cycles of 94 ℃ for 30 s, 55 ℃ for 30 s, and 72 ℃ for 30 s, followed with a final extension at 72 ℃ for 5 min. PCR products of RNA1, RNA2 and RNA3 were digested with *Dde*I, *Bst*XI and *Xho*I respectively. These CAPS markers were later used to confirm the origin of each RNA in recombinant viruses made between CMV-M6 and CMV-FNY.

13 Genetic map construction

The genetic map was constructed using the JoinMap 4.1 software (Stam, 1993). Linkage groups were calculated using a LOD score of 10, the regression mapping algorithm and the Kosambi's function. The rest of parameters were set as default.

14 QTL analysis

The QTL mapping was performed with MapQTL® 6 (VanOoijen and Maliepard, 1996). QTL analysis was performed by Interval Mapping and non-parametric Kruskal-Wallis test. A QTL was considered as significant when LOD (logarithm of odds) values were higher than 2 or had a significance level $P \leq 0.01$.

15 Sanger sequencing

All Sanger sequencing was performed at CRAG by using the technology *ABI 3730 DNA Analyzer* (Applied Biosystems) for capillary electrophoresis and fluorescent dye terminator detection.

Results

Part I QTL analysis for resistance to the aggressive CMV-FNY strain

A screening of our DHL population showed that the resistance to the CMV subgroup I strain M6 requires the presence of *cmv1* acting together with the QTLs *cmvqw3.1* and *cmqw10.1*(Guiu-Aragonés et al., 2014). However, further analysis showed that some double haploid lines, resistant to M6, did not carry either *cmvqw10.1* (DHL1046 and DHL140), or *cmvqw3.1* (DHL1123). This suggests that although *cmvqw3.1* and *cmvqw10.1* are necessary to confer resistance to CMV-M6, they can be substituted by other QTLs present in the parental genotype SC. This unidentified QTLs would be present in DHLs 1046 and DHL140, substituting for *cmvqw10.1*, and in DHL 1123 substituting for *cmvqw3.1*. Hence, it is of great importance to understand the genetics of this complex resistance and to elucidate all the QTLs involved to manage the resistance in a breeding program.

I.1 Screening for CMV-FNY resistance

To check this hypothesis, the 12 DHLs, resistant to CMV-M6 found by Guiu-Aragonés et al (2014) were evaluated for CMV-FNY resistance. The parental genotype SC was used as a negative control, while the susceptible genotype PS was used as a positive control. The infection assay of each DHL was performed with six biological replicates. At 14 dpi, the susceptible control PS showed mosaic symptoms in all leaves while the resistant control SC did not show any infection symptom.

Among those screened DHLs, only two, DHL142 and DHL69 (Figure R1-1), showed resistance, while the other ten lines, were susceptible (Table R1-1). Five out of six DHL142 plants were asymptomatic, while one of them was infected with only mild mosaic in firstly developed leaves and the newly developed leaf recovered from infection. Four out of six DHL69 plants were also symptomless, whereas two were infected. The infection was also confirmed by DAS-ELISAas described in Material and Methods (section 10.1). Both DHL69 and DHL142 harbor *cmv1, cmvqw3.1, cmvqw10.*1. However, they performed differently upon CMV-FNY infection. DHL142 is resistant whereas DHL69 is moderately resistant, which indicates that they contain different additional QTLs conferring CMV-FNY resistance.

Table R1-1. Screening of the 12 CMV-M6-resistant DHLs against CMV-FNY

	cmv1	*cmvqw3.1*	*cmvqw10.1*	Resistance to FNY
DHL29	SC	SC	SC	S
DHL41	SC	SC	SC	S
DHL46	SC	SC	SC	S
DHL69	SC	SC	SC	r (4/6)
DHL85	SC	SC	SC	S
DHL128	SC	SC	SC	S
DHL142	SC	SC	SC	R(6/6)
DHL2012	SC	SC	SC	S
DHL140	SC	SC	PS	S
DHL1046	SC	SC	PS	S
DHL1123	SC	PS	SC	S
DHL135	SC	PS	SC	S
SC	SC	SC	SC	R
PS	PS	PS	PS	S

Note: First column indicates DHLs and controls. 2nd, 3rd and 4th rows indicate the allele of QTLs *cmv1, cmvqw3.1* and *cmvqw10.1* respectively. SC indicates the allele from the resistant line SC and PS indicates the allele from the susceptible line PS. The last row indicates the resistance or susceptibility to CMV-FNY of each melon line. “S”, “r” and “R” mean susceptible, moderately resistant and fully resistant, respectively. The numbers in the brackets indicate the number of resistant plants against the total number of plants evaluated.

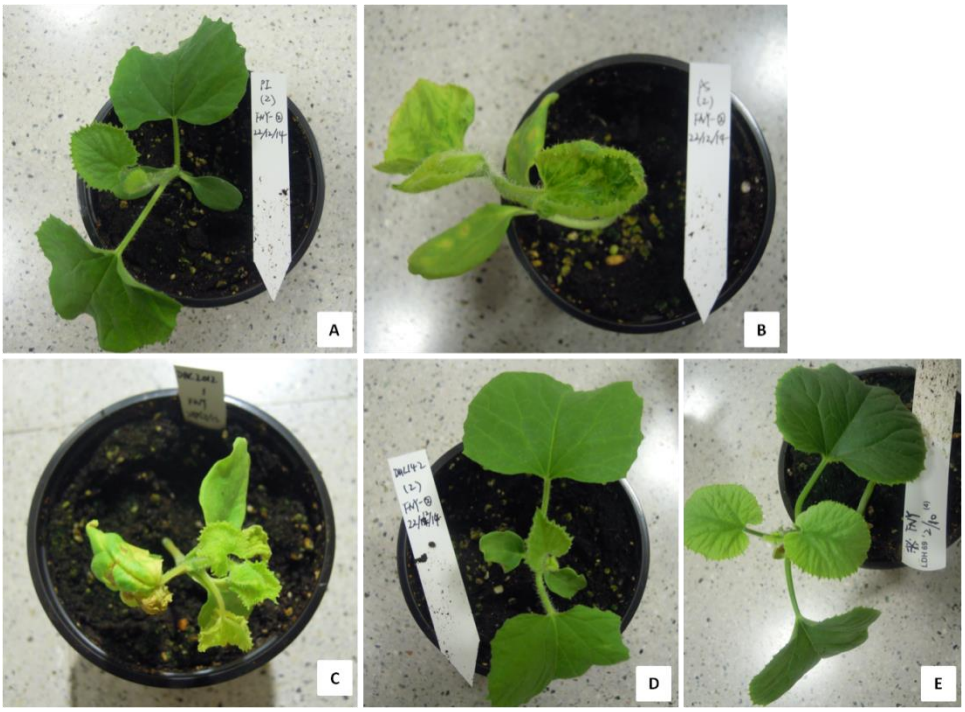

Figure R1-1. Phenotype of melon line upon CMV-FNY inoculation. A) Resistant genotype SC;B) Susceptible genotype PS; C) Susceptible DHL2012; D) Resistant DHL142 and E) Resistant DHL69 .

I.2 Production of F_2 populations

In order to identify additional QTLs responsible for the resistance to CMV- FNY, eight F_2 populations were produced between different susceptible and resistant melon lines. The F_2 populations produced are listed in Table R1-2. The F_2 populations were done by crossing the corresponding lines, with no attention to the direction of the cross, and then self-pollinating the F_1. In this thesis work finally, four F_2 populations were used for the QTL analysis: those obtained from the crosses between DHL142 x DHL2012, DHL69 x DHL2012, DHL142 x 20-91-15 and DHL142 x DHL1046.

Table R1-2. F_2 populations generated by crossing resistant and susceptible parental lines

Line	DHL2012	DHL1046	20-91-15
DHL142	√	√	√
DHL69	√	√	√
SC	√	√	-

Note: "√" indicates that the F_2 population between the two corresponding melon lines was developed. "-" indicates that it was not developed. 20-91-15 is a melon introgression line harboring three QTLs: *cmv1, cmvqw3.1* and *cmvqw10.1* (see Results part II).

I.3 QTL analysis with the F_2 population made from the cross DHL142 x DHL2012

I.3.1 Phenotypic analysis of CMV-FNY resistance

The infection of F_2 population from the cross DHL142 x DHL2012 was performed in two versatile environmental test chambers as described in Material and Methods (section 4.1). In total, 78 F_2 individuals were inoculated with CMV-FNY. Six SC plants and six DHL142 plants were inoculated as negative controls. Six PS plants were inoculated as positive controls. Two PS, two SC and two DHL142 plants were left as non-inoculated controls. The infection degree of both individuals and controls were scored at 6 dpi, 9 dpi, 12 dpi, 13 dpi and 19 dpi, with symptoms severity scoring from "0" to "4".

The systemic infection of PS started at 6 dpi, while none of the DHL142 and nearly none of the SC showed any infection symptom. One out of six inoculated SC plants, showed typical mosaic on the first two leaves but it was recovered at the third leaf. Among the F_2 population, four individuals started the infection at 6 dpi while the rest of the population did not show any visible infection symptom at this time (Table R1-3). As the infection progressed, more individuals were infected with higher infection degree. At the end of the experiment, i.e. 19dpi, 44.87% individuals were symptomless, while 55.13% of the population showed different

infection degrees. The segregation test of non-infected against infected plants in this population did not agree with any Mendelian inheritance model for one or two genes (Chi-square test). It should be noted that 20 individuals were infected with strong mosaic, and their growth was compromised.

Table R1-3. Infection degrees of the F_2 population from the cross DHL142 x DHL2012 at different days post inoculation with CMV-FNY

Infection degree	6dpi	9dpi	12dpi	13dpi	19dpi
0	74	66	50	45	35
1	0	3	12	15	11
2	2	4	6	1	5
3	2	2	2	8	7
4	0	3	8	9	20

Note: The first column indicates the infection degrees from “0” to “4”. Fist rowindicates therecorded time points. The numbers in the cells indicate the number of infected plants under a certain infection degree at a certain time point.

The infection was later confirmed using DAS-ELISA at the end of the experiment. The distribution of ELISA value among individuals was shown in Figure R1-2B. The plants with ELISA value bigger than two times that of non-inoculated plants were considered as infected, and the others were considered as non-infected. No clear correlation (correlation factor = 0.743) was observed between the ELISA determined infection and visible observed infection or between the ELISA value and the infection degrees (correlation factor = 0.703). Therefore, ELISA was not performed in the following experiments.

The AUSPC value of each individual, which could be a simulation factor that represents the whole infection process, was calculated according to the equation (in Material and Methods 10.2) and presented in Figure R1-2. The smaller the values are, the more resistant the plants are, and vice versa. The AUSPC value of SC, DHL142 and PS were 4.75, 0 and 50.5 respectively. Among all the individuals, the average AUSPC value was 11. More than half of the individuals

had the value smaller than 10. The minimum AUSPC value was 0 (as SC) while the maximum value was 50.5 (as PS). The median among all the individuals was 3.

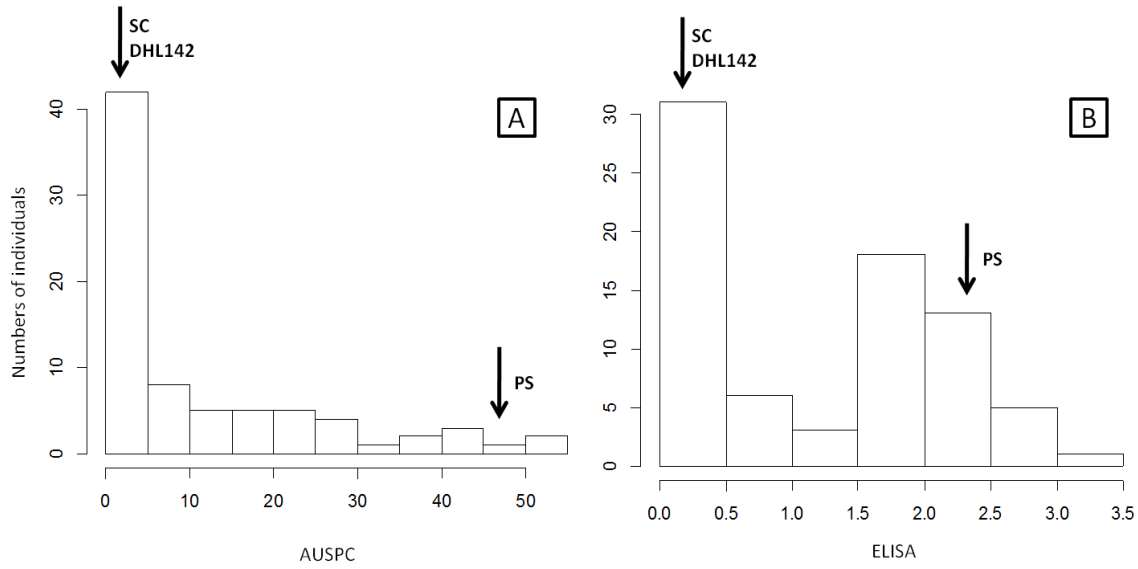

Figure R1-2. A) The AUSPC value and B) DAS-ELISA value among the F_2 individuals. The arrows indicate the corresponding values of PS, SC and DHL142.

I.3.2 Genotyping and construction of genetic map

The DHL population had previously been genotyped by 892 markers (Michael Bourgeois, personal communication) Therefore, we knew which regions were shared by the two DHL and which regions were not. Using these data, the segregating profile between DHL142 and DHL2012 was obtained and represented in a map chart (Figure R1-3) using GGT 2.0 software (van Berloo, 2008). Some polymorphic and monomorphic markers between DHL142 and DHL2012 were selected to define the polymorphic areas. From these defined polymorphic areas, a total of 33 SNP markers were selected to genotype the F2 population (underlined in Figure R1-3). No markers were selected in LG I and LG XI as there were only small polymorphic areas between DHL142 and DHL2012. The alleles of DHL142 in those regions were from PS, which indicated that it was unlikely that the additional QTLs were located in those regions. The results of the KASPAR genotyping for the 78 individuals with 33 markers are shown in Table S1.

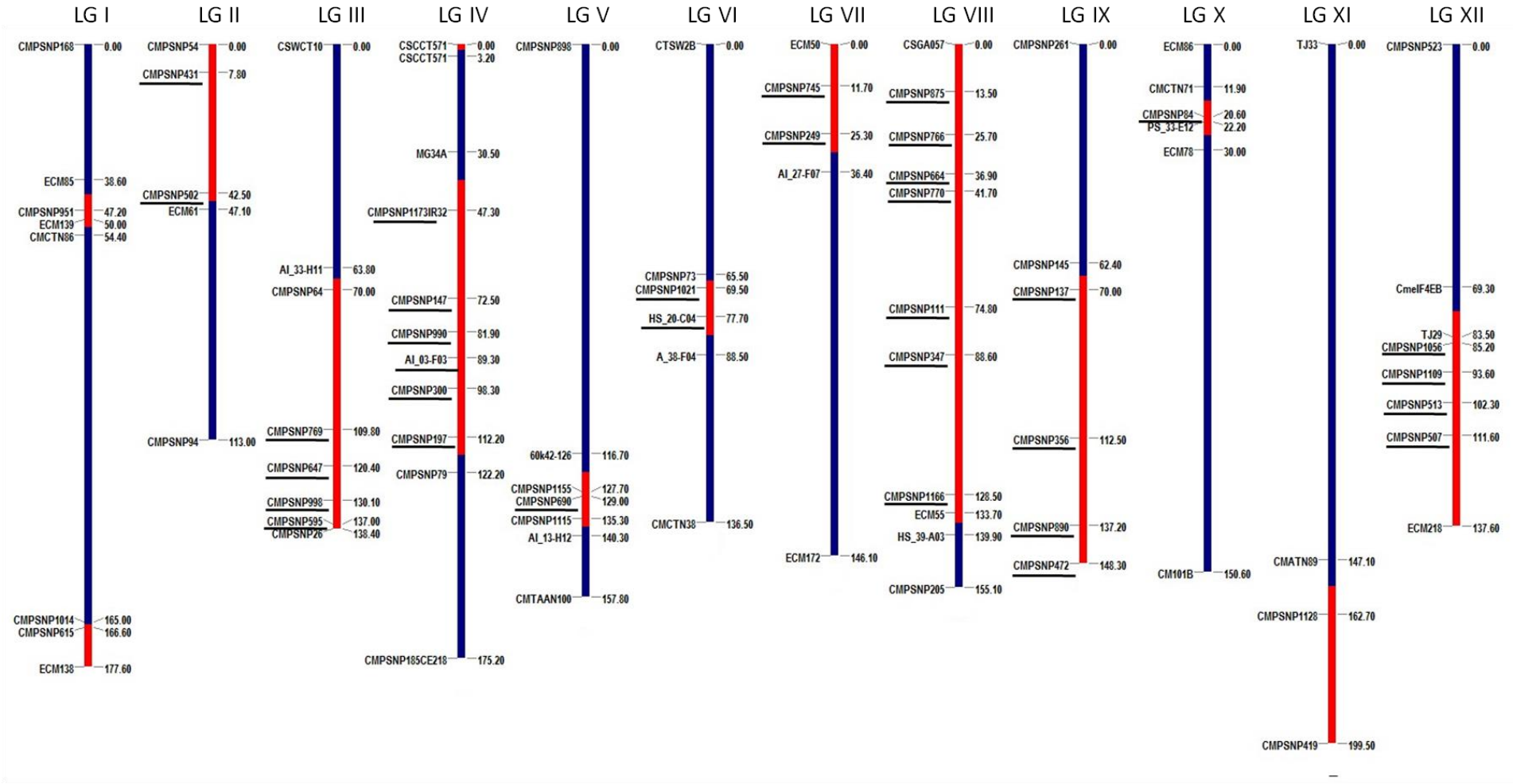

Figure R1-3. Map chart used to select polymorphic markers for the population F_2 made from the cross DHL142 x DHL2012. Each bar represents one linkage group. The names of makers are on the left side of the bar and the genetic distance of the makers on the right. Bar in red color indicates the polymorphic regions between DHL142 and DHL2012 while in blue indicates that this region is monomorphic. The underlined markers were selected for genotyping and QTL analysis.

The genetic map was constructed using JoinMap 4.1 as described in Material and Methods (section 13). The data used were the genotypic data of 78 F_2 individuals with 33 polymorphic SNP markers. In total, 10 LGs were constructed (Figure R1-4). Since LG V and LG X have only one maker, they are not included in the figure.

In total, the map spanned a distance of 287.7cM with an average distance of 9.3 cM between two markers. The maximum distance was 23.1 cM between markers CMPSNP137 and CMPSNP356 in LG IX. The minimum distance was 2.2 cM between markers AI_03-F03 and CMPSNP990 in LG IV.

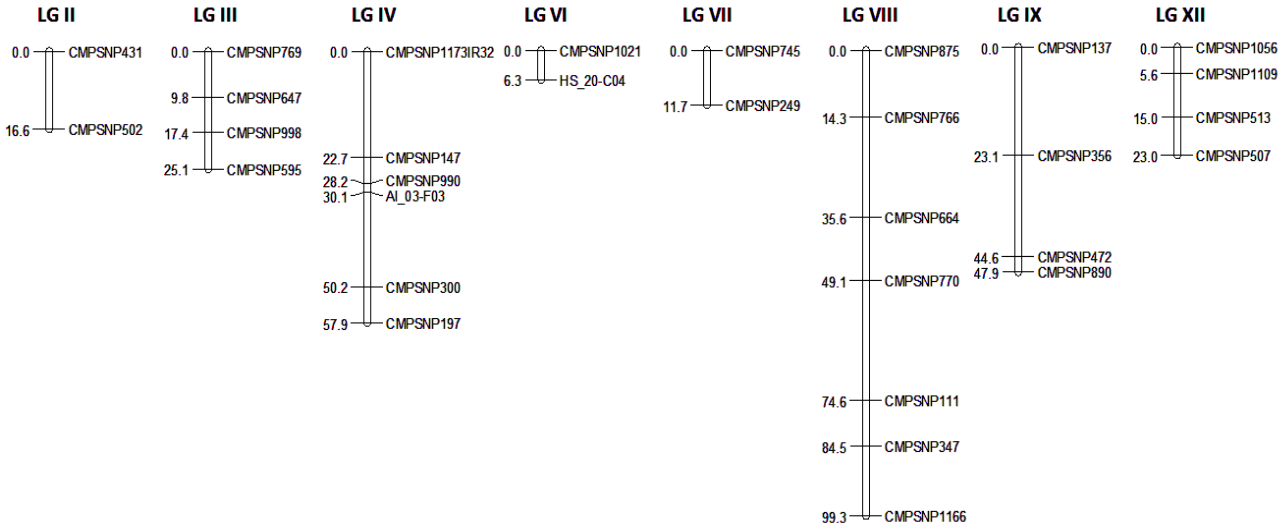

Figure R1-4. Genetic map of the F_2 population made from the cross DHL142 x DHL2012 defined using 33 SNP markers and 78 individuals. Each bar represents one linkage group. The name of the makers are shown on the right side of the bar and the numbers on the left are their genetic position of each marker in cM.

I.3.3 QTL analysis

QTL analysis was performed using all the phenotyping data (Table S5) obtained, including the infection degree at 6, 9, 12, 13 and 19 dpi, the calculated AUSPC value, or the ELISA value. The QTL analysis was performed as described in Material and Methods (Section 14).

We defined a threshold of LOD 2 (for the interval mapping (IM) analysis) or level of significance $p \leq 0.001$ (for non-parametric Kruskal-Wallis (KW)) test to consider a putative QTL.

After the analysis, no LOD value bigger than 2 was found in this population for any of the phenotypic data evaluated. The biggest LOD value obtained was 1.85, corresponding to the marker CMPSNP147 in LG IV, for the infection degree at 12 dpi. In the KW test, we observed a $P \leq 0.01$ for CMPSNP147 and also the same value for the marker CMPSNP300 in LG IX, in this case correlated with the ELISA data. Since the LOD and KW values were so low, we did not consider any of the QTLs as putative QTLs for CMV-FNY resistance. Moreover, they were not consistent for at least two different phenotypic data.

The same experiment was repeated using another set of 40 F_2 individuals and a QTL analysis was performed merging the data of both experiments to increase the number of individuals evaluated from 78 to 118. However, no significant QTLs were obtained in both, independent and merged, analysis.

Table R1-4. QTL analysis for the resistance to CMV-FNY from the cross DHL142 x DHL2012.

	LG	Marker	Test statistics	
			LOD	KW
12 dpi	IV	CMPSNP147	1.85	*K* 6.03 (**)
ELISA	IX	CMPSNP300	1.62	*K* 7.33 (**)

The significance of Kruskal-Wallis test is presented using "*", where ** to $P \leq 0.01$.

I.4 QTL analysis with the F_2 population made from the cross DHL142 x IL 20-91-15

The IL 20-91-15 harbors three resistant QTLs, *cmv1, cmvqw3.1* and *cmvqw10.1,* introgressed from SC in the genetic background of PS. Therefore if contains much less SC background than DHL2012 and there will be less background noise during QTL analysis using an F_2 population produced between DHL142 and IL 20-91-15 than between DHL142 and DHL2012.

I.4.1 Phenotypic analysis of CMV-FNY resistance

A population of 120 F_2 individuals was tested for CMV-FNY susceptibility or resistance. Three SC plants and three DHL142 plants were inoculated as negative controls. Three plants from each line 20-91-15, PS and the F_1 hybrid DHL142 x IL 20-91-15 were inoculated as positive controls. The phenotype of this infection assay was recorded from 7to23 dpi. All three PS started showing mild infection from 7 dpi and became severely infected at 13 dpi. One of 20-91-15 plants showed infection at 7 dpi, and the other two plants were infected at 13 dpi and 18 dpi, respectively. Finally, all the IL 20-91-15 plants resulted with a severe infection degree of 4 or 5. One of F_1 hybrid was infectedat7 dpi while the other two were infected later but finally all the F_1 hybrid plants were heavily infected. Few mosaic spots were observed in SC, but the plants recovered without any systemic symptom. One out of three DHL142 were heavily infected at 13 dpi, while the other two did not show any infection symptom until the end of the experiment.

Overall, the infection in this F_2 population showed heavier infection symptoms than the F_2 population made from the cross DHL142 x DHL2012 tested before. In this population, the infection points at 7, 13, 18 and 23 dpi were selected representing different infection stages (Table R1-5). Some individuals started showing infection symptomsat7 dpi, while 107 out of 120 (89.17%) plants were symptomless. More plants showed infection symptoms at 13 dpi. Later on, when the infection progressed, the number of infected plants as well as the infection degree increased. At the end of the infection assay, only 5.8% of the population was absent of any infection symptom. Considering all the plants with infection degree 0 to be not infected, and infection degree from 1 to 5 to be infected, the ratio of non-infected versus infected plants was 7:113, which fits the mendelian inheritance model of two recessive genes (chi-square test, ****).

Table R1-5. Infection degree of the F_2 population made from the cross DHL142 x IL 20-91-15 at different days post inoculation with CMV-FNY

Infection degree	7 dpi	13 dpi	18 dpi	23 dpi
0	107	45	16	7
1	7	29	19	1
2	3	24	23	6
3	3	8	30	11
4	0	11	17	65
5	0	3	15	30

The first column indicates the infection degrees from “0” to “5”. Fist row indicatesthe recorded time points. The numbers in the cells indicate the number of infected plants under a certain infection degree at a certain time point.

The AUSPC value was calculated as described in Material and Methods (Section 10.2). The distribution of the AUSPC among all the individuals is presented in Figure R1-5. The average AUSPC value for all the individuals was 29.86 with most of AUSPC values distributed from 20 to 50. The minimum AUSPC value was 0 while the maximum value was 70, and the median was 28.5.

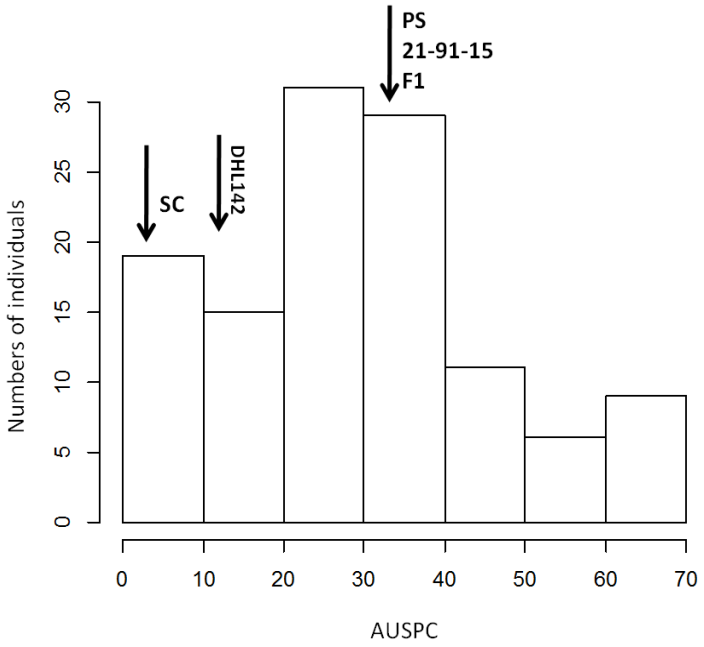

Figure R1-5. AUSPC distribution of the F_2 population made from the cross DHL142 x IL 20-91-15.The X axis indicates the AUSPC value and Y axis indicates the number of plants at AUSPC value.The arrows indicate the AUSPC values of the control lines.

I.4.2 Genotyping and construction of genetic map

A map chart based on the polymorphisms between IL 20-91-15 and DHL142 was drawn as described before in section 3.2. Within the polymorphic regions, 39 markers were selected for genotyping the F_2 population (underlined in Figure R1-6). No marker was selected in LG I because the small polymorphic region in LG I does not segregate between DHL142 and DHL2012 (susceptible) (see section 3.2), which indicates that the additional QTL should not be there. Also, no marker was selected in LG XI as no polymorphism existed between DHL142 and IL 20-91-15 in this LG. Among the 39 polymorphic markers designed, four markers, CMPSNP1021 from LG VI, CMPSNP111from LG VIII, CMPSNP1056 and CMPSNP 1109 from LGXII were discarded because they do not segregate as expected. The other 35 markers worked correctly in the Fluidigm genotyping platform and could differentiate genotypes among F_2 individuals. The genotyping data of the 120 F_2 individuals generated by 35 SNP markers were finally used to construct the genetic map (Figure R1-6 and Table S2).

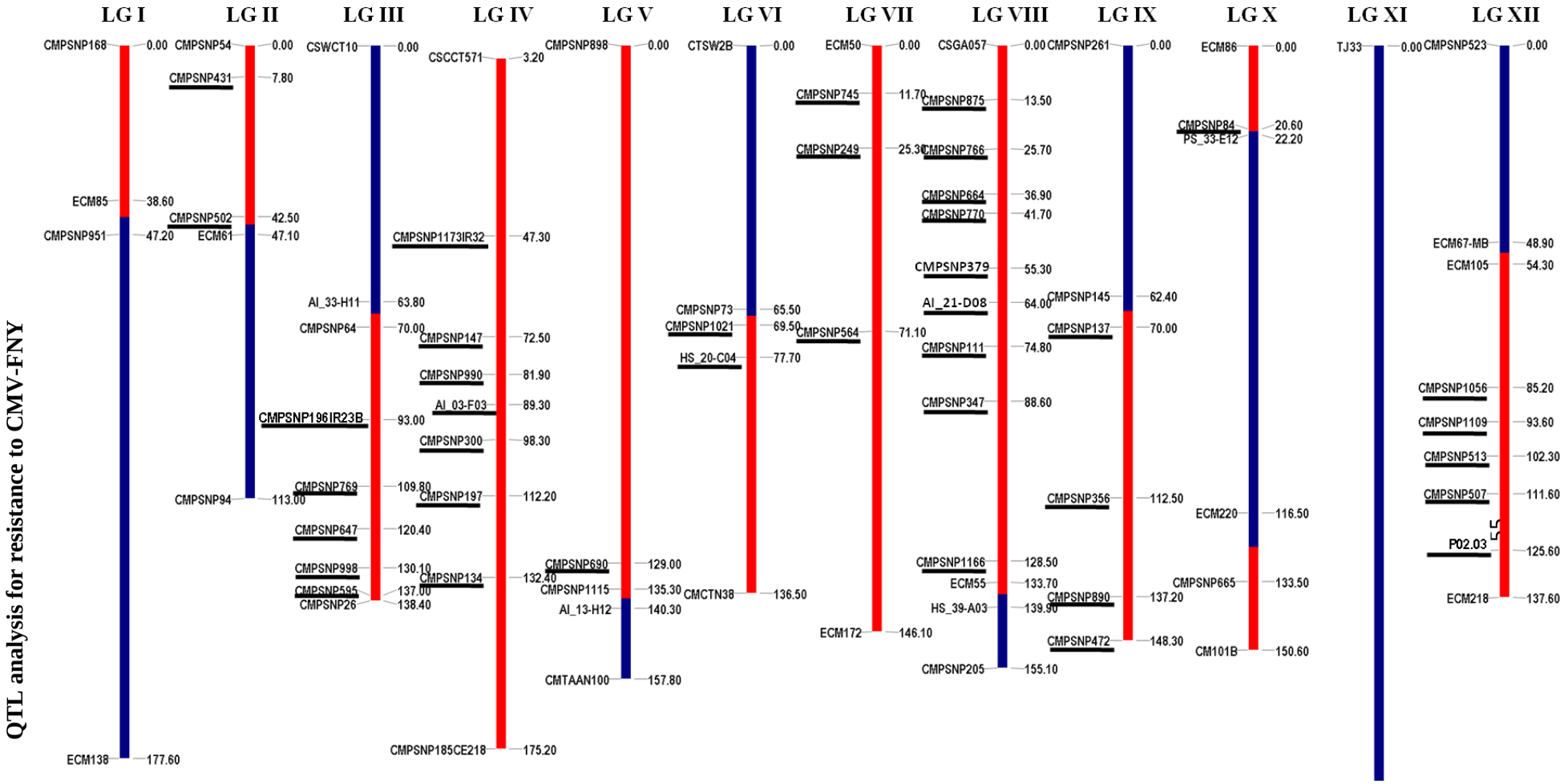

Figure R1-6. Map chart used to select polymorphic markers for the F_2population made from the cross DHL142 x 20-91-15. Each bar represents one linkage group. The names of the makers are on the left side of the bar and the genetic distance of the makers, on the right. Bar in red color indicates the polymorphism between DHL142and 20-91-15 while in blue indicates a monomorphic region . The underlined markers were selected for genotyping and QTL analysis.

The genetic map contained seven LGs (Figure R1-7). In total, the map covered 418.1 Cm of distance with an average distance of 11.9 cM between two markers. The maximum distance was 44.3 cM between markers CMPSNP347 and AI_21-D08 in LG VIII. The minimum distance was 2.2 cM between markers CMPSNP890 and CMPSNP472 in LG IX.

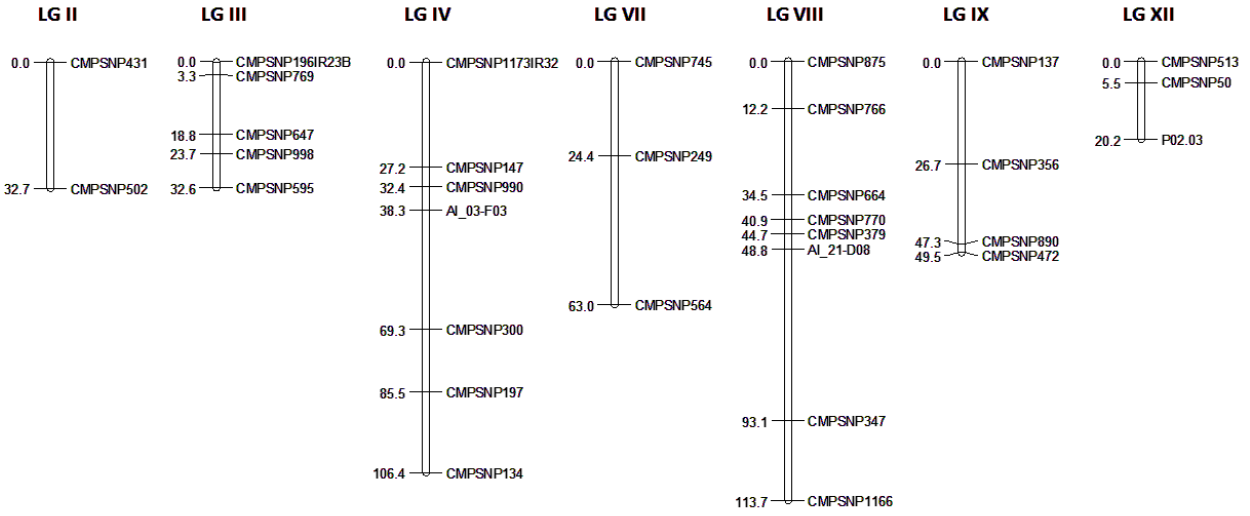

Figure R1-7. Genetic map the of F_2 population made from the cross DHL142 x IL 20-91-15 defined using 35 SNP markers and 120 individuals. Each bar represents one linkage group. The name of the makers is shown on the right side of the bar and the numbers on the left are their genetic position in cM.

I.4.3 QTL analysis

The QTL analysis was performed combining the genotypic data and all the phenotypic data (Table S6) including the infection degree at different days post inoculation and the AUSPC value using MapQTL® 6. All the LOD values bigger than 2 in the IM analysis, or significance with a $P \leq 0.001$ in the KW test are presented in Table R1-6. QTL analysis using the infection degree at 14, 15 and 16 dpi showed one putative QTL in LGXII correlated with the marker P02.03. With KW test, it also showed significance at 20dpi.

Another putative QTL was found using the qualitative data "infected versus non-infected" plant, associated with the SNP marker CMPSNP502 in LG II, with a LOD value of 2.80 and P ≤ 0.0001 (Table R1-6).

The result of QTL analysis using the phenotypic trait AUSPC did not show any significant LOD value.

Table R1-6. QTL analysis for the resistance to CMV-FNY from the cross DHL142 x IL 20-91-15. LOD values >2 for infection degree at different dpi (14, 15, 16 and 20 dpi), and "infected versus non-infected" (Y/N) phenotype.

	LG	Markers	Statistic test	
			LOD	KW
14 dpi	XII	P02.03	2.07	8.34 (**)
15 dpi	XII	P02.03	2.26	9.36 (***)
16 dpi	XII	P02.03	2.22	9.36 (***)
20 dpi	XII	P02.03	ns	9.82 (***)
Y/N	II	CMPSNP502	2.80	11.29 (****)

The significance of Kruskal-Wallis test is presented using "*", where * equal to $P \leq 0.05$, ** to $P \leq 0.01$, *** to $P \leq 0.001$, **** to $P \leq 0.0001$. "ns" indicates non significant value.

I.5 QTL analysis with the F_2 population from the cross DHL69 x DHL2012

I.5.1 Phenotypic analysis of CMV-FNY resistance

Two PS, two SC, three DHL69 and three DHL2012 plants and 80 F_2 individuals were inoculated with CMV-FNY. All the PS started showing infection from 7 dpi and finally were heavily infected with severe typical mosaic. DHL2012 started showing infection two days later than PS but finally resulted fully infected, with small and curling plants. One out of three inoculated DHL69 plants was infected 17 dpi with mild symptoms. One out three SC was infected with mild mosaic in first two leaves at 10 dpi, but finally recovered without any

infection symptom. The infection degree of the 80 F_2 individuals was recorded at different days post inoculation (Table R1-7).The infection started around 7 dpi in some F_2 individuals. At this time, most plants (62 out of 80) did not show visible infection symptoms. At 10 dpi, almost 75% were infected with visible symptoms. At the end of the experiment, 19 dpi, only eight plants (10%) were not infected. The segregation of non-infected versus infected plants was 8:72, which does not fit the mendelian inheritance model for one or two genes (chi-square test).

The AUSPC value of the F_2 population is presented in Figure R1-8. The AUSPC values of the resistant lines DHL69 and SC were 2.3 and 6.6, respectively, while the values of the susceptible lines DHL2012 and PS were 47.5 and 48 respectively. The average AUSPC value of the population was 25.6. The minimum AUSPC value was 0 and the maximum value was 58.5. The median among all the individuals was 27.

Table R1-7. Infection degree of the F_2 population made from the crossDHL69 x DHL2012 at different days post inoculation with CMV-FNY

Infection degree	7 dpi	10 dpi	11 dpi	12 dpi	13 dpi	14 dpi	17 dpi	18 dpi	19 dpi
0	62	23	20	16	15	15	9	8	8
1	10	25	23	20	16	10	9	8	6
2	4	14	5	7	6	10	11	12	12
3	3	11	18	14	14	17	16	10	12
4	1	3	9	16	15	13	18	24	25
5	0	4	5	7	14	15	17	18	17

The first column indicates the infection degrees from “0” to “5”. The fistrow indicates the recorded time points. The numbers in the cells indicate the number of infected plants under a certain infection degree at a certain time point.

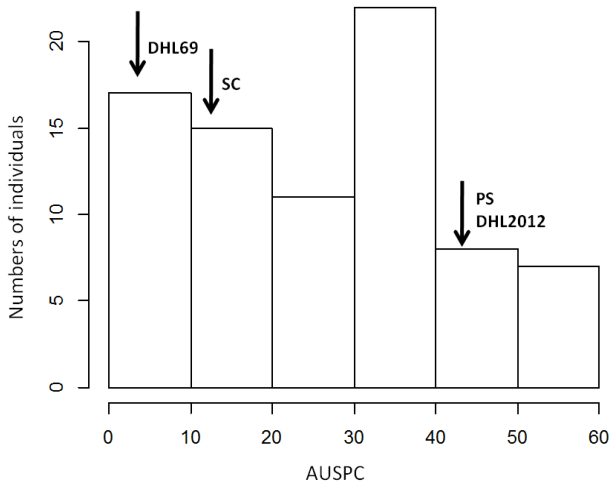

Figure R1-8. AUSPC distribution of the F_2 population made from the cross DHL69 x DHL2012. The X axis indicates the AUSPC value and Y axis indicates the number of plants at AUSPC value.The arrows indicate the AUSPC value of the control lines.

I.5.2 Genotyping and construction of the genetic map

A map based on the polymorphisms between DHL69 and DHL2012was constructed as described in section 3.2 to define the interesting polymorphic regions (Figure R1-9). With this information, 37 polymorphic markers (underlined in Figure R1-9) were selected across different linkage groups. Although polymorphic areas exist in LG VI and LG XI as shown in the map, any marker was selected because the alleles of the resistant parental DHL69 in these polymorphic areas are from PS. Only one marker was selected for each one of the small polymorphic regions of LG V and LG X, respectively. One marker was also selected for LG VII even the whole chromosome is PS allelic in DHL69. The selected markers were later used for genotyping (Table S3), map construction and QTL analysis.

The genetic map was obtained with the genotypic data of 37 markers and 80 F_2 individuals (Figure R1-10). In total, the map covered 286.9 cM with an average distance 8.7 cM between two markers. The maximum distance was 41.1 cM between markers CMPSNP173 and CMPSNP320 in LG IX. The minimum distance was 0 cM between marker CMPSNP379 and CMPSNP770 in LG VIII.LG I was separated into two pieces, LG1-1 and LG1-2, because of the high recombination rate between markers CMPSNP484 and CMPSNP521 in this F_2 population.

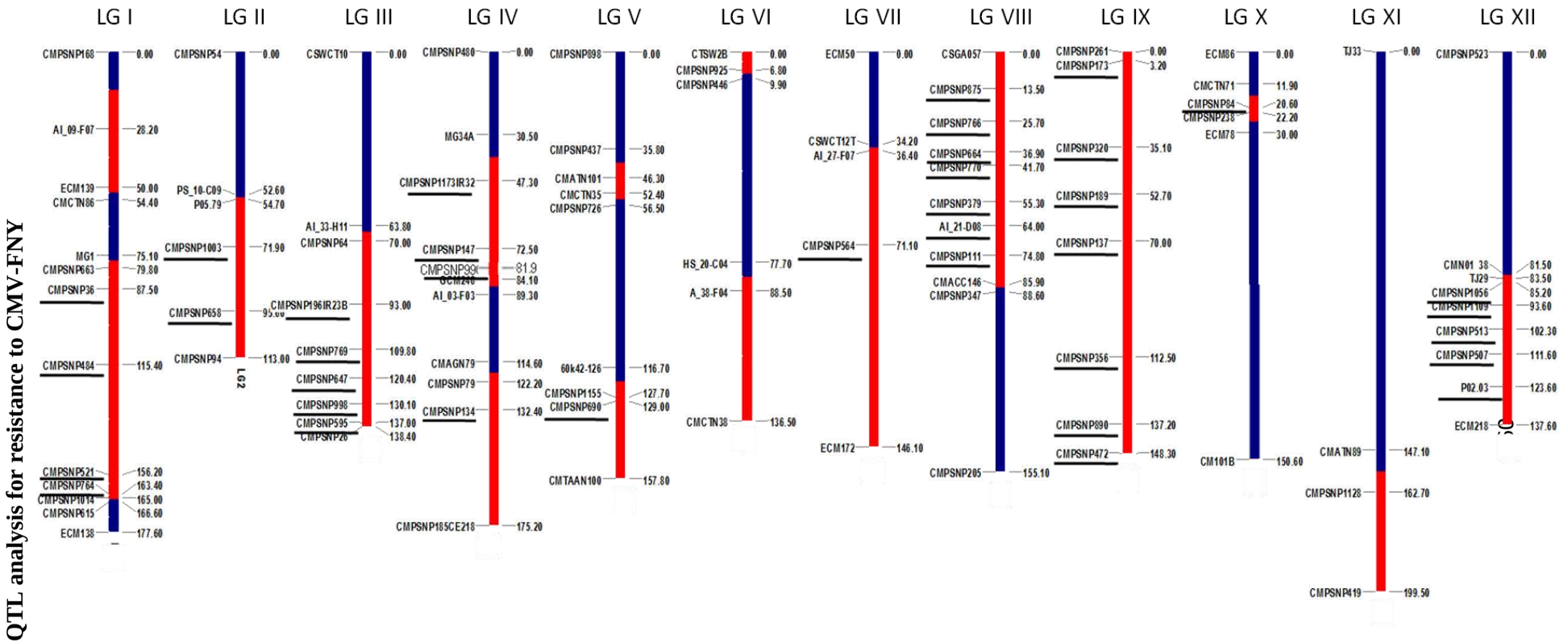

Figure R1-9. Map chart used to select the polymorphic markers for the F_2population made from the cross DHL69 x DHL2012. Each barrepresentsone linkage group. The names of the makers are on the left side of the bar and the genetic distance of the makers on the right. Bar in red color indicatesthe polymorphic regions between DHL69 and DHL2012, while in blue color indicates the monomorphic regions. The underlined markers were selected for genotyping and QTL analysis.

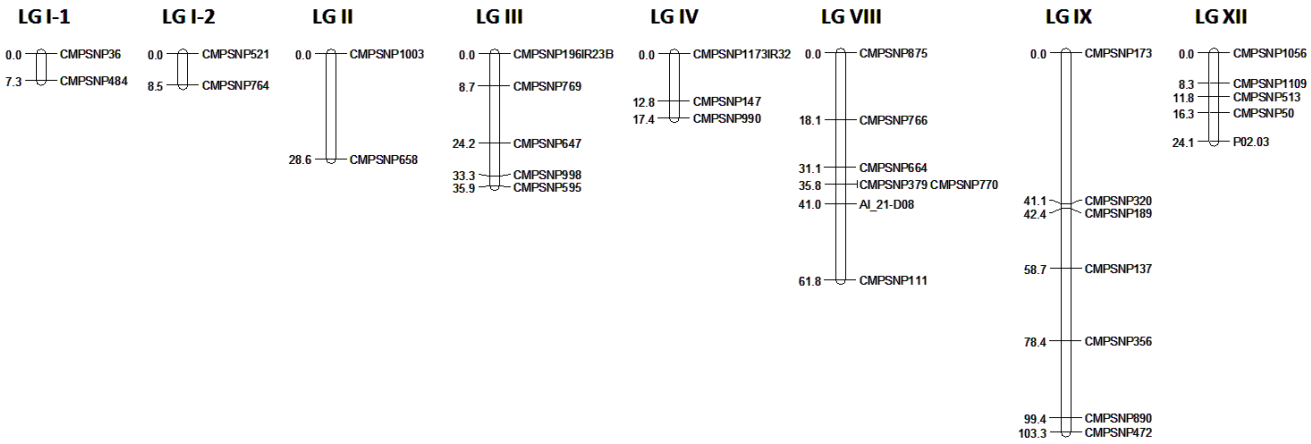

Figure R1-10. Genetic map of the F_2 population made from the cross DHL69 x DHL2012 defined using 37 SNP markers and 80 individuals. Each bar represents one linkage group. The name of the makers are shown on the right side of the bar and the numbers on the left correlate with the genetic position of each marker in cM.

I.5.3 QTL analysis

QTL analysis was performed combining genotypic data with all the phenotypic data (Table S7). The QTL analysis that resulted in LOD values bigger than 2 or KW significance $P \leq 0.001$ are shown in Table R1-8. QTL analysis using infection degrees at 17 and 18 dpi showed one putative QTL in LG IX correlated with marker CMPSNP137 with LOD value 2.15 for the IM test. Another putative QTL was observed in LG X from the KW test, associated with the marker CMPSNP84 for the infection trait at 11 dpi, and with qualitative phenotyping at the end of the assay considering the plants as infected or not infected.

Any other putative QTL was detected using the AUSPC data.

Table R1-8. QTL analysis for the resistance to CMV-FNY from the cross DHL69 x DHL2012. LOD values >2 for infection degree at different dpi (11, 17, and 18 dpi), and "infected versus non-infected" (Y/N) phenotype.

	LG	Markers	Statistic test	
			LOD	KW
11 dpi	X	CMPSNP84	ns	9.230 (***)
17 dpi	IX	CMPSNP137	2.15	8.254 (**)
18 dpi	IX	CMPSNP137	2.15	8.288 (**)
Y/N	X	CMPSNP84	2.86	12.008 (****)

The significance of the Kruskal-Wallis test is presented using "*", where ** equal to $P \leq 0.01$, *** to $P \leq 0.001$, **** to $P \leq 0.0001$. "ns" indicates non-significance values.

I.6 QTL analysis with F_2 population made from the cross DHL142 x DHL1046

Since along the previous F_2 populations and corresponding QTL analysis no common significant QTLs were detected, it is reasonable to think that either the phenotypic methods or the genotyping are not working. To test our method, we made a cross where we should detect a QTL already identified, so that, if the method was correct, we could identify it.The melon DHL1046, resistant to CMV-M6 but susceptible to CMV-FNY, contains *cmv1* and *cmvqw3.1*, but not *qwcmv10.1*. The melon DHL142, resistant to both CMV-M6 and CMV-FNY,harbors *cmv1*, *cmvqw3.1* and *cmvqw10.1*. The F_2 population made between DHL142 and DHL1046 should segregate for locus *cmvqw10.1*. Then, this F_2population was chosen for QTL analysis that should detect at least *cmvqw10.1* and perhaps additional minor QTLs.

I.6.1 Phenotypic analysis for CMV-FNY resistance

Eighty F_2 individuals were tested for CMV-FNY resistance. Four PS and four F_1 hybrid (DHL142 x DHL1046) were inoculated as positive controls. Four SC and four DHL142 were inoculated as negative controls. The infection symptom of this population was recorded at 13, 14,

15, 18, 20, 21 and 26 dpi. The results of the infection assay are presented in Table R1-9. Four out of 80 plants had a delay in growth affecting the phenotyping, so they were excluded. At 13 and 14 dpi, around 35% plants did not show infection symptoms. Later on, more plants became infected, with an increase in the infection degree. At the end of the experiment, i.e., 26 dpi, 25% of the plants were healthy without any visible infection symptom. The segregation of resistance to CMV-FNY in this F_2 population was 19: 57 (None infected/ Infected), which did not deviate from the theoretical segregation 1:3 (chi-square test, ****) based on the genetic control by one recessive gene model. Then, this suggests that these two parental lines would share the additional QTL, since the single recessive gene would be *cmvqw10.1*.

Table R1-9. Infection degrees of the F_2 population made from the cross DHL142 x DHL1046 at different days post inoculation with CMV-FNY.

Infection degree	13 dpi	14 dpi	15 dpi	18 dpi	20 dpi	21 dpi	26 dpi
0	29	26	23	19	18	17	19
1	16	18	20	8	6	5	3
2	12	13	11	13	6	6	5
3	12	11	14	17	23	24	10
4	7	8	6	17	17	17	27
5	0	0	2	2	6	7	12

Each number in the table indicates the number of plants in the population infected with a certain infection degree at certain time point.

The AUSPC value of SC and DHL142 was 0 and 9.3, respectively. The value of PS and the F_1 hybrid was 51.5 and 50 respectively. The distribution of AUSPC value of all the individuals is presented in Figure R1-11. The biggest value among the individuals was 63 while the smallest one was 0. The mean and median among the population were 28.76 and 31.75, respectively.

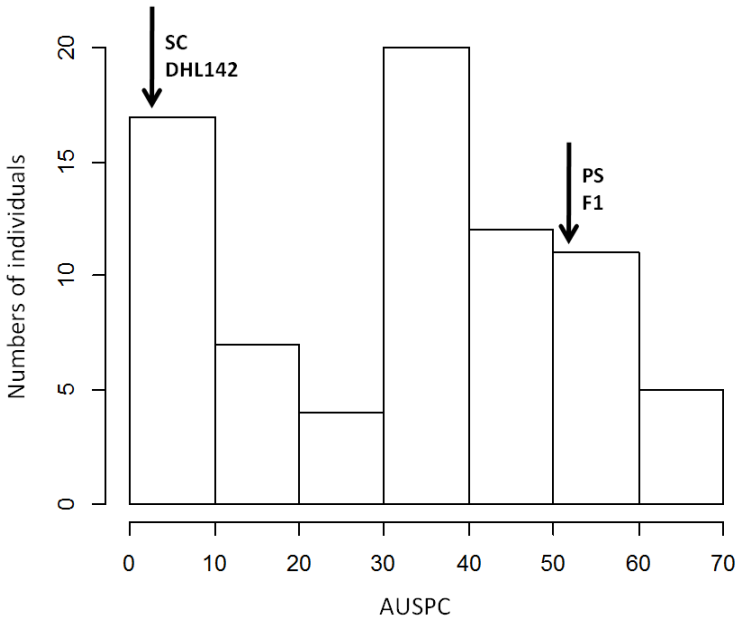

Figure R1-11. AUSPC distribution of the F_2 population made from the cross DHL142 x DHL1046. The X axis indicates the AUSPC value and Y axis indicates the number of individuals under certain AUSPC value ranges. The arrows indicate the AUSPC values of resistant lines DHL142, SC and susceptible lines PS and F_1 hybrid.

I.6.2 Genotyping and construction of genetic map

The polymorphic or monomorphic flanking markers between DHL142 and DHL1046 were selected to define the polymorphic area (Figure R1-12). Forty-eight SNP markers (underlined in Figure R1-12) were selected across 11 LGs. No marker was selected in LG VII because it was not segregating in this population. Only one marker was selected for LG I and LG II, respectively. Forty-one out of 48 SNP markers worked in the Fluidigm platform while the other seven markers CMPSNP1176IR89, CMPSNP183, CMPSNP1117, CMPSNP762, CMPSNP238, CMPSNP671 and CMPSNP456 were excluded as they failed amplifying. In order to fill the gap in LG X where the SNP markers failed, one microsatellite ECM116 and two CAPS markers PS-15-H02 and PS-40-E11 were used to genotype the same populations. Finally, the genotyping data of 80 F_2 individuals based on the 44 markers were used for genetic map construction and QTL analysis (Table S4, Figure S1, S2 and Figure S3).

The generated map is shown in the Figure R1-13. In total, 12 LGs were constructed. The map covered 275.8 cM and the average distance between two markers was 6.3 cM. The maximum

distance was 27.6 cM between marker CMPSNP845 and marker CMPSNP253. The minimum distance was 0 cM between marker CMPSNP65 and marker PS-15-H02. LG X was separated into two pieces because there is high recombination rate between markers PS-40-E11 and ECM116.

I.6.3 QTL analysis

In the QTL analysis, maker CMPSNP113 from LG X had the most significance LOD value (2.40) for IM, and a $P \leq 0.001$ in the KW test, concerning the infection degree at 26 dpi. However, CMPSNP113 is far from the region where QTL *qwcmv10.1* maps. Apart from that, one marker CMPSNP159 in LG IX was found to be significant with LOD value equal to 2.15, corresponding to the trait infected/ non-infected at 26 dpi, where the analysis of KW showed a significance level $P \leq 0.01$ (Table R1-10).

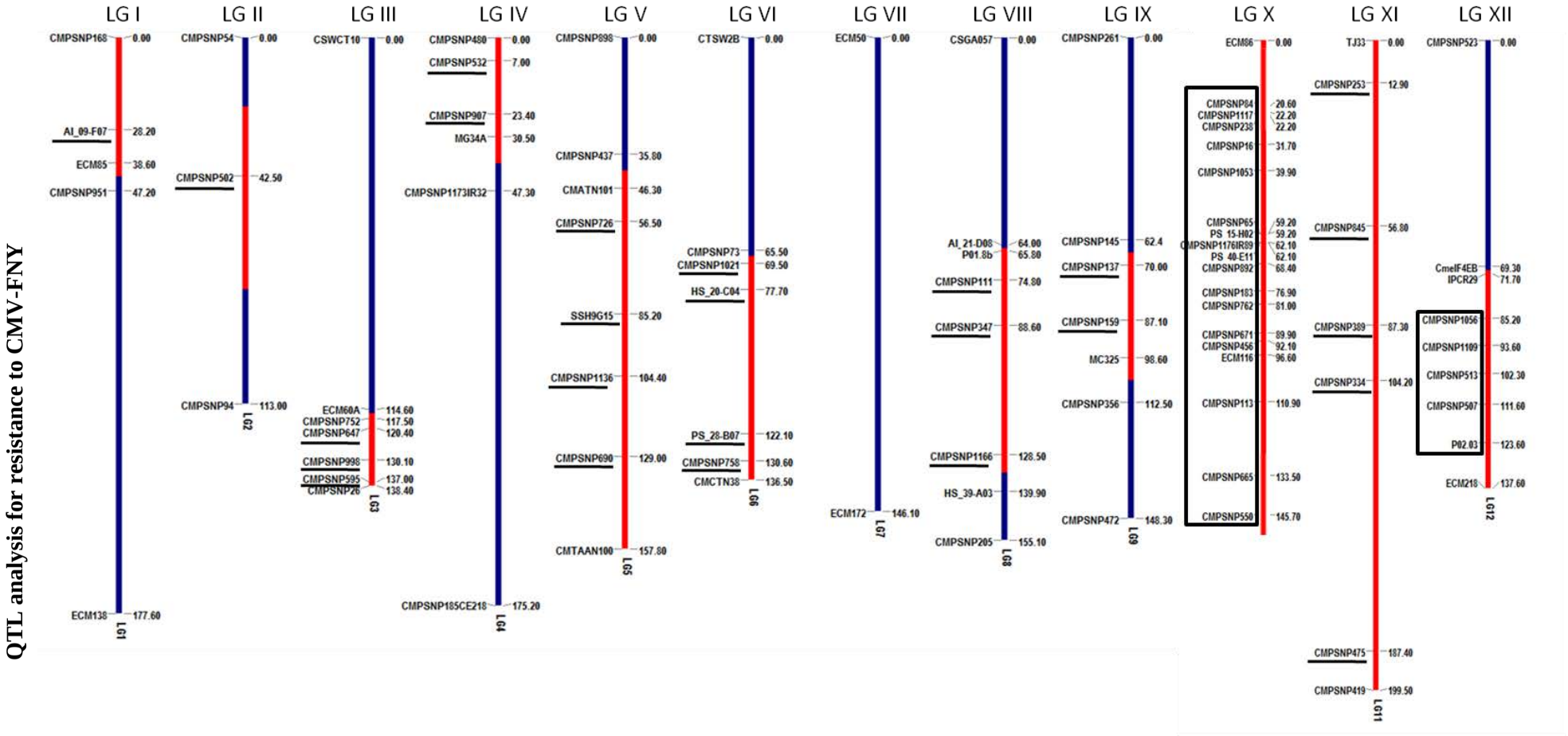

Figure R1-12. Map chart used to select polymorphic markers for the F_2population made from the cross DHL142 x DHL1046. Each barrepresentsone linkage group. The names of the makers are on the left side of the bar and the genetic distance of the makers, on the right. Bar in red color indicatesthe polymorphic regions between DHL142 and DHL1046 while in blue indicates the monomorphic regions. The underlined markers were selected for genotyping and QTL analysis.

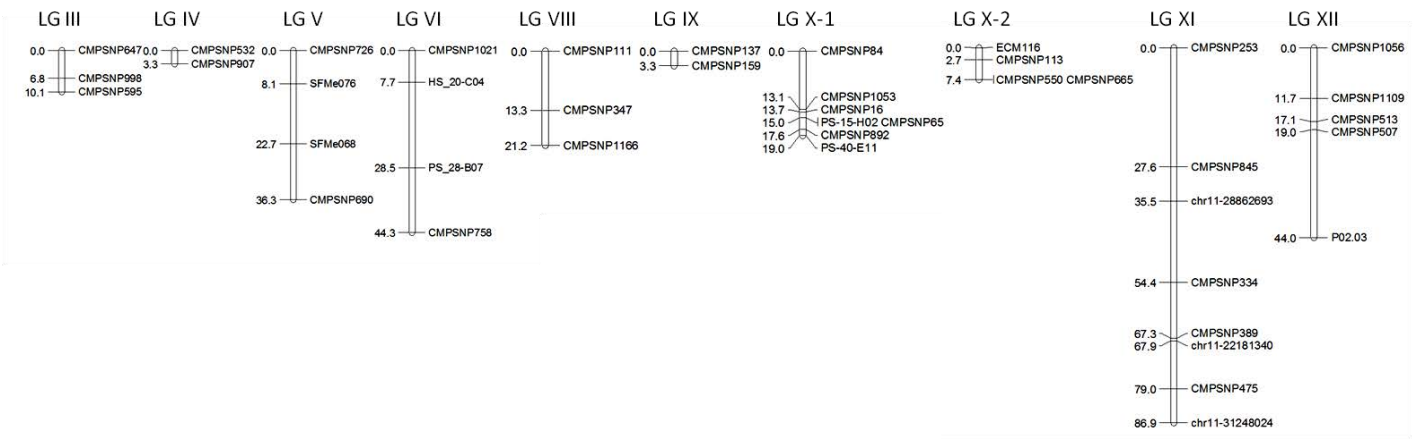

Figure R1-13. Genetic map of the F_2 population made from the cross DHL142 x DHL1046 defined using 37 SNP markers and 80 individuals. Each bar represents one linkage group. The name of the makers are shown on the right side of the bar and the numbers on the left correlate with the genetic position of each marker in cM.

Therefore, as our F_2 control population DHL142xDHL1046 did not allow us to detect the QTL *qwcmv10.1*, which had previously been identified in the DHL population (Guiu-Aragonés et al., 2014), we concluded that the method we were using to detect new minor unidentified QTLs, was not the appropriate and need further improvement.

Table R1-10. QTL analysis for the resistance to CMV-FNY from the cross DHL142 x DHL1046. LOD values >2 for infection degree at 26 dpi and "infected versus non-infected" (Y/N) phenotype.

	LG	Markers	Statistic test	
			LOD	KW
26 dpi	X	CMPSNP113	2.40	10.40 (***)
Y/N	IX	CMPSNP159	2.15	9.17 (**)

The significance of the Kruskal-Wallis test is presented using "*", where ** equal to $P \leq 0.01$, *** to $P \leq 0.001$.

Part II Production and re-sequencing of melon introgression lines 5-123, 20-28-62 and 20-91-15

Production and re-sequencing of ILs

The melon IL 5-123, harboring the introgression containing the QTLs *cmv1* and *cmvqw3.1*; IL 20-28-62, harboring the introgression containing *cmv1* and *cmvqw10.1*; and IL 20-91-15, harboring the introgression containing *cmv1*, *cmvqw3.1* and *cmvqw10.1* were produced previously by our research group using marker assisted selection.

The QTL *cmvqw3.1*, was mapped in a 15.2 cM introgression, between markers HS10A02 and A21C11; and the QTL *cmvqw10.1* was mapped in a 7.4 cM introgression, between markers CMSNP65 and CMSNP183 (Guiu-Aragonés et al, 2014). To obtain the IL with QTLs *cmv1* and *cmvqw3.1*, the NIL SC12-1-99, which contains *cmv1* within an introgression of 2.2 cM, from CMN61_14 to CMN21_55 markers (Essafi et al, 2009) was crossed with the NIL SC3-3, which contains *cmvqw3.1* within an introgression of 27.5 cM, from SNP marker AI_14-B01 to CMPSNP979. To obtain the IL with QTLs *cmv1* and *cmvqw10.1* the SC12-1-99 was crossed with the NIL SC10-2, which contains an introgression of the whole LG X and includes *cmvqw10.1*. The F_1 from both crosses were self-pollinated to obtain two F_2 populations for selection of plants with introgression lines containing two QTLs each in homozygosis. First, the molecular marker sca02318.8 was used in both populations to select plants containing *cmv1*. Second, from these plants, the line with QTLs *cmv1* and *cmvqw3.1* was selected using flanking SNP markers AI_14-B01 and CMPSNP64, very close to the mapping flanking markers for this QTL. To obtain the line with QTLs *cmv1* and *cmvqw10.1*, flanking markers CMPSNP1117 and SNP671, again, very close to the flanking markers of the QTL were used.

To obtain the IL with the three QTLs, these ILs harboring two QTLs were crossed to obtain a F_1 population that was later self-pollinated to obtain the F_2 population where *cmv1* was fixed and *cmvqw3.1* and *cmvqw10.1* were segregating. From this population double and triple homozygous ILs were selected using molecular markers. To obtain the line 5-123 SNP markers AI_14-B01 and CMPSNP64, from LG III, were used to select the allele SC and markers CMPSNP1117 and SNP671, from LG X, were used to select for allele PS. To obtain the IL 20-28-62, the same markers were used but in this case, AI_14-B01 and CMPSNP64 selected for allele PS and CMPSNP1117 and SNP671 selected for allele SC. To obtain the line 20-91-15, all these markers were used to select plants with the SC allele in all positions. The scheme of development of ILs is presented in Figure R2-1.

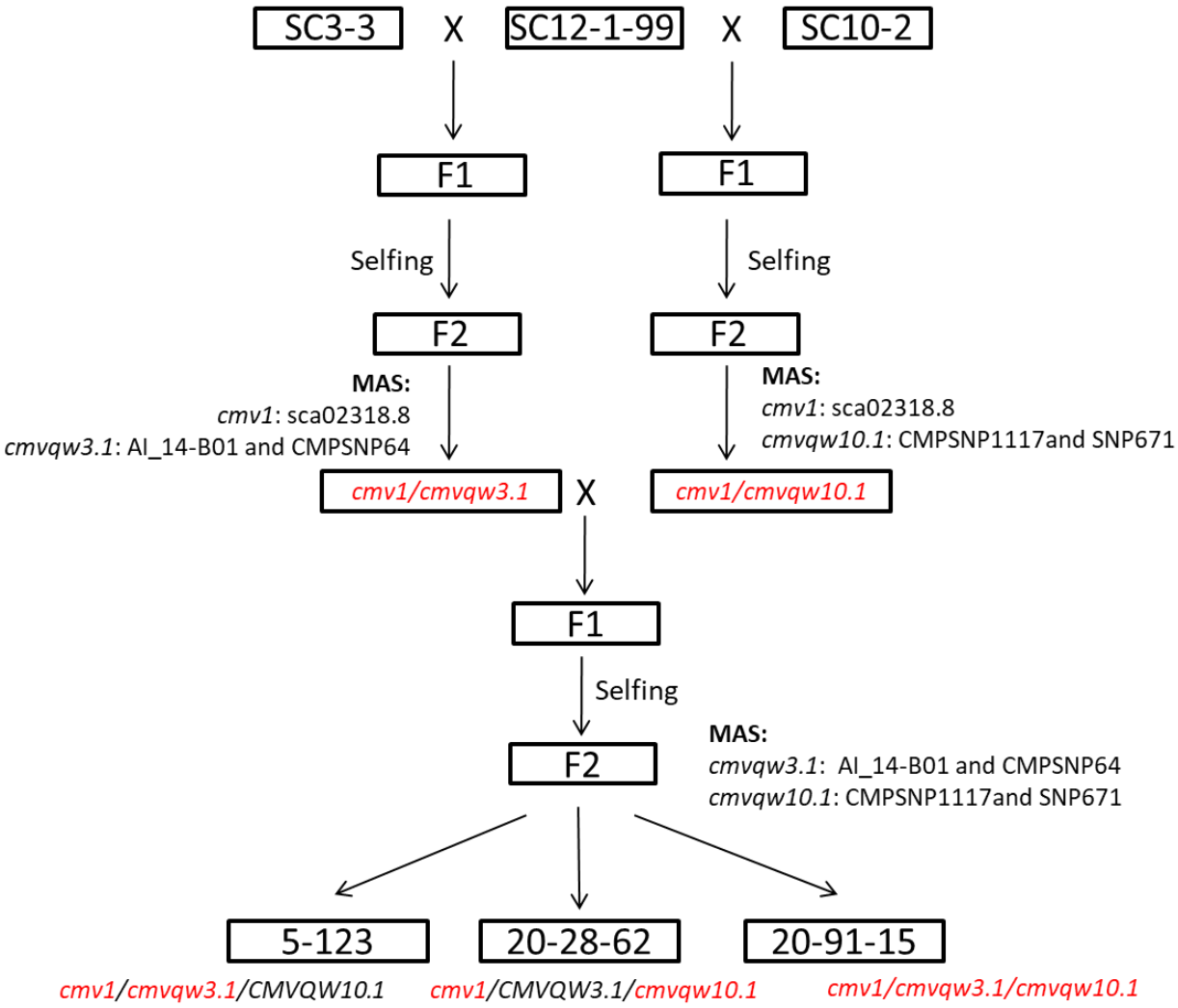

Figure R2-1. Scheme of the development of introgression lines containing resistance QTL combinations at the background PS. In the figure, SC alleles are marked in red.

To gain deeper knowledge about any possible additional unintended introgression from the resistant parental line SC introduced during the generation of these three lines, they were re-sequenced. Fifteen plants of each line were grown and leaf material was collected and pooled for high quality DNA extraction, as indicated in Materials and Methods, section 5. Samples were sent for sequencing to the Centre Nacional de Analisi Genomicos (CNAG). HiSeq2000 Illumina paired-end sequencing (2 × 125) was used for re-sequencing.

II.1 Mapping of Illumina reads

The mapping statistics of re-sequencing data for the three ILs is listed in Table R2-1. In total, the genome-wide re-sequencing data yielded 150,379,786, 168,739,842 and 155,136,326 reads for melon ILs 5-123, 20-28-62 and 20-91-15, respectively. Out of them, 76.02%, 74.65% and 79.19% of reads, respectively, were mapped to the melon reference genome (v3.6.1) (https://www.melonomics.net/melonomics.html#/) after filtering for quality parameters. The average sequencing depth was 41.22 x for line 5-123, 44.67 x for line 20-28-62 and 43.54 x for line 20-91-15.

Table R2-1. Mapping statistics of re-sequencing data for the three ILs

IL	5-123	20-28-62	20-91-15
Number of reads	150,379,786	168,739,842	155,136,326
Number of reads after mapping and filtering	114,316,278	125,968,713	122,863,615
Percentage of reads mapped after filtering	76.02%	74.65%	79.19%
Average sequencing depth	41.22x	44.67x	43.54x

II.2 Genomic patterns in three re-sequenced ILs

The SNP mining for three ILs 5-123, 20-28-62 and 20-91-15 was performed against melon reference genome version 3.6.1. The assignment of genotype was performed every 250 kb by comparing the re-sequencing data of the ILs against PS and SC (Figure R2-2, R2-3, R2-4). The detailed genotyping of all three ILs is listed in Table S9.

The introgression line 5-123 contains the introgression for the SC allele in homozygosis in LG III between physical positions 1,771,744 and 26,560,062 bp. The QTL *cmvqw3.1* had been selected using SNP markers AI_14-B01 and CMPSNP64, which map at physical positions 2,804,355 and 24,802,380 bp. Therefore, the introgression is larger than the QTL. The same is true for the introgression containing *cmv1* in LG XII, although in this case, the region containing *cmv1* (7,026,378 to 14,137,772 bp) is homozygous, but there is a large adjacent region in heterozygosis that has been undetected during the development of this line. There is also a heterozygous area in chromosome 8 between physical position 6,579,259 and

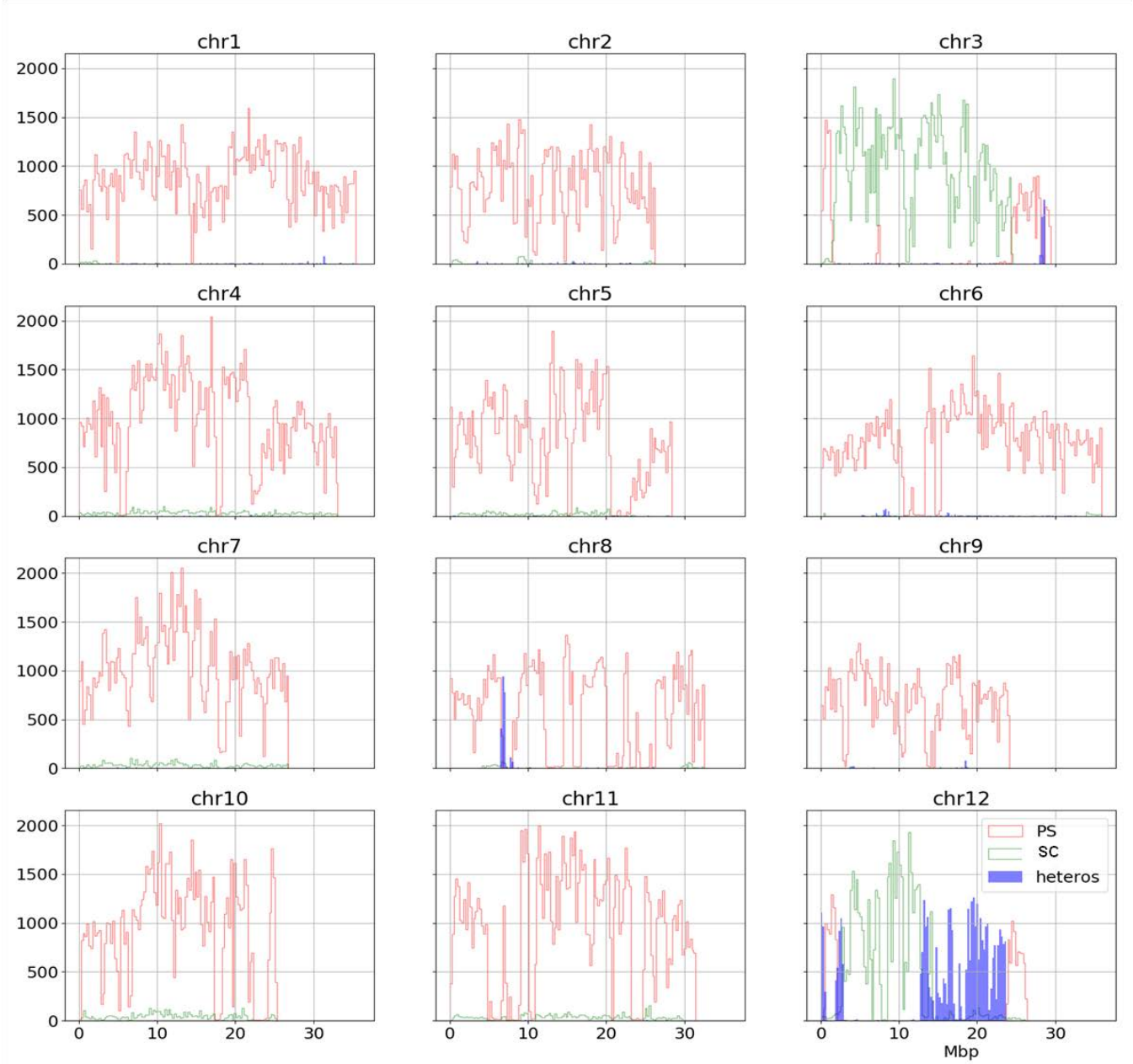

Figure R2-2. Re-sequencing genotyping of melon introgression line **5-123** across 12 chromosomes (Chr). X axis indicated each chromosome divided by 10 Mbp. Y axis indicates the numbers of SNPs. The bars in pink indicates PS background, in green indicates SC introgression while in light purple indicates a heterozygous region between PS and SC. The blank area indicates low density or no SNP identified.

7,104,662 bp (Figure R2-2). Therefore, the IL 5-123, apart from carrying the desired SC introgressions selected with the flanking markers used for LG III and LG XII, contained an additional 5.1 % of SC contamination, of which 3.7 % were in heterozygosity and 1.4 % in homozygosity.

The introgression line 20-28-62 contains the introgression for the SC allele in homozygosis in LG X between physical position 512,065 and 4,586,254 bp. The QTL *cmvqw10.1* had been selected using markers CMPSNP1117 and CMPSNP671, which map at physical positions 1,122,337 and 4,747,628 bp. The rest of LG X was almost covered in heterozygosity. Two homozygous SC alleles were detected in LG XII, one between physical position 10,878 bp and 3,388,963 bp, containing *cmv1* and another small introgression between 13,546,117 bp and 13,745,919 bp. Two unintended small homozygous introgressions, each around 0.15 Mb, were also detected in LG VI. Moreover, some heterozygosis were detected in LG II, IV, VI, VII, VIII and IX ranging from size 10,545 bp (LG IV) to 1,505,061 bp (LG II). In total, the IL 20-28-62 although containing the targeted introgressions that had been selected with the flanking markers used for LG X and LG XII, had also 8 % of SC contaminations, from which 6.4 % are in heterozygosity and 1.6 % in homozygosity.

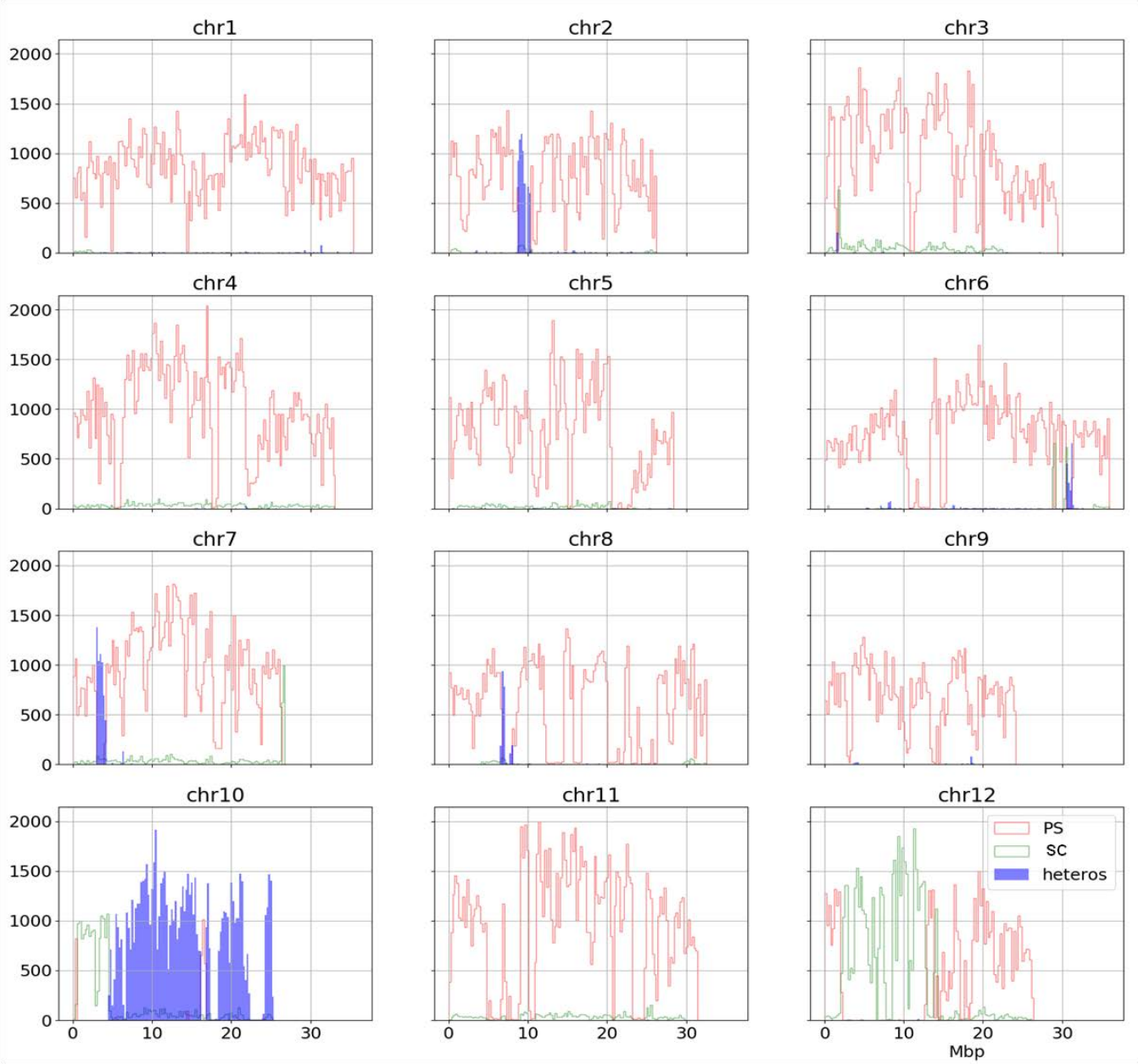

Figure R2-3. Re-sequencing genotyping of melon introgression line **20-28-62** across 12 chromosomes (Chr). X axis indicated each chromosome divided by 10 Mbp. Y axis indicates the numbers of SNPs. The bars in pink indicates PS background, in green indicates SC introgression while in light purple indicates a heterozygous region between PS and SC. The blank area indicates low density or no SNP identified.

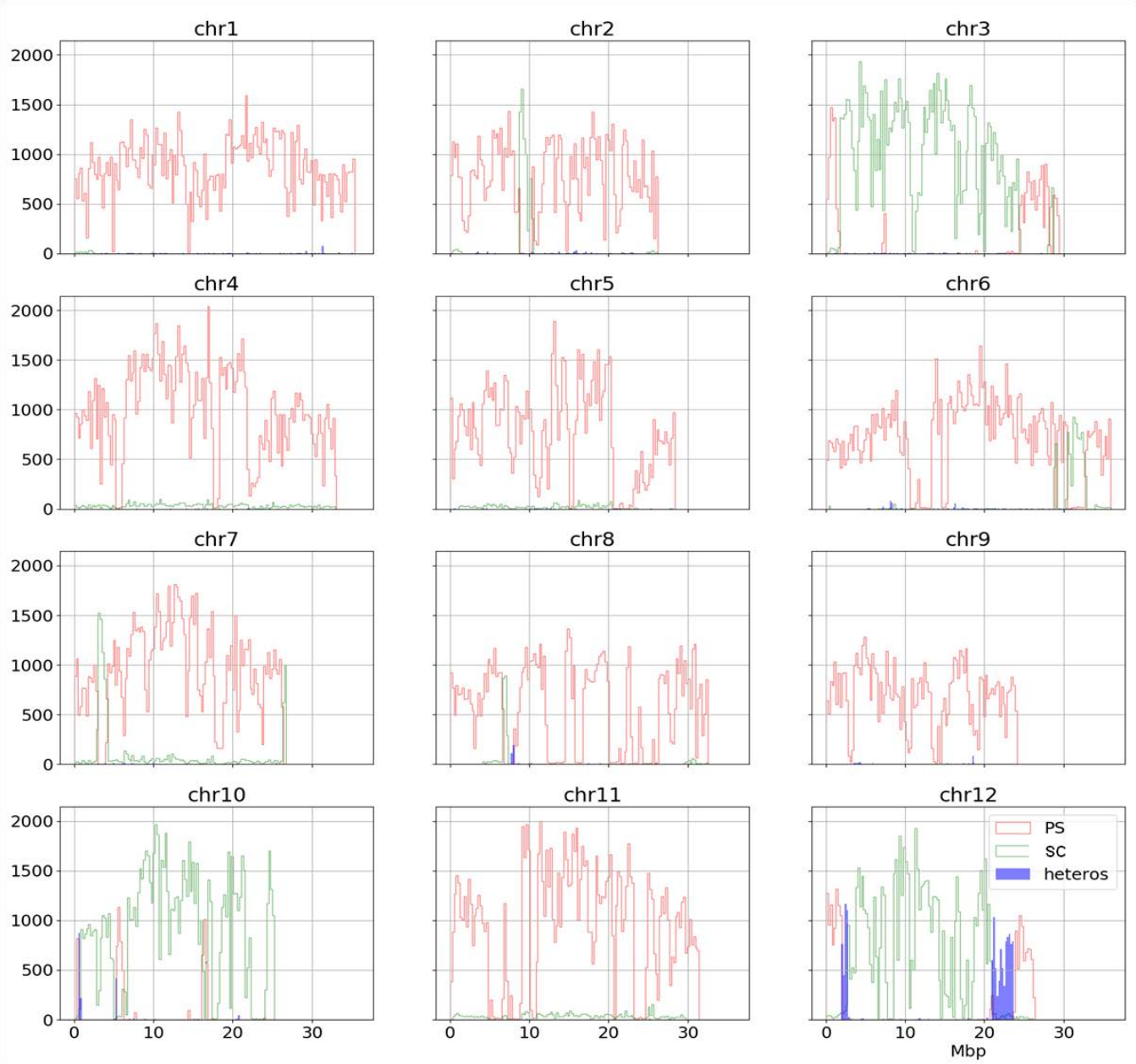

Figure R2-4. Re-sequencing genotyping of melon introgression line **20-91-15** across 12 chromosomes (Chr). X axis indicated each chromosome divided by 10Mbp. Y axis indicates the numbers of SNPs. The bars in pink indicates PS background, in green indicates SC introgression while in light purple indicates a heterozygous region between PS and SC. The blank area indicates low density or no SNP identified.

Production and re-sequencing of ILs

The introgression line 20-91-15 contains the SC introgression in LG XII between 2,809,018 and 21,992,847 bp where *cmv1* lays, the introgression in LG X between 834,447 and 5,145,816 bp where *cmvqw10.1* lays, and the introgression in LG III between 1,587,220 and 26,644,880 bp where *cmvqw3.1* lays. Apart from these intended homozygous introgressions, some other homozygous introgressions in LG II, III, VI, VII and VIII were detected. In total, the IL 20-91-15 contains around 12.5 % of background contamination in the whole genome during the process of IL development, from which 10.9 % is in homozygosity and 1.6% in heterozygosity.

Overall, according to the re-sequencing results, 5-123 harbors the expected resistance SC loci *cmv1* and *cmvqw3.1;* 20-28-62 harbors the resistance SC loci *cmv1* and *cmvqw10.1*; and 20-91-15 harbors the resistance loci *cmv1, cmvqw3.1* and *cmvqw10.1*. All three ILs contain some unintended homozygous and heterozygous small introgression contaminations in some chromosomes. All of them were susceptible to CMV-FNY, and only 20-91-15 (*cmv1/cmvqw3.1/cmvqw10.1*) was found to be resistant to CMV-M6 (data not shown). Our results indicated that even though they had some unintended extra introgressions, the ILs could be used for further analysis regarding the characterization of the resistance to CMV-FNY or the study of the determinants of virulence.

Part III Characterization of melon resistance to the aggressive CMV-FNY strain

Recent studies have shown that in the resistance against CMV conferred by SC melon accession, there are at least three QTLs involved: *cmv1, cmvqw3.1 and cmvqw10.1* (Guiu-Aragonés et al., 2014). The inheritance of *cmv1* has been characterized previously to be recessive (Essafi et al., 2009). The gene *cmv1* prevents the virus movement from the bundle sheath cells to the intermediary cells or vascular parenchyma cells, hindering a systemic infection (Guiu-Aragonés et al., 2016). Here, we aim to characterize the resistance conferred by the other described QTLs, *cmvqw3.1, cmvqw10.1,* and unknown QTLs to the aggressive CMV strains belonging to subgroup I.

III.1 Melon lines harboring different QTL combinations delayed the systemic infection.

We evaluated three ILs containing different QTL combinations: 5-123, carrying *cmv1* and *cmvqw3.1*, 20-28-62, carrying *cmv1* and *cmvqw10.1*, 20-91-15, carrying *cmv1*, *cmvqw3.1* and *cmvqw10.* All ILs are susceptible to CMV-FNY. The first leaf of seven plants from each line (5-123, 20-28-62, 20-91-15), PS and SC were inoculated with CMV-FNY, and symptoms were evaluated at 7 and 14 dpi (Figure R3-1). One plant from each line was also mock inoculated as control. At 7 dpi, only the control PS showed viral symptoms, whereas lines with different QTL combinations and SC were completely symptomless.

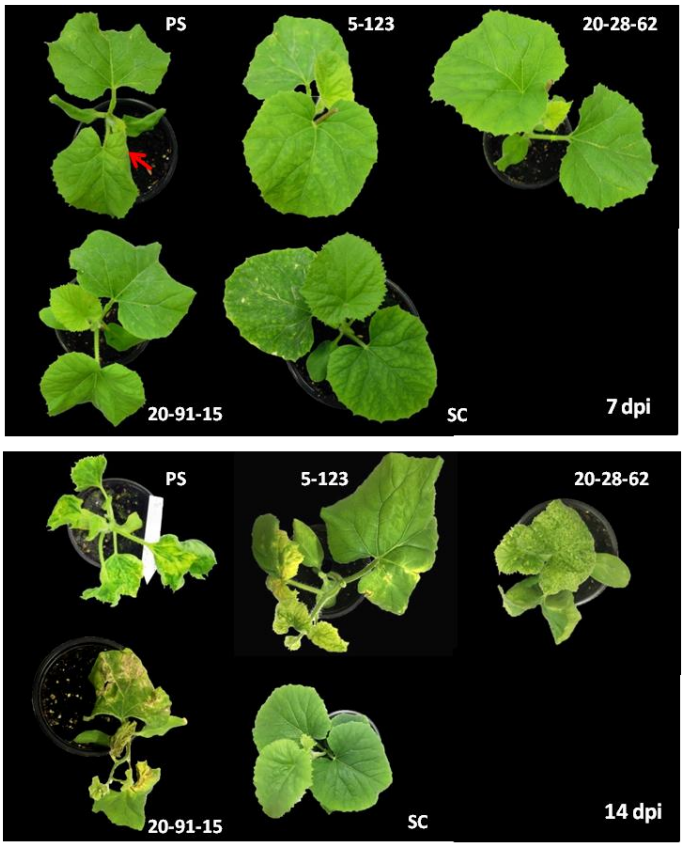

Figure R3-1. Infection symptoms of different melon lines after inoculation with CMV-FNY at 7 dpi and 14 dpi. The red arrow in the figure indicates the systemic infection symptoms in the new leaf of PS at 7dpi.

However, at 14 dpi, all lines except SC were systemically infected and showed different infection phenotypes. PS showed the typical severe mosaic and curling leaves, and resulted in relatively small plants compared with mock inoculated plants. In the case of lines 5-123, 20-28-62 and 20-91-15, they showed even more severe symptoms than PS, such as curling, necrosis in leaves and petioles, and some of the plants dead. SC remained symptomless until the plants were removed (around 20 dpi).

The delay of the systemic infection was confirmed by RT-PCR using CMV-FNY specific primer pair (F109-400F and F109-1400R amplifying a 1,019 bp fragment) in the newly developed leaves. At 7 dpi, we only detected CMV-FNY in PS samples, whereas it was not detected in any of the other lines evaluated. At 14 dpi, the virus was detected in all samples, with the exception of the resistant control SC (Figure R3-2).

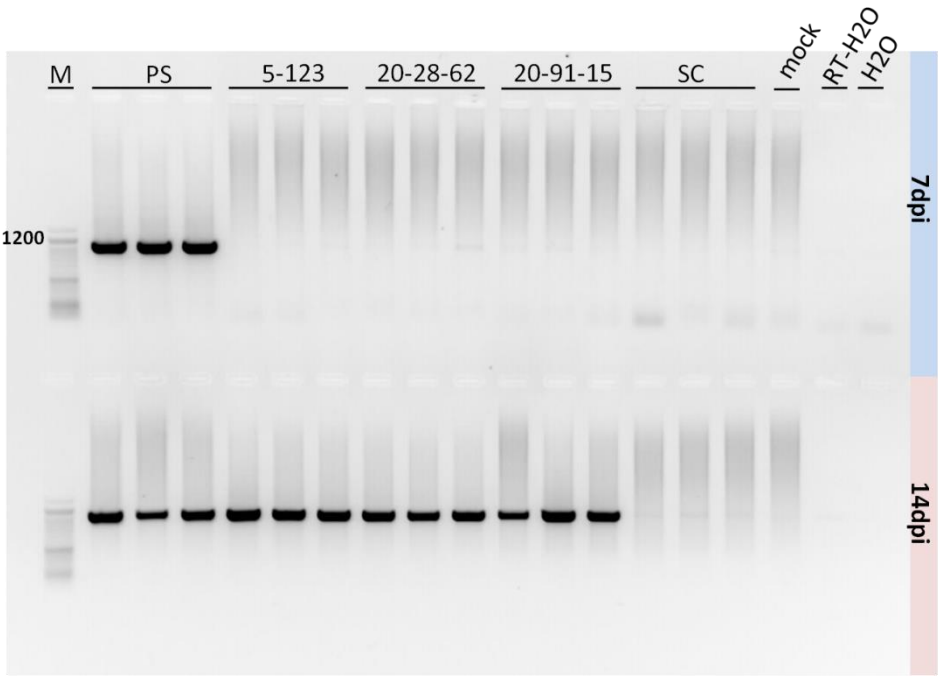

Figure R3-2. RT-PCR for CMV-FNY detection in the new leaves of melon lines (PS, 5-123, 20-28-62, 20-91-15, SC) inoculated with CMV-FNY. M: size marker (50 bp DNA ladder); mock: mock inoculated PS; RT-H_2O: negative control for reverse transcription using H_2O instead of RNA; H_2O: negative control for PCR with H_2O instead of cDNA.

Thus, we concluded that melon lines harboring resistance QTL combinations, even though they are susceptible to CMV-FNY, they differ in the timing of systemic infection. Melon lines harboring only *cmv1/cmvqw3.1* (5-123), *cmv1/cmv10.1* (20-28-62) or *cmv1/cmvqw3.1/cmvqw10.1* (20-91-15) could not prevent CMV-FNY systemic infection, but the presence of these combinations of QTLs contribute to its delay, suggesting that they are involved in viral movement, like *cmv1*. In the resistant melon accession SC, which carries additional QTL(s) still undetected, the virus systemic infection was inhibited.

III.2 Lines harboring at least two QTLs delayed virus accumulation in the petiole of the inoculated leaf

The delay in CMV-FNY systemic infection in melon lines harboring different QTL combinations suggests that the function of these QTLs is related to preventing the transport of the virus within the plant tissue. Therefore, these lines should carry fewer viruses in their phloem

than PS at the beginning of the infection. To confirm this, we quantified by qRT-PCR the relative viral accumulation in the petioles of inoculated leaves at 7 and 14 dpi.

In experiment 1, twelve plants of each melon line 5-123, 20-28-62, 21-91-15, PS and SC were rub inoculated with CMV-FNY in the first true leaf. After 7 dpi, the petioles of the inoculated leaves from six plants of each melon line were cut and immediately frozen in liquid N_2. The same was done at 14 dpi. At this point, symptoms in the plants that had been infected were truly visible. Since not all the inoculated plants could be infected, at least three plants showing visible symptom of each line per time point were processed for RNA extraction, cDNA synthesis and qRT-PCR analysis. The detailed processes were carried out as indicated in Materials and Methods (section 6 and section 10). As shown in Figure R3-3 and Table R3-1, at 7 dpi the virus accumulation in the petiole of SC was lower compared with all other melon lines. This difference was statistically significant between SC and PS, and SC and 5-123. Melon lines 20-28-62 and 20-91-15 had less virus compared with the susceptible line PS, although the difference was not statistically significant. Among the biological replicates of each melon line, PS did not show much dispersion, while lines harboring QTL combinations had more variation among biological replicates at the beginning of the infection (7 dpi).

At 14 dpi, however, there was less dispersion of biological replicates. In this case, virus accumulation in the petioles of lines 20-28-62 (*cmvqw10.1/cmv1*) and 20-91-15 (*cmvqw3.1/cmvqw10.1/cmv1*) were significantly lower than in those of PS, indicating that the QTL combinations present in these lines were somehow affecting the entry or the transport of the virus in the phloem. For line 5-123, although there was less virus accumulation than in PS, the difference was not significant, indicating that the QTLs present in this line (*cmvqw3.1/ cmv1*) delayed viral transport less efficiently than the other combinations. The resistant line SC had significantly less virus than nearly all the susceptible lines.

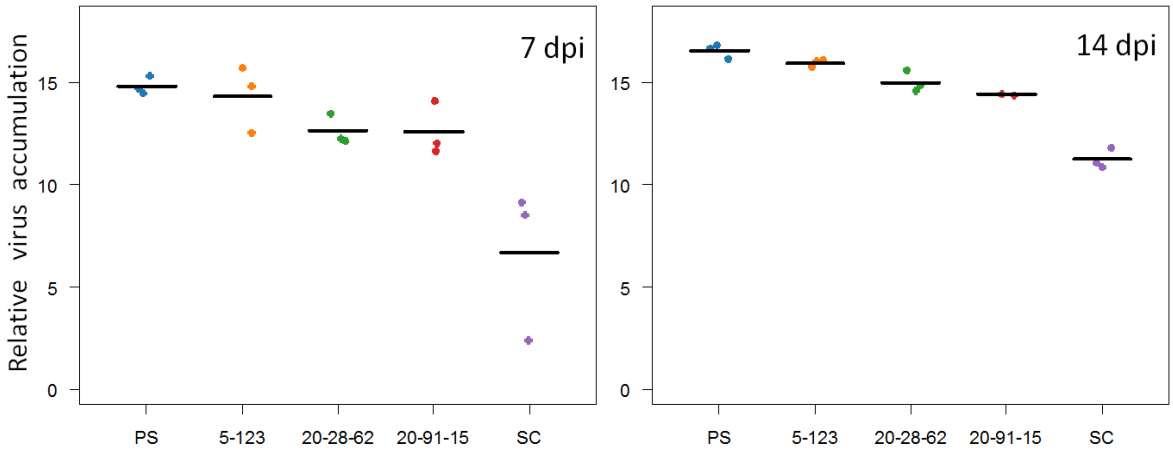

Figure R3-3. Relative virus accumulation (ddCt) in the petioles of the first leaf inoculated with CMV-FNY of different melon lines at 7 dpi and 14 dpi (experiment 1). X axis indicates melon lines and Y axis indicates the amount of relative virus accumulation. The line in the figure indicates the mean of ddCt of each line.

Table R3-1. Significance test for the relative virus accumulation (ddCt) in the petiole of inoculated leaves among different melon lines at 7 dpi and 14 dpi (experiment 1) using Dunn test.

	Melon lines	5-123	20-28-62	20-91-15	SC
7 dpi	PS	0.4636	0.0855	0.0502	0.0023
	5-123		0.1006	0.0603	0.0031
	20-28-62			0.3921	0.0721
	20-91-15				0.1177
14 dpi	PS	0.1899	0.0395	0.0130	0.0006
	5-123		0.1899	0.0749	0.0096
	20-28-62			0.2563	0.0716
	20-91-15				0.2563

Note: The numbers shaded in dark grey indicate significance value $p < 0.05$.

To confirm the results obtained in experiment 1, we performed a second experiment under the same conditions. In experiment 2, a total of 20 plants per line were inoculated with CMV-FNY,

and petioles from three infected plants of each line per time point were processed as described in the experiment 1. The same virus accumulation trend was observed in the experiment 2 (Figure R3-4, Table R3-2). The susceptible line PS always had more virus accumulation compared with SC and other susceptible lines harboring different QTLs. The resistant line SC had the lowest level of virus compared with the rest of the lines evaluated. The melon line 20-91-15, harboring *cmv1*, *cmvqw3.1* and *cmvqw10.1*, at 14 dpi seemed to have less virus accumulation compared with 20-28-62 and 5-123, although the results were not significant. In general, in the second experiment we saw a bigger dispersion of the data at 7 and 14 dpi compared to the first experiment, which can explain the lack of significant differences between lines.

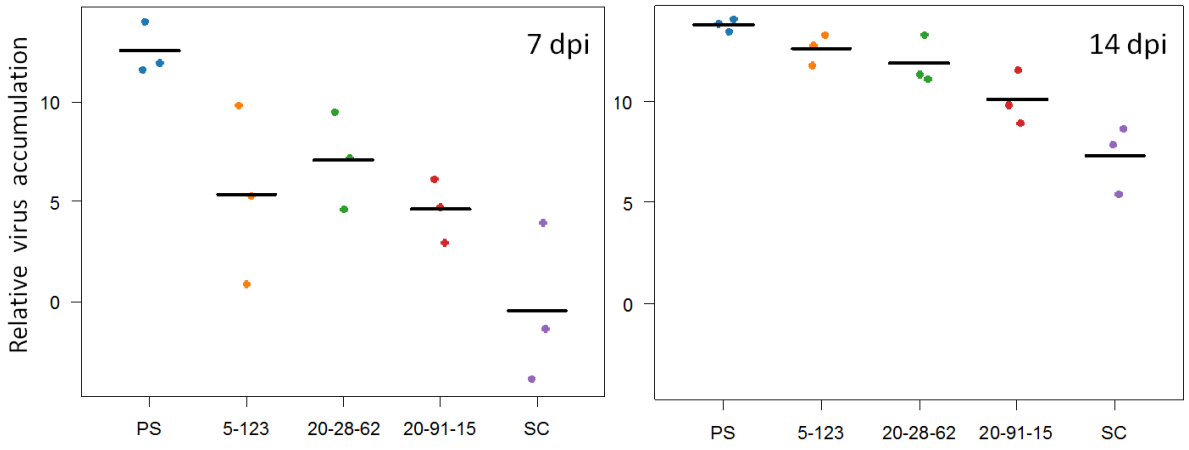

Figure R3-4. Relative virus accumulation (ddCt) in the petioles of first leaves inoculated with CMV-FNY of different melon lines at 7 and 14 dpi (experiment 2). X axis indicates melon lines and Y axis indicates the amount of relative virus accumulation (ddCt). The line in the figure indicates the mean of ddCt of each line.

Table R3-2. Significance test for the relative virus accumulation (ddCt) in the petiole of the inoculated leaves among different melon lines at 7 dpi and 14 dpi (experiment 2) using Dunn test.

	Melon lines	5-123	20-28-62	20-91-15	SC
7 dpi	PS	0.0414	0.0855	0.0223	0.0010
	5-123		0.3575	0.3921	0.0855
	20-28-62			0.2614	0.0414
	20-91-15				0.1367
14 dpi	PS	0.1577	0.0502	0.0112	0.0005
	5-123		0.2614	0.1006	0.0112
	20-28-62			0.2614	0.0502
	20-91-15				0.1577

Note: The numbers shaded in dark grey indicate significance value $p < 0.05$.

Combining both experiments, we can conclude that the resistant melon line SC is able to prevent the virus movement to the vein to produce a systemic infection. Even all the other melon lines are susceptible to CMV-FNY, they differ in the infection they produce. The most susceptible melon line PS, without any QTL described in this study, had shown visible systemic infection and accumulated a high amount of virus at the early stage of infection (7 dpi). Melon lines harboring QTL combinations took much longer to accummulate enough virus in the petiole of the inoculated leaf and, consequently, viral symptoms can only be observed at later stages. All these results should indicate that the QTLs *cmv1*, *cmvqw3.1*, *cmvqw10.1* and uncharacterized additional QTLs can somehow hinder long distance virus movement to produce a systemic infection.

III.3 Movement of CMV-FNY is not affected within the vein

Once shown that the virus movement is affected in all the melon lines harboring QTLs of resistance, we decided to determine whether these QTLs work at the level of phloem entry, as *cmv1* does (Guiu‐Aragonés et al., 2016), or if they act preventing the viral movement within the vein once CMV-FNY has already invaded the phloem.

To decipher this, the petioles of the inoculated first leaves were cut into two parts, proximal and distal with respect to the leaf (Figure R3-5), and then the virus accumulation was quantified using qRT-PCR in the proximal and distal parts. We hypothesized that if the virus movement within the phloem was affected, a gradient of virus concentration would be observed from the proximal part to the distal part of the petiole, being the quantity in the proximal part consistently higher than that in the distal part. On the other hand, if the virus entry into the phloem was affected by the presence of the QTLs, the gradient of virus in the petiole would only be observed at the very early stages of the infection, and then later, the quantity of virus would be homogeneous in both petiole parts.

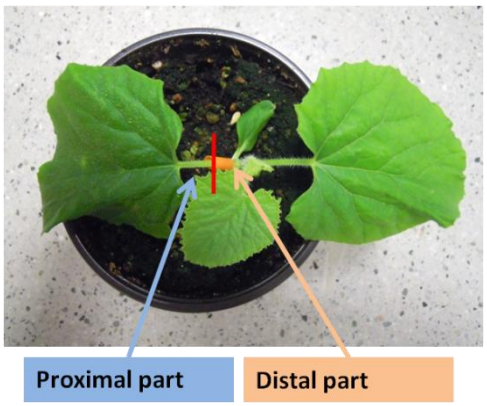

Figure R3-5. Proximal and distal petiole of the inoculated melon first leaf.

In total, the first leaf of 30 plants of each line 5-123, 20-28-60, 20-91-15, PS and SC were inoculated with CMV-FNY. The petioles of ten plants from each melon line per time point were collected and cut into proximal and distal halves. Sampling was performed at 7, 10 and 14 dpi. Finally, petioles from three to five infected plants of each line per time point were processed for RNA extraction, cDNA synthesis and qRT-PCR analysis. The detailed processes were the same as described in the virus quantification for whole petioles.

Consistently with the previous experiment, in the susceptible line PS the virus accumulation was already high at 7 dpi in both parts of the petiole (Figure R3-6), whereas the rest of the lines showed lower virus accumulation, being SC the lowest value. At this very early stage of infection, a dispersion of virus accumulation in both proximal and distal petioles was seen in the

melon lines 20-28-62 and 20-91-15, in the distal part of 5-123, but not in the resistant line SC and susceptible line PS. At 7 dpi was difficult to compare both halves of the petiole because of the high dispersion of data. We only could observe that in lines 5-123 and 20-28-62 the virus accumulation was slightly higher in the proximal part of the petiole compared with that in distal petiole. For PS, 20-91-15 and SC we did not observe differences between both parts of the petiole. . Overall, at 7 dpi, no significant differences were observed between virus accumulations in both parts of the petiole for any of the lines tested (Table R3-3).

At 10 dpi (Figure R3-6), more virus accumulation but less dispersion was observed in all the lines compared to 7 dpi. In line SC, a relative higher virus accumulation in proximal petiole was seen, while all the other lines had equivalent virus accumulation in the proximal and the distal petiole parts. No significant difference was observed between virus accumulation in both parts of the petiole for any of the lines tested (Table R3-3).

At 14 dpi (Figure R3-6), the amount of virus was increased in all the lines compared with values at 7 and 10 dpi. In all cases, all lines showed equal virus accumulation in both halves of the petiole of the inoculated leaves, with no significant differences between proximal and distal parts (Table R3-3). The higher dispersion of the data was observed in the resistant line SC for both proximal and distal petiole, suggesting that not all the SC replicates accumulated virus at the same level.

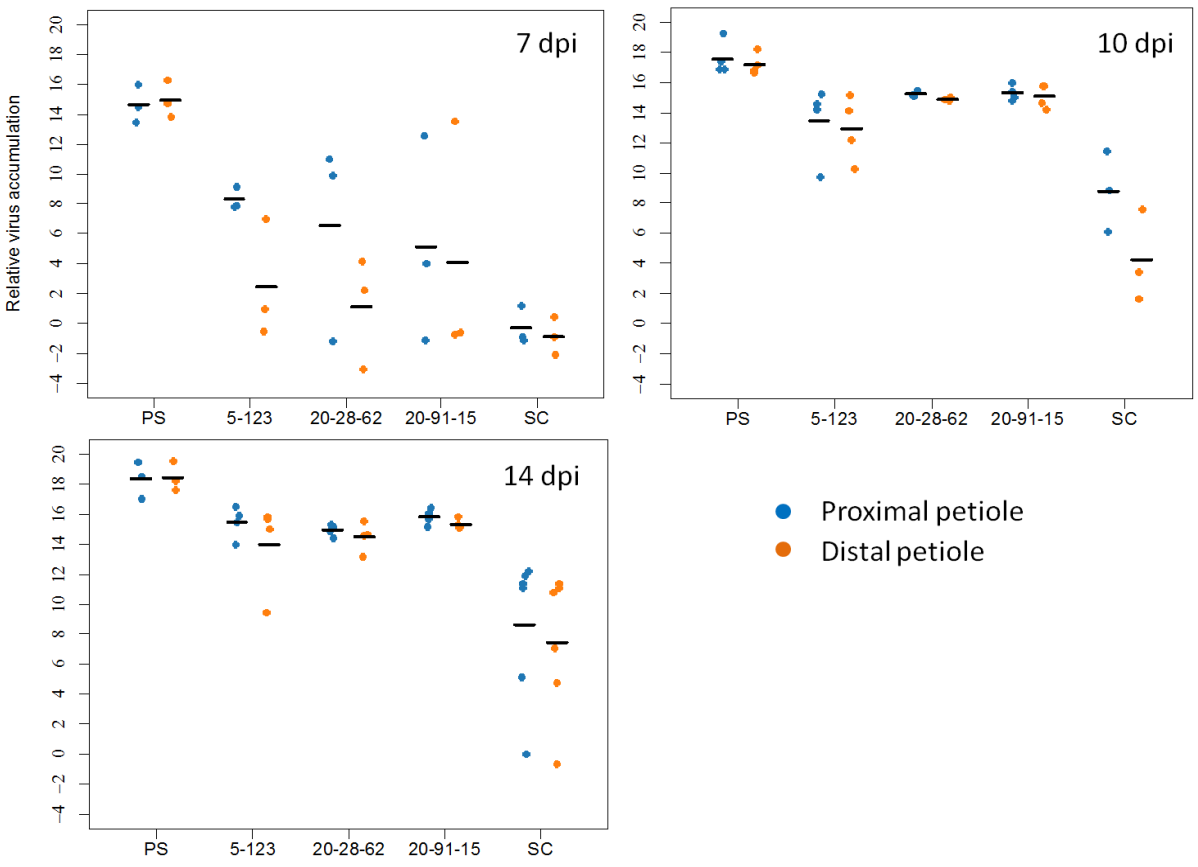

Figure R3-6. Relative virus accumulation (ddCt) in proximal petioles and distal petioles of CMV-FNY inoculated first leaves among melon lines at 7, 10 and 14 dpi. In each figure, X axis indicates melon lines and Y axis indicates the value of relative virus accumulation (ddCt).

The absence of significant differences between the virus accumulation in both parts of the petiole for all the lines evaluated allowed us to conclude that once the virus enters the phloem, it moves within the phloem with no further restriction. Therefore, the combination of QTLs present in the introgression lines 5-123, 20-28-62 and 20-91-15 participate in restricting the entrance of CMV-FNY in the phloem, as does *cmv1* for CMV strains of subgroup II (Guiu-Aragonés et al, 2016).

Table R3-3. Two-tailed t-test for the relative virus accumulation (ddCt) between proximal petiole and distal petiole of inoculated first leaves of each melon line at different days post inoculation.

		PS	5-123	20-28-62	20-91-15	SC
p value	7dpi	0.7836	0.0690	0.2892	0.8701	0.6187
	10dpi	0.5980	0.7685	0.0507	0.6644	0.1213
	14dpi	0.8899	0.4037	0.4064	0.1600	0.6761
t value	7dpi	0.2937	2.4695	1.2207	0.1743	0.5387
	10dpi	0.5565	0.3080	2.7636	0.4561	1.9619
	14dpi	0.1475	0.8981	0.8928	1.6031	0.4303

To further determine if the viral movement is restricted in the bundle sheath (BS) cells, as is the case of *cmv1* (Guiu-Aragonés et al., 2016), transmission electron microscopy combined with immune-gold labeling experiments will be necessary. In the course of this thesis it was not possible to address these experiments.

III-4 A virus threshold can affect the resistance or susceptibility of SC

Even though SC is an accession resistant to CMV-FNY, positive values of relative virus accumulation were observed in all experiments (Figure R3-3, Figure R3-4 and Figure R3-6). This means that a certain amount of virus can still reach the phloem of SC without causing any infection symptom. Interestingly, during some inoculation sets, some of SC plants showed mild mosaic infection symptoms in first leaf that then disappear in new leaves. Hereby, we hypothesize that a virus accumulation threshold might exist affecting the resistance of SC. Beyond the virus accumulation threshold, the plants will not show symptoms; but when the virus accumulation exceeds the threshold, mild symptoms will appear.

Synergism between ZYMV and CMV was reported, showing that after co-inoculation of both viruses the amount of CMV was increased while ZYMV amount was maintained (Wang et al., 2004). An engineered attenuated ZYMV-AG strain was found to be less pathogenic, without affecting plant growth, but it was still able to increase the CMV amount when co-inoculated. The

binary clone of this strain, named ZYMV-AGII provided by Dr. Gal-on, was hereby used as a tool to increase the amount of CMV-FNY in this experiment (Arazi et al., 2001).

To see if an increase of CMV-FNY amount could be enough to overcome the putative threshold and induce systemic symptoms in SC, we designed an experiment in which SC cotyledons were inoculated with three different treatments: (i) infiltrated with ZYMV-AGII, (ii) inoculated with CMV-FNY, and (iii) co-inoculated with ZYMV-AGII and CMV-FNY. As a control, we used non-inoculated SC plants, and three biological replicates were done per treatment. For the co-inoculated treatment, CMV-FNY was inoculated two days after ZYMV-AGII infiltration. The infection of SC was observed at 14 dpi, and a piece of the newly developed leaf of each SC was collected for ZYMV and CMV molecular detection. RNA extraction, cDNA synthesis and RT-PCR were performed as described in Material and Methods (Section 10.2).

At 14 dpi, CMV-FNY inoculated SC plants did not show any visual infection symptom, as in the non-treated plants. ZYMV-AGII infiltrated SC plants showed mild mosaic with vein clearing. In the case of co-inoculated plants with ZYMV-AGII and CMV-FNY plants had much stronger symptoms with leaf curling and typical mosaic in all leaves (Figure R3-7).

The detection of ZYMV-AGII infection in all SC plants was performed by RT-PCR using ZYMV specific primer pair pAG68F and pAG68R, which amplify a 790 bp fragment. ZYMV was detected in all ZYMV-AGII infiltrated plants, and ZYMV-AGII_CMV-FNY co-inoculated plants (Figure R3-8). The amplification in non-inoculated SC plants was assumed as contamination during PCR process (Figure R3-8A).

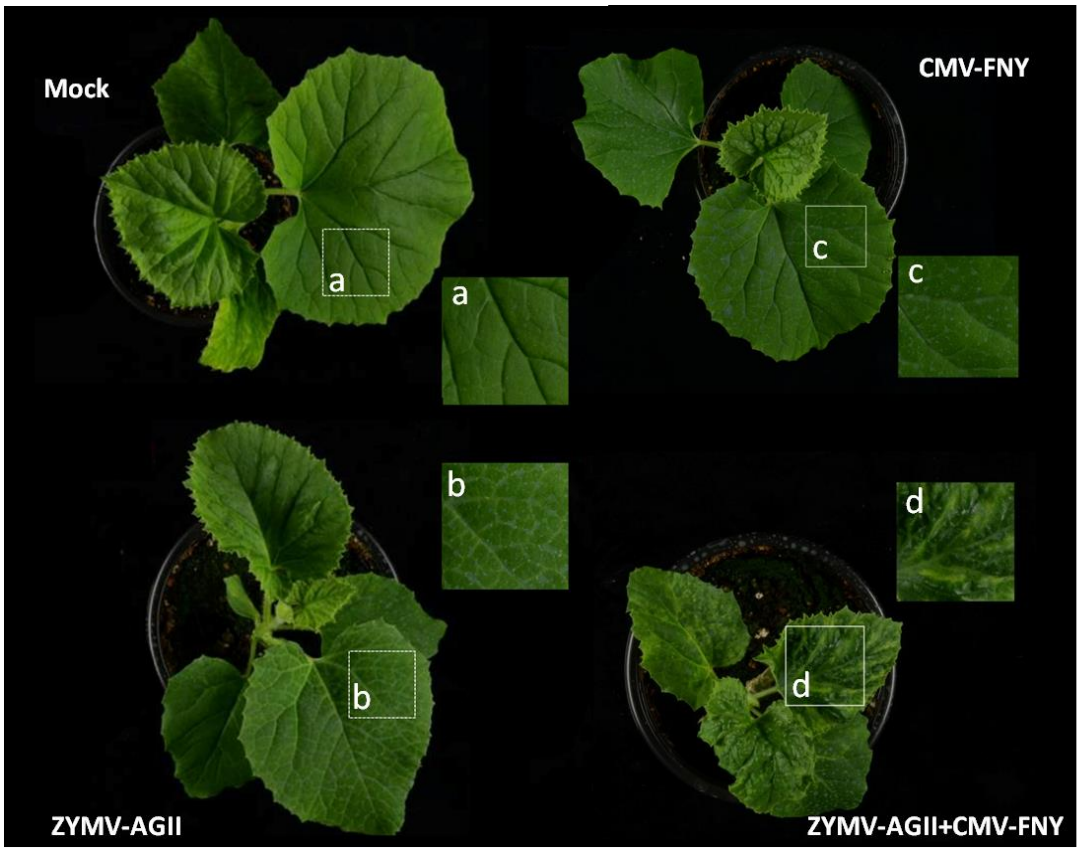

Figure R3-7. Phenotype of melon SC plants inoculated with CMV-FNY, infiltrated with ZYMV-AGII, co-inoculated with CMV-FNY + ZYMV-AGII, and mock inoculated at 14 dpi. Magnification leaf area of a) mock inoculated, b) ZYMV-AGII infected, c) CMV-FNY inoculated and d) ZYMV-AGII + CMV-FNY co-inoculated SC including minor veins.

The detection of CMV-FNY infection was performed by RT-PCR using the same specific primer pair used for qRT-PCR which could amplify a 123 bp fragment (see table M-2 in Materials and Methids. CMV-FNY specific amplification was detected only in ZYMV-AGII_CMV-FNY co-inoculated SC plants, while it was not detected in CMV-FNY inoculated plants (Figure R3-8B).

ZYMV-AGII and CMV-FNY co-inoculated SC plants were systemically infected while CMV-FNY inoculated SC kept resistant, which indicated that the resistance of SC could be broken when the amount of CMV-FNY increases.

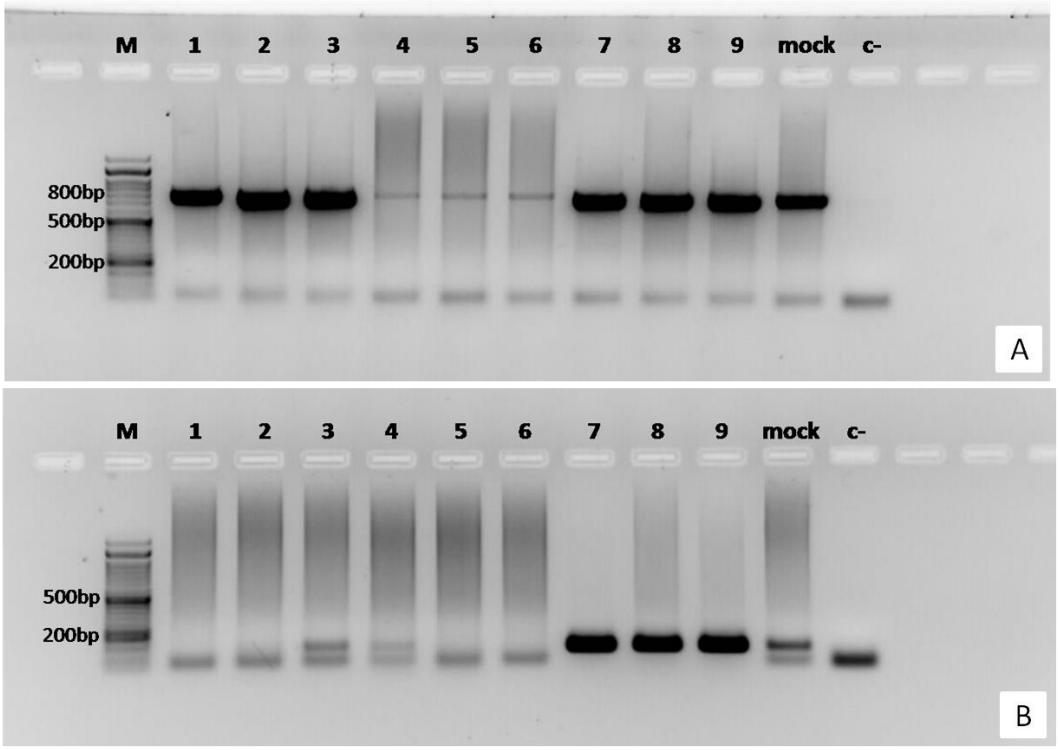

Figure R3-8. Detection of A) ZYMV-AGII and B) CMV-FNY infection in SC plants at 14 dpi using RT-PCR. M) size marker (50bp DNA ladder); 1-3) ZYMV-AGII infiltrated; 4-6) CMV-FNY inoculated; 7-9) ZYMV-AGII and CMV-FNY co-inoculated; mock) mock inoculated; and c-) H2O.

Part IV Virulence determinants responsible for overcoming the resistance mediated by *cmv1*, *cmvqw3.1* and *cmvqw10.1*

Previously, it has been described that the viral determinants against recessive QTL *cmv1* resided in the movement protein of CMV-FNY (Guiu-Aragonés et al., 2015). The melon introgression line 20-91-15, harboring the resistance QTLs *cmv1*, *cmvqw3.1* and *cmvqw10.1*, is resistant to subgroup II strain CMV-LS. When testing 20-91-15 against subgroup I strains, this IL was shown to be resistant to CMV-M6, but susceptible to CMV-FNY. The total genome similarity between CMV-FNY and CMV-M6 was 98.5 %, and between CMV-FNY and CMV-LS was 72.7% (Cèlia Guiu, PhD thesis). Here, we aim to determine the viral factor(s) of CMV-FNY responsible for overcoming the resistance conferred together by *cmv1, cmvqw3.1* and *cmvqw10.1* via producing pseudo recombinants between CMV-FNY and CMV-LS or between CMV-FNY and CMV-M6.

IV.1 Development of molecular markers to differentiate between CMV-FNY and CMV-M6.

To differentiate RNAs between CMV-FNY and CMV-M6 in our experiments of generating combinations of these two viruses, one CAPS marker was developed for each RNA as described in Material and Methods (section 12.3).

For RNA1, primer pair F109-3000F and F109-3'R was used for PCR amplification. Both viruses amplify a 338 bp fragment. The CMV-FNY fragment was digested with *DdeI*, producing four fragments of 29 bp, 51bp, 129 bp and 129 bp. The CMV-M6 fragment produced only three fragments of 51 bp, 129 bp and 158 bp (Figure R4-1).

For RNA2, primer pair F209-2200F and F209-3'R was used for PCR amplification. CMV-FNY could amplify an 863 bp fragment and, after digestion with *BstXI*, producing two fragments with size 30 bp and 833 bp. CMV-M6 amplified an 860 bp fragment and, after digestion with the same enzyme, produced three fragments of 30 bp, 405 bp and 425 bp (Figure R4-6).

For RNA3, primer pair F309-1600F and F309-3'R was used for PCR amplification. CMV-FNY amplified a 635 bp fragment and after digestion with *XhoI*, the amplicon was digested into two fragments of 255 bp and 380 bp. CMV-M6 amplified a 633 bp fragment that will not be digested by *XhoI* (Figure R4-6).

The CAPS markers developed for differentiating RNA1, RNA2 and RNA3 between CMV-M6 and CMV-FNY were named CAPS-M6FNY-1, CAPS-M6FNY-2 and CAPS-M6FNY-3

respectively. These three CAPS markers were later used to confirm the RNA origin in the chimeric viruses when necessary.

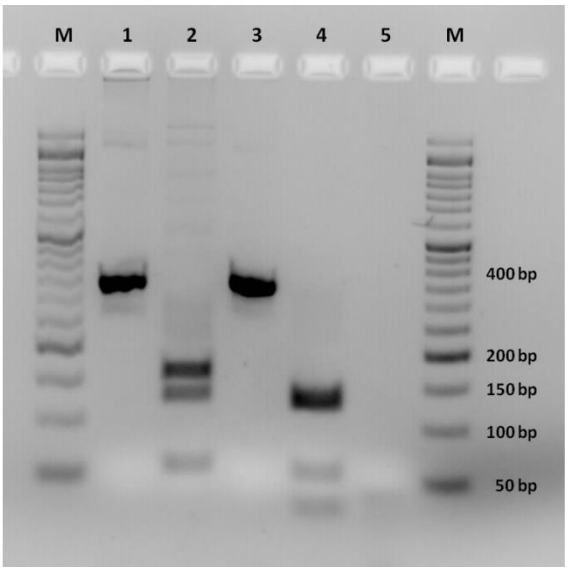

Figure R4-1. CAPS-M6FNY-1 marker used to differentiate RNA1 between CMV-FNY and CMV-M6. M) 50bp DNA mass marker, the size of corresponding bands is listed on the right.1) PCR amplicon of pGEM-M6; 2) pGEM-M6.1 *DdeI* digested; 3) PCR amplicon of pFny; 4) pFny1 *DdeI* digested 3; 5) negative control for PCR, with H_2O.

IV.2 Construction of binary vectors of CMV-M6

To establish an agroinfiltration based system to get the chimeric virus combinations, binary vectors were constructed. Binary vectors pCR1(+), pCR2(+) and pCR3(+), which express respectively, RNA1, RNA2 and RNA3 of CMV-FNY, were kindly provided by Dr. Kim Kook-Hyung (Seo et al., 2009). Binary vector pGREEN-M6.3 for agroinoculation of CMV-M6 RNA3, was constructed previously (Guiu-Aragonés, PhD thesis) in our laboratory. In order to get RNA1 and RNA2 binary vector for CMV-M6, the corresponding cDNAs of RNA1 and RNA2 were inserted into pCR1(+), pCR2(+) based binary vector pSNU1 after removing the CMV-FNY genomes, as described in Material and Methods (section 9). The expected constructs were named as pCR-M6.1 and pCR-M6.2, respectively.

As most of RNA1s from CMV strains were unstable in E. *coli* (A. M. Martín-Hernández, personal communication), the Gibson assembly (see Material and Methods, section 9) of CMV-

M6 RNA1 product was transformed in commercial E.*coli* 10β and also into Stbl4, which is deficient in recombination. Some colonies were obtained using both strains of competent cells.

Eight colonies from Stbl4 and two colonies from10β cells were selected. The plasmids were checked by PCR using M6.1-2650F and pCR3V-R primers (see Material and Methods, section 9) that must amplify a 900 bp fragment. All colonies tested, except Stbl4-4, produced the right band (Figure R4-2A). Nevertheless we digested all clones to confirm the results. When digested with *SacI* and *XbaI*, only colony Stbl4-2 produced the expected fragments of 2,992 and 7,967 bp (Figure R4-2B and C).The colony was sequenced and compared with the original M6 RNA1 in the construct pGEM-M6.1, showing a T to A transition at position 2,153 of the coding sequence of the 1a protein, and a 7 nt deletion 7 nt downstream the SNP T/A (Figure R4-2 D). As this construct would not be functional due to a change of frame in the coding sequence of the 1a protein, we assumed that a sequence around this area would be detrimental for *E. coli*, which would tend to eliminate it. Therefore, to break this putative sequence, we decided to introduce an intron IV2 from the potato ST-LS1 gene (Eckes et al., 1986) upstream or downstream of the deletion detected, to avoid the recombination in the bacteria. However, finally we did not get any colonies in both upstream or downstream cases (data not shown). Therefore, we could not use a binary vector for CMV-M6 RNA1 and we continued with the in vitro transcription vector pGEM-M6.1 to generate the recombinant viruses carrying CMV-M6 RNA1.

The Gibson assembly reaction of CMV-M6 RNA2 into the vector pSNU1 produced only one colony after transformation into competent *E.coli* strain JM109. After analysis by digestion with the restriction enzymes *PstI*, *SalI* and *XmaI*, the plasmid produced bands with the expected size (896 pb, 2,929 bp and 6,820 bp) (Figure R4-3). The construct was confirmed by sequencing. Then, the construct was transformed to agrobacteria strain C58C1.

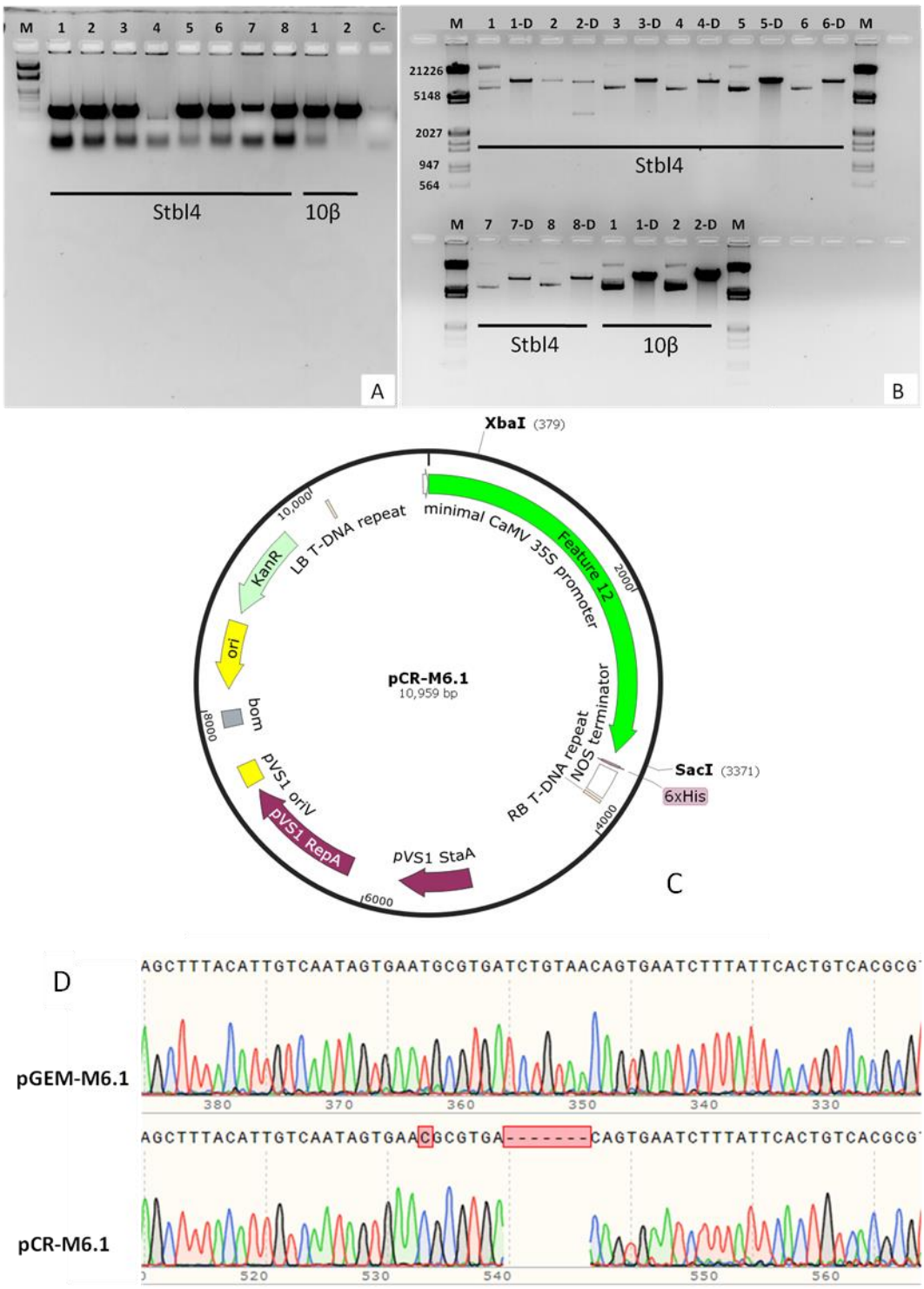

Figure R4-2. Confirmation of the pCR-M6.1 colonies. A) Colony PCR, Stbl4-1 to Stbl4-8 represent eight colonies selected in the assembly transformed to competent cells Stbl4, while 10 β-1 and 10 β-2 represent two colonies selected in the assembly transformed to competent cells 10 β; B) enzyme digestion of the constucts with *SacI* and *XbaI*. 1 to 8 indicate the constructs non-digested and 1-D to 8-D digested

with *SacI* and *XbaI*.C) In silico construction of pCR-M6.1 showing the RNA1 genome in green and the restriction enzyme sites for *SacI* and *XbaI*. D) The deletion found in the construct pCR-M6.1 compared with template pGEM-M6.1. In A and B, letter M indicats DNA molocular marker Promega™ Lambda DNA/EcoRI + HindIII, the numbers on the left side of M indicate the size of the corresponding marker bands. c- indicates negative control for PCR, with H_2O.

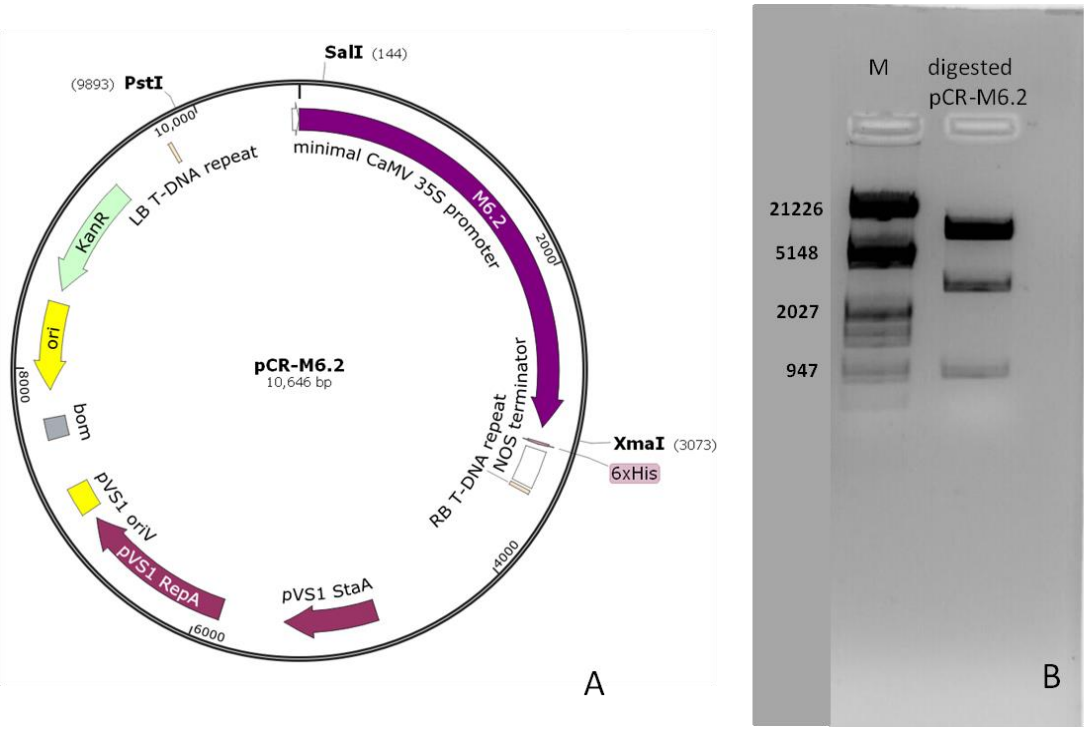

Figure R4-3. Construction of the plasmid pCR-M6.2. A) In silico construction of pCR-M6.2; B) Digestion of the construct with the enzymes *PstI, SalI* and *XmaI*. M, Promega™ Lambda DNA/EcoRI + HindIII marker showing the size of corresponding bands.

IV.3 Production of pseudo recombinant viruses

Once we had generated the viral vectors, we were able to make combinations between RNAs from both strains. In theory, eight recombinants could be produced between CMV-M6 and CMV-FNY (Figure R4-4).

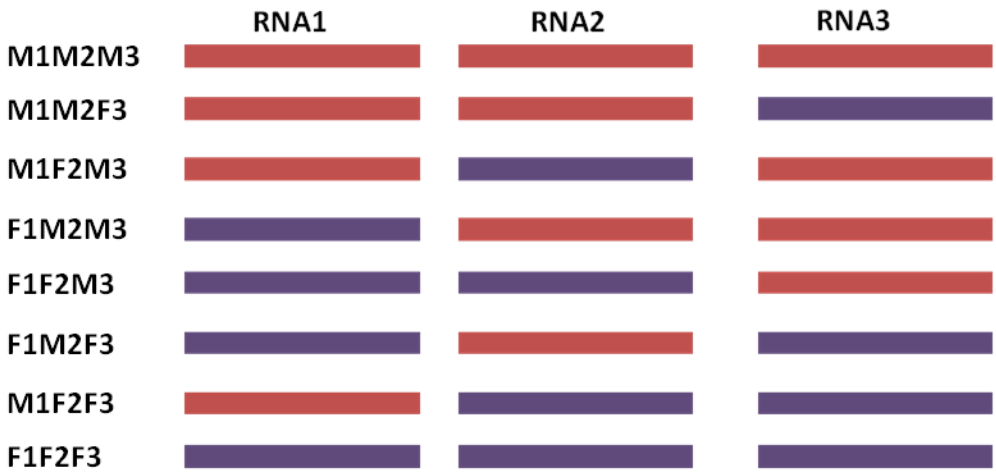

Figure R4-4. Theoretical pseudo recombinants between CMV-FNY and CMV-M6. Purple bar indicates RNAs with CMV-FNY origin. Red bar indicates RNAs with CMV-M6 origin. The name of each recombinant is listed on the left.

IV.3.1. Recombinants produced between CMV-FNY and CMV-M6.

The infectious vectors pCR1(+)/pFny1, pCR2(+), pCR3(+) were used to produce RNA1, RNA2 and RNA3 of CMV-FNY, represented by F1/F1', F2 and F3 in the recombinants, respectively. The infectious vectors M6.1, pCR-M6.2 and pGreen-M6.3 were used to produce RNA1, RNA2 and RNA3 of CMV-M6, represented by M1, M2 and M3 in the recombinants, respectively. The production of recombinant viruses was performed via mixed inoculation, as described in Material and Methods (section 4.2). Several sets of experiments were carried out to inoculate *N. benthamiana* plants. In each experiment set, for each recombinant, at least two *N. benthamiana* plants were inoculated. Two mock inoculated *N. benthamiana* plants were also included as negative control. CMV-M6 inoculated *N. benthamiana* was used as positive control.

None of recombinants carrying RNA1 from CMV-M6 infected *N. benthamiana* plants. All the recombinants with RNA1 from CMV-FNY produced infection in *N. benthamiana* plants, showing mild systemic infection in the upper leaves (Figure R4-5 A-E). The infections of CMV-FNY resembled F1F2F3/F1'F2F3 and recombinant F1F2M3/F1'F2M3 were slightly more symptomatic than other recombinants.

The infection of *N. benthamiana* was confirmed by RT-PCR using the primer pair F109-900F and F109-2000R, amplifying 1,115 bp to detect the presence of RNA1 from CMV-FNY (Figure

R4-5 F). The mock-inoculated plant showed certain background amplification, negligible compared with the intensity of the bands in the infected plants.

The infection of some *N. benthamiana* plants was also confirmed by RT-PCR amplifying specific fragments around 860 bp from RNA 2 and fragments around 630 bp from RNA3 (Figure R4-6A). As shown in Figure R-4-6 B, CAPS-M6FNY-2 confirmed CMV-FNY origin of RNA2 in recombinant F1F2M3 and F1F2F3; and CMV-M6 origin of RNA2 in recombinants F1M2F3 and F1M2M3. The control inoculated with CMV-M6 virus surprisingly showed a less intense amplification with the FNY genotype in RNA2, which probably was an error in sampling or a contamination during amplification. The CAPS–M6FNY-3 confirmed that in combination F1F2F3 and F1M2F3 the RNA3 is from CMV-FNY origin, whereas combinations F1F2M3 and F1M2M3 corresponded to CMV-M6 origin. In lane 2, CMV-M6 control, the RNA3 was CMV-M6 genotype, although there are mild bands in the gel, suggesting a slight contamination with CMV-FNY in this sample.

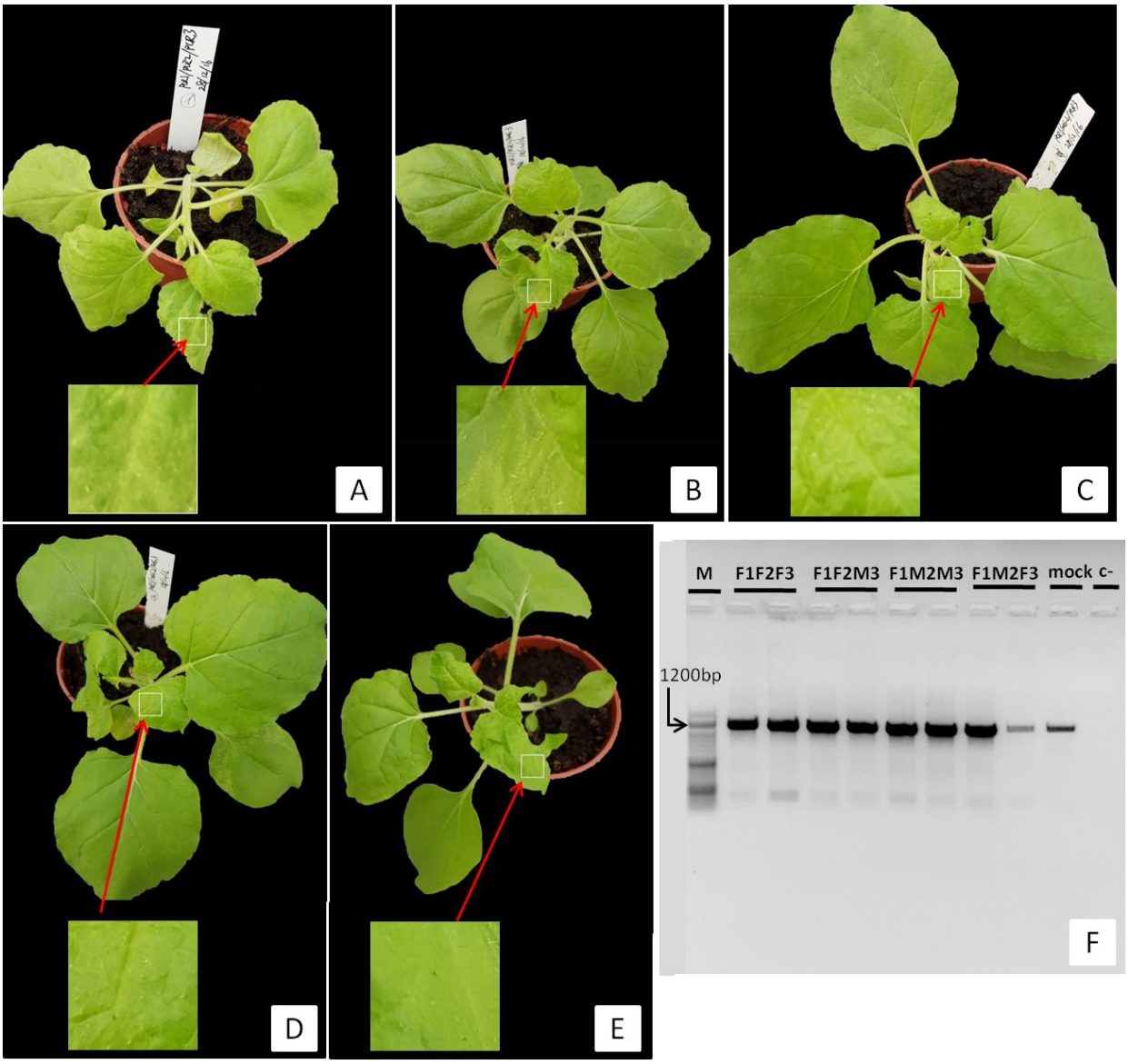

Figure R4-5. Phenotype of *N. benthamiana* plants inoculated with recombinants generated between CMV-FNY and CMV-M6. **A)** F1F2F3, **B)** F1F2M3, **C)** F1M2F3, **D)** F1M2M3 and **E)** mock inoculated *N.benthamiana* plants. Red arrows indicate the magnification of leaf area. **F)** RT-PCR for virus detection in the plants inoculated with different recombinants, c- indicates negative control for PCR with H_2O, M represents 50 bp DNA mass marker with the arrow indicating the corresponding size band on the left.

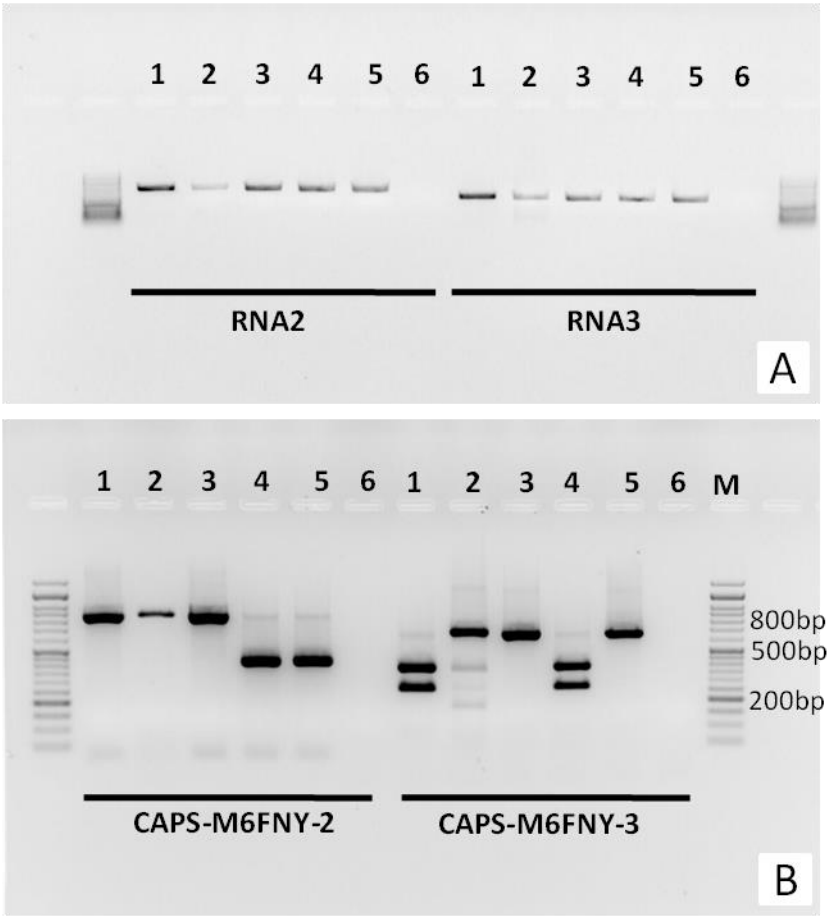

Figure R4-6. Confirmation of the infection and RNA origin of recombinants produced between CMV-M6 and CMV-FNY in *N. benthamiana*. A) RT-PCR amplification of RNA2 and RNA3 used to confirm the infection of *N. benthamiana* plants with pseudo recombinants; 1: F1F2F3; 2: CMV-M6; 3: F1F2M3; 4: F1M2F3; 5: F1M2M3 and 6: H_2O. B) CAPS markers to differentiate RNA2 and RNA3 between CMV-FNY and CMV-M6. M) 50 bp DNA Mass marker, corresponding size of some bands are listed on the right.

The sap from verified infected *N. benthamiana* plants was used to inoculate the cotyledons of the three testing melon lines PS, 20-91-15 (*cmv1/cmvqw3.1/cmvqw10.1*) and SC. At least, four biological replicates of each melon line were inoculated with each viral recombinant. The phenotype was recorded at 14 dpi.

The results summarizing all sets of experiments are listed in Table R4-1. All the recombinants could infect the susceptible melon line PS but with different infection degrees (Figure R4-7).

F1F2F3/F1'F2F3, F1F2F3/F1'F2M3 and CMV-M6 infected nearly all the PS plants with severe mosaic and leaf curling, while F1M2F3/F1'M2F3 and F1M2M3/F1'M2M3 were able to infect PS plants with only mild mosaic spots in all the leaves. Only the recombinant F1'F2M3 was able to infect all inoculated 20-91-15 plants, with mosaic and curling in all leaves (Figure R4-8). However, since there was no infection in line 20-91-15 inoculated with F1F2F3/F1'F2F3, we can only conclude that the viral factor of CMV-FNY that could overcome the resistance conferred by *cmv1, cmvqw3.1* and *cmvqw10.1* lay in RNA1 or RNA2. We could not determine the virulence in more detail with this information.

Table R4-1. Melon infection of viral recombinants produced between CMV-FNY and CMV-M6

	PS	20-91-15	SC
CMV-M6	15/15	0/15	0/15
F1F2F3	4/5	0/5	0/5
F1'F2F3	21/21	0/21	0/21
F1F2M3	5/5	0/5	0/5
F1'F2M3	4/4	4/4	0/4
F1M2F3	5/5	0/5	0/5
F1'M2F3	9/17	0/17	0/17
F1M2M3	5/5	0/5	0/5
F1'M2M3	4/8	0/8	0/8

Note: The numbers in the table indicate numbers of infected plants/ inoculated plants

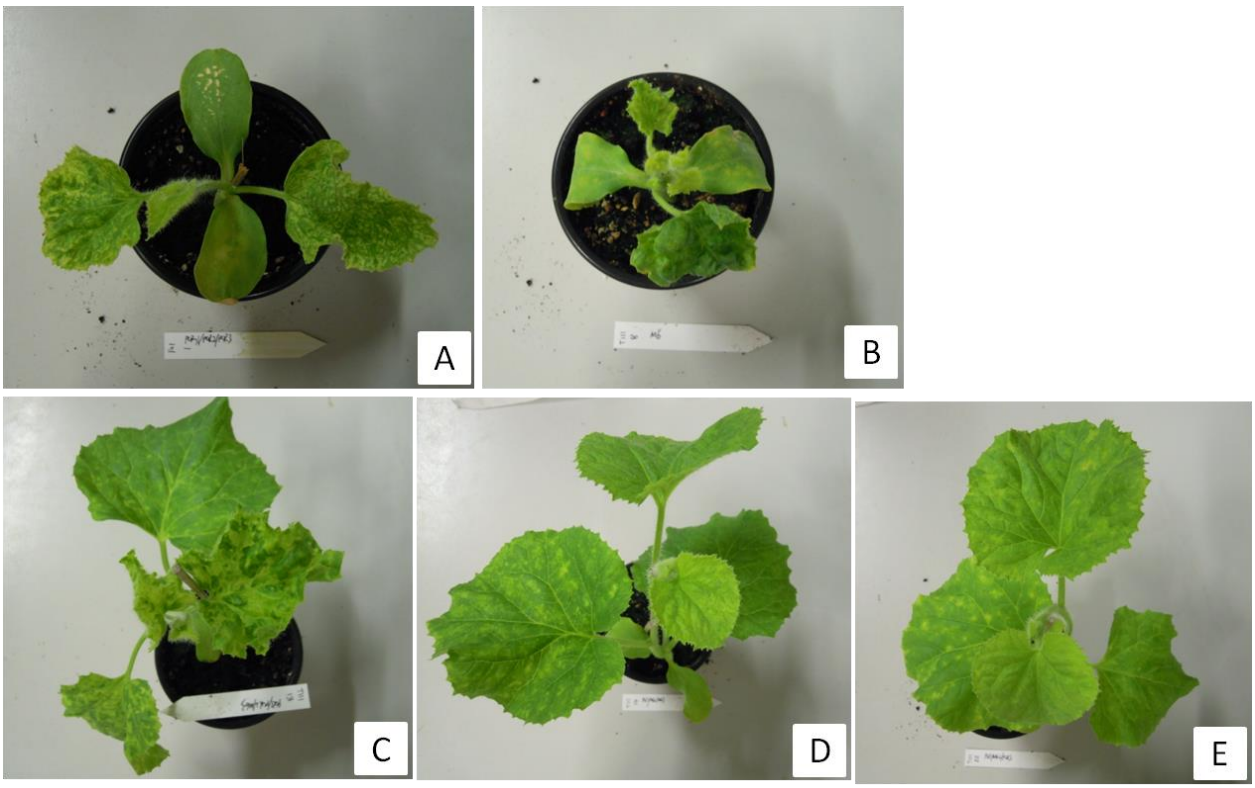

Figure R4-7. Phenotype of PS inoculated with viral recombinants between CMV-FNY and CMV-M6 A) F1F2F3, B) CMV-M6, C) F1F2M3, D) F1M2M3, E) F1M2F3.

Figure R4-8. Infection of melon lines PS, 20-91-15 and SC by the viral recombinant F1'F2M3

Since none of the recombinants containing F1 could infect the line 20-91-15, while the recombinant F1'F2M3, containing F1' from the construct pFny1 , was able to infect 20-91-15, we hypothesize that there was a problem in the F1 original vector pCR1(+). Therefore, the viral genome of the construct pCR1(+) was sequenced. A point mutation T to C was detected in pCR1(+) at position 2,568 compared to the original viral sequence of CMV-FNY RNA1 (Figure R4-9), but no mutation in F1' original vector pFny1 was found. This point mutation changes the amino acid from Met (ATG) to Thr (ACG) at position 825 in 1a protein, which is predicted as a deleterious change. This deleterious change might change the secondary structure or tertiary structure of the CMV 1a protein, hence affecting the virulence.

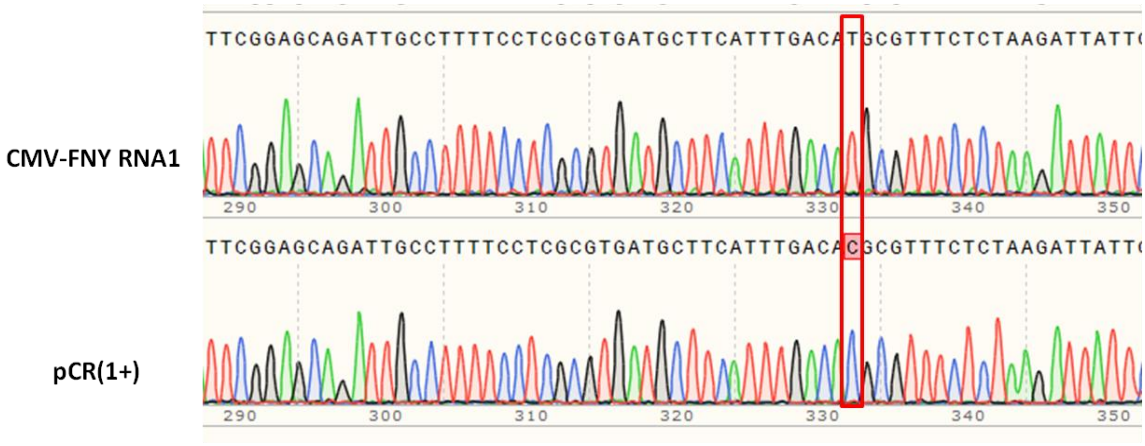

Figure R4-9. The point mutation detected in the binary vector pCR1(+) compared with the sequence of CMV-FNY RNA1. The red rectangle shows the T to C mutation.

IV.3.2 Recombinants produced between CMV-FNY and CMV-LS

Here, we aimed to produce the recombinants between CMV-FNY and CMV-LS to gain more knowledge about virulence determinants of CMV-FNY. RNA1 of CMV-FNY and all RNAs of CMV-LS were obtained using in vitro transcription as described in Material and Methods (section 8). RNA2 and RNA3 for CMV-FNY were based on agro-infiltration. The mixed inoculation was performed as described in Material and Methods (section 4.2). RNAs of CMV-FNY were represented by F1-F2-F3 and CMV-LS by L1-L2-L3.

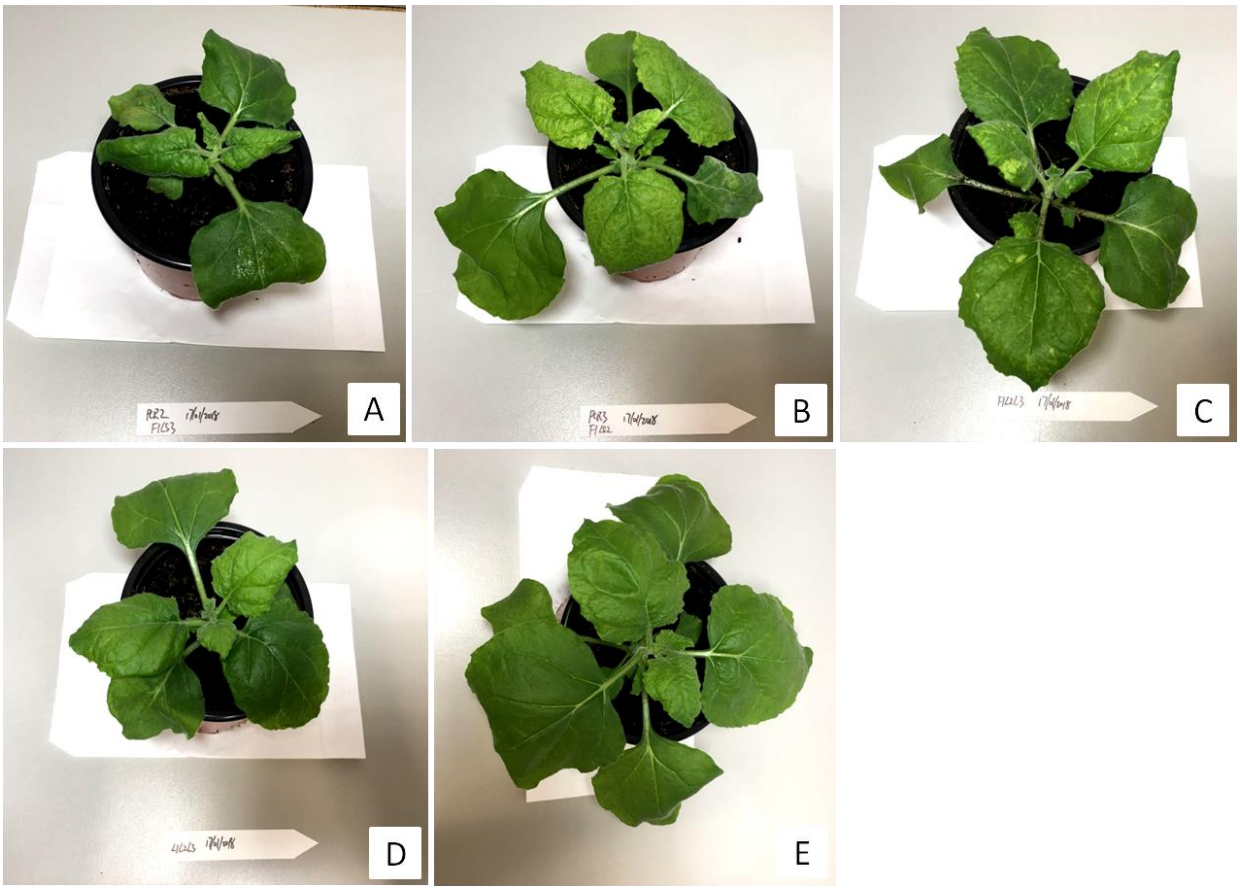

Figure R4-10. Phenotype of *N. benthamiana* plants inoculated with different viral recombinants between CMV-FNY and CMV-LS A**)** F1F2L3, B) F1L2F3, C) F1L2L3, D) L1L2L3 and E) mock inoculated.

Four out of eight possible recombinants were found able to infect *N. benthamiana* plants in this experiment set. The infection of *N. benthamiana* plants was recorded at 14 dpi (Figure R4-10). The recombinant F1F2L3 heavily infected *N. benthamiana* plants producing curling leaves and small plants. Recombinant F1L2F3 produced mosaic and yellowing in leaves, and F1L2L3 produced spotty mosaic. L1L2L3, resembling CMV-LS, could only produce mild mosaic symptoms. Sap from infected *N. benthamiana* new leaves was used to inoculate cotyledon of melon lines PS, 20-91-15 and SC as well as cotyledons of squash. The squash Chapin F1 (Semillas Fitó SA, Barcelona, Spain) could accumulate high amount of virus compared to *N. benthamiana*, making easier the mechanical inoculation. Three individuals of the melon lines and

two individuals of squash plants were inoculated with each viral recombinant at the same time. Only L1L2L3 and F1F2L3 produced the systemic infection symptoms on squash. Recombinant F1L2L3 produced mild mosaic in the first leaf of squash but the infection was disappearing and finally lost in the upper leaves. Thereafter, the systemically infected squash were also used as viral sap to inoculate cotyledon of melon lines PS, 20-91-15 and SC.

The infection of melon lines PS, 20-91-15 and SC by both *N. benthamiana* sap or by squash sap was recorded at 14 dpi and is summarized in Table R4-2. Two out of three and one out of three PS plants were infected by L1L2L3 and F1L2F3 using sap from infected *N.benthamiana*, respectively, while five out of five (hundred percent efficiency) PS were infected by L1L2L3 and F1L2F3 using sap from infected squash (Figure R4-11). The other recombinants did not produce visible infection symptoms. None of the recombinants infected 20-91-15 or SC.

Table R4-2 Melon infection with viral recombinants produced between CMV-FNY and CMV-LS

	PS	**20-91-15**	**SC**
F1F2L3	0/3	0/3	0/3
F1L2F3	1/3	0/3	0/3
F1L2L3	0/3	0/3	0/3
L1L2L3	2/3	0/3	0/3
F1F2L3 (squash)	5/5	0/5	0/5
L1L2L3 (squash)	5/5	0/5	0/5

Note: The numbers in the table indicated numbers of infected plants/ inoculated plants. F1F2L3 (squash) and L1L2L3 (squash) indicate the sap origin, whilst others with sap from *N.benthamiana*.

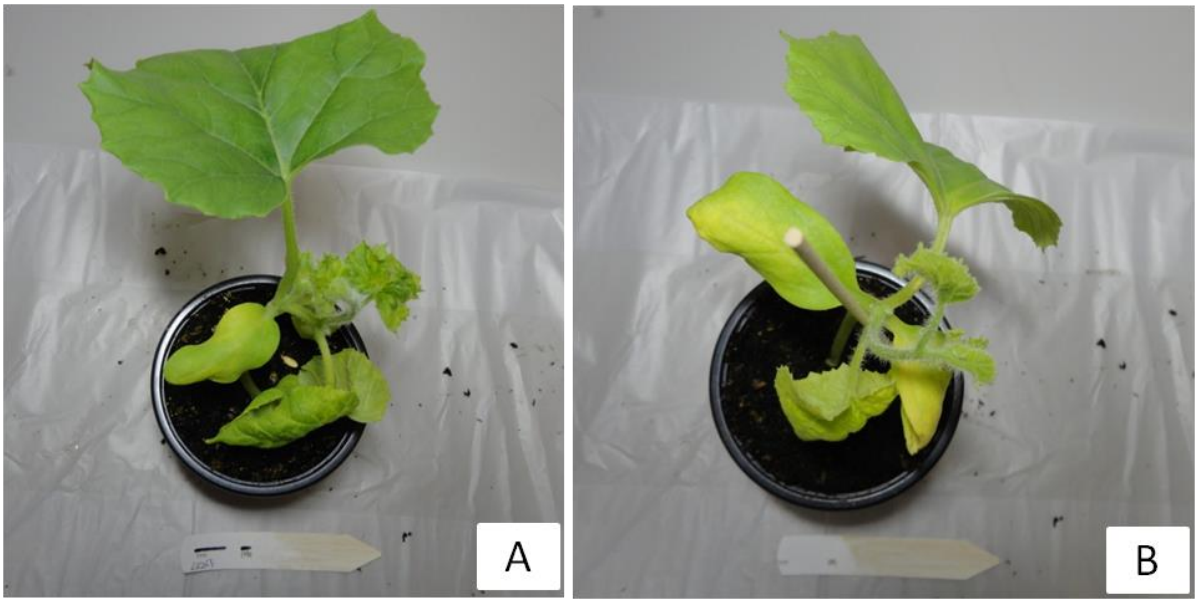

Figure R4-11. Infection of the melon line PS with viral recombinants produced between CMV-FNY and CMV-LS using infected squash as viral sap. A) L1L2L3 and B) F1F2L3**.**

This experiment did not give us enough information to identify the RNA that carries the determinant for *cmvqw3.1* and *cmvqw10.1*. Additionally, we found that squash infected by the viral recombinants produced in *N. benthamiana* plants, could produce a more efficient infection in melon plants and hence can be used as viral sap to inoculate melon plants to determine virulence in the following experiments.

Discussion

The resistance to CMV mediated by the gene *cmv1* was studied in our laboratory and was described as impairing the transport from the BS cells to the phloem. In this thesis, we have addressed the study of the resistance provided by the other QTLs present in the resistant accession, which is effective against CMV strains of subgroup I.

1. QTL analysis for the resistance to aggressive CMV-FNY strain

The resistance of SC to different CMV strains is complex. The recessive cmv1 allele was found to confer resistance to CMV subgroup II strains like CMV-LS and CMV-P9 (Essafi et al., 2009). However, cmv1 is insufficient to confer resistance to CMV subgroup I strains like CMV-M6 (Guiu-Aragonés et al., 2014). Two other QTLs have been described, cmvqw3.1 and cmvqw10.1, that together with cmv1 can confer resistance to CMV-M6. However, a more aggressive subgroup I strain, CMV-FNY, can overcome the resistance conferred by the three QTLs together (cmv1, cmvqw3.1 and cmvqw10.1). When dissecting the resistance of SC, we observed that some SC derived DHLs, DHL142 and DHL69 and SC itself were still resistant to CMV-FNY. Hence, we hypothesized that there must be other still unidentified QTLs conferring resistance to CMV-FNY.

F2 populations have been successfully used in QTL analysis for plant development, flowering, disease resistance or fruit ripening traits in different plants species as Arabidopsis thaliana (Kowalski et al., 1994; Rabanal et al., 2017), rice (Kitomi et al., 2015; McCormick, 2017), tomato (Wang et al., 2015; Soyk et al., 2017) and melon (Yuste-Lisbona et al., 2011; Vegas et al., 2013). The minimum size usually accepted for QTL mapping in a bi-parental population is 100 individuals. In this study, we aimed to identify the additional QTLs controlling CMV-FNY resistance by using multiple F2 populations made between different SC derived parental lines with population size between 78 to 120 individuals. Hence, the population and size of population in our study is surrounding the acceptable threshold, so we should expect a good performance.

Phenotyping for disease resistance or susceptibility is complex. In the literature, depending on the pathogen type or the severity of isolates, different disease evaluation categories have been applied. Some studies used qualitative traits (infected vs non-infected plants) for QTL analysis or map based cloning (Essafi et al., 2009; Rawat et al., 2016), but most of researches applied severity index ranging from no symptom, to slightly infection symptoms until strong severe plant

infection (Buerstmayr et al., 2002; Buerstmayr et al., 2003; Gutiérrez et al., 2015; Cockerton et al., 2018). Some indexes described are DSI (Disease Severity Index) (Friedmann et al., 1998; Anbinder et al., 2009; Cheng et al., 2017) and AUSPC (Area Under the Symptom Progress Curve (AUSPC) (Shaner and Finney, 1977; Dintinger et al., 2014; Sallam et al., 2016), where the later takes into account the progress and severity of the disease in a time course.

Phenotyping for CMV inoculated plants has been complex. The severity of CMV infection is affected by environmental factors, such as temperature (Zhao et al., 2016). Moreover, as an RNA virus, CMV has a relatively high mutation rate. Both genetic and environmental factors mentioned could influence the severity of CMV. In our studies, we observed that CMV-FNY sometimes could infect the resistant parental line SC with very mild mosaic symptoms in the first leaf. The F2 populations became infected with mild to severe symptoms, but not at the same level for all the populations tested. For this reason, we have evaluated all the aspects of the development of the disease, from the end-point qualitative trait infected vs non-infected, to the AUSPC that considers the evolution of symptomatology of each individual during the whole process. Despite the accuracy in the phenotypic evaluation, the use of an F2 population has some limitations, being the most important, the lack of biological replicates that can cause the appearance of false negatives, when some individuals escape the infection by rub inoculation. In a previous work for dissecting resistance of SC to CMV subgroup II strains, qualitative trait (infected or non-infected) was applied to evaluate CMV infection in the SC x PS NIL collection with at least five replicates per NIL (Essafi et al., 2009). In the analysis of SC resistance to subgroup I strain CMV-M6, the resistance was evaluated in the SC x PS DHL collection as a quantitative trait with different infection degrees, using 6-10 replicates for each DHL (Guiu-Aragonés et al., 2014). In both works, the evaluation of CMV infection using biological replicates increased the accuracy of phenotyping and the robustness of the QTL detection. In our QTL analysis, sets of around 100 individuals were inoculated for each F2 population without any replicate. This would probably cause a big effect even if only one or two individuals were false negatives, due to the size of the population. Therefore, the accuracy of disease evaluation for each individual could be the most feasible factor affecting the accuracy of our mapping results. In order to have robust data, F2:3 populations have been widely successfully used in QTL analysis for disease resistance (Huang et al., 2001; Li et al., 2001; Huynh et al., 2016; Kumar et al., 2017). The facilities at CRAG during this work did not allow us to perform the analysis of

F2:3, however we consider to continue the QTL analysis for the resistance to CMV-FNY, producing F2:3 populations based on the F2 population described before for QTL analysis to improve the results of this project.

The marker selection in our work was performed based on the previous knowledge of the genotype of our DHL collection, from which we selected markers in the segregating regions for each population. Since we have different segregating populations, we took advantage on the comparison between them to avoid the selection of markers in regions where one population was not segregating. After map construction for each population, the average distance between two markers varied from 6.3 cM (F2 population made from the cross DHL142 x DHL1046) to 11.9 cM (F2 population made from the cross DHL142 x 20-91-15). Most of the polymorphic regions were covered, however, we could not neglect that there were some small uncovered regions that could prevent the QTL detection if it was located in those regions.

QTL analysis resulted in several putative minor QTLs in different LGs, with LOD value comprises between 2.07 and 2.86. One putative QTL in LG II and another in LG XII were detected, using the infected vs non-infected phenotypic trait with LOD value of 2.80 and 2.86 respectively. QTLs in LG IX (LOD 2.15), LG X (LOD 1.62) and LG XII (LOD 2.07-2.26) were detected using the infection degree. Therefore, we were not able to see a consistent QTL using different phenotyping methods, or with high LOD values, which could guarantee its reliability. The QTL analysis to different CMV strains was also performed by Dogimont et al. (2000) using a 122 RILs collection made between SC and the susceptible Charentais type cultivar Védrantais . In their study, apart from the major QTL mapping in LG XII, several minor QTLs in LG II, LG III, LG VIII, LG IX and LG XII were detected putatively involved in the resistance to different CMV strains. Among these QTLs, most of them were related with CMV subgroup II resistance. Nevertheless, Essafi et al. (2009) demonstrated that cmv1 on its own is enough to confer resistance to these strains. Also, regarding the resistance to the CMV subgroup I strain CMV-M6, QTLs cmvqw3.1 and cmvqw10.1 were detected in a DHL population made between SC and PS (Guiu-Aragonés et al., 2014) and none of QTLs detected by Dogimont et al. (2000) in their RILs collection co-localized with cmvqw3.1or cmvqw10.1 (Guiu-Aragonés et al., 2014). Furthermore, few RILs were resistant to another subgroup I strain, CMV-TL (Dogimont et al., 2000), which suggests that using this RIL collection might hinder the QTL analysis to subgroup I CMV strains.

To test whether our QTL analysis system was capable for detecting minor QTLs responsible for CMV-FNY resistance, an F2 population made between DHL142 and DHL1046 was used. This population segregates for the previously known cmvqw10.1 QTL, and should present also some minor QTLs. The QTL analysis using this population resulted in one putative minor QTL in LG X, with LOD value equal to 2.40, corresponding to marker CMPSNP113. However, this SNP marker is outside of the described cmvqw10.1interval, which is located between the markers PS_15-H02 and CMPSNP183 (Guiu-Aragonés et al., 2014).The result suggests that our QTL detection is not sensitive enough for mining minor QTLs for resistance to CMV-FNY.

2. Re-sequencing of ILs

ILs containing combinations of two or three QTLs were re-sequenced, to confirm whether the QTLs have been successfully introgressed and whether there were unintended introgressions apart from the expected regions.

The ILs 5-123, 20-28-62 and 20-91-15, contain the desired SC intervals known to carry the resistance QTLs cmv1, cmvqw3.1 and cmvqw10.1in homozygosis. However, the introgressions were bigger than the QTL regions. During the development of these ILs, flanking markers were used for selecting the SC alleles in the QTL regions. However, although the genotype of these markers confirmed the desired regions, the regions outside of the QTL were not analyzed to ensure that no additional SC introgressions were unintendedly dragged. Additionally, some heterozygous and homozygous unintended introgressions were also detected. In 5-123, a small heterozygous region was found in LG VIII. In 20-28-62, some homozygous SC alleles were detected in LG III and LG VI. Even the region in LG III is inside the QTL cmvqw3.1, but far away from the peak of the QTL. Some heterozygous regions in LG II, LG VI, LG VII, LG VIII and LG X were also detected. In 20-91-15, homozygous SC alleles were detected in LG II, LG III, LG VI, LG VII, LG VIII and LG X. Some heterozygous regions in LG VI, LG VIII, LG IX, LG X and LG XII were also detected.

The PS x SC NIL collection and sub NILs were genotyped using a 768 SNPs set (Esteras et al., 2013) (J. Argyris, personal communication). In the line SC12-1-99, apart from cmv1, other two SC introgressions were from 28,267,327 to 28,907,412 in LG VII and from 20,566,525 to 21,676,078 in LG IX. In the line SC3-3, apart from cmvqw3.1, two SC regions, from 36,382,412 to 38,106,882 in LG VI and from 6,629,064 to 7,022,329 in LG VIII. The line SC10-2 was

missing for SNP genotyping (Argyris et al, personal communication). Therefore, we do not know what contaminant introgressions were present. Hence, we could conclude that in the ILs 5-123, 20-28-62 and 20-91-15, the contaminations in LG VI and LG VIII were originated from SC3-3, the contaminations in LG VII and LG IX were originated from SC12-1-99 while the other contaminations probably originated from SC10-2.

The ILs were also tested for the resistance to CMV-M6 and CMV-FNY. All the ILs were susceptible to CMV-FNY. Only 20-91-15 was resistant to CMV-M6 infection while the other two were susceptible (A. M. Martín-Hernández, personal communication). Both results indicate that our ILs contain the desired resistance QTL combinations and, despite the presence of some contaminant introgressions, they could be used for the characterization of the resistance mechanism of these QTLs. However, for fine mapping of cmvqw3.1 and cmvqw10.1, further works should be done to obtain introgression lines without background contaminations.

3. The resistance to subgroup I CMV strains

In this study, we aimed to characterize the resistance conferred by cmvqw3.1, cmvqw10.1 and unidentified QTLs to subgroup I CMV strains. The resistance of lines 5-123 (cmv1/cmvqw3.1), 20-28-62 (cmv1/cmvqw10.1) and 20-91-15 (cmv1/cmvqw3.1/cmvqw10.1) to CMV-FNY, which can overcome the resistance conferred by cmv1/cmvqw3.1/cmvqw10.1 was tested. By using CMV-FNY challenging different melon lines, we could advance in the understanding of the resistance mechanism of cmv1/cmvqw3.1/cmvqw10.1/unidentified QTLs, and whether and how the QTL combinations, cmv1/cmvqw3.1, cmv1/cmvqw10.1 and cmv1/cmvqw3.1/cmvqw10.1 could collaborate in the resistance.

Plant viruses are obligate intracellular parasites, dependent on their hosts (Moon and Park, 2016). Plant resistance or susceptibility to virus is an outcome of the interaction between plant host and viral factors. This interaction between viral particles and host factors will affect the virus replication, cell-to-cell movement and long-distance movement. Thereby, plant resistance or susceptibility is finally influenced. Different plant host factors have been described affecting either virus replication or virus movement (for a review see (Wang, 2015)). As it has been described that the replication and cell-to-cell movement of CMV-FNY is not affected in the resistant line SC (Guiu‐Aragonés et al., 2016), we concentrate on how these resistance QTLs affect the movement of CMV-FNY.

The delay in CMV-FNY infection observed in our experiments could not be due to different virus input in the inoculation, since we kept the inoculation conditions constant and the experiments were reproducible several times. We did not inoculate the melon lines using titrated virus, since we always inoculated first squash plants to produce fresh virus to inoculate melon. Instead, we always used the same area of squash-infected leaf, grinded in the same volume of DIECA buffer and inoculated the melon leaf by rub-inoculation making the same number of rubs on the leaf. This, together with the fact that in repeated experiments, the relative virus accumulation was reproducible, indicated that the differences in virus accumulation in the phloem of the different lines was not due to different virus input during the inoculation.

The delay of infection in melon lines harboring resistance QTL combinations (cmv1/cmvqw3.1, cmv1/cmvqw10.1 and cmv1/cmvqw3.1/cmvqw10.1) compared with PS indicated that the resistance plant factors cmvqw3.1 and cmvqw10.1 were affecting the efficiency of movement of CMV-FNY, but were not sufficient to stop CMV-FNY systemic infection. For this, additional resistance QTLs should be involved as is the case of the resistant parental line SC, which carries all of them.

In both CMV-FNY resistant and susceptible melon lines, equivalent virus accumulation in the proximal and distal petioles of the inoculated leaves was detected. This indicated that the resistance was not working in the phloem movement but in phloem entry, similarly to cmv1-mediated resistance to CMV-LS. In this case, by immunogold experiments, Guiu-Aragonés et al. (2016) demonstrated that the virus remained restricted to the BS cells, and was not able to proceed to the phloem cells. Given that the characterization of the resistance conferred by cmv1/cmvqw3.1/cmvqw10.1/additional QTLs, indicates that the same phloem entry step is impaired, we foresee that the virus will be delayed in the BS cells again. To demonstrate this, further work should be done using immunogold labeling at TEM experiments, to quantify and compare CMV-FNY accumulation in the BS cells and in vascular parenchyma and companion cells. Our hypothesis is that CMV-FNY will be present in the phloem cells, but in much lower amount than in BS cells.

Though SC is resistant to CMV-FNY, some viruses could still be detected in the petioles of SC compared with non-inoculated melon plants. This results indicated that small amounts of viruses could still enter the phloem of the resistant line even though they could not produce a systemic infection. The effective population size is defined as the number of individuals that

could pass their genes to the next generation (Elena and Sanjuán, 2007). Effective population size is a key parameter and could be affected during all the virus infection steps (Tamisier et al., 2017). For a successful virus infection, virus has to enter into plant cells, invade from cell-to-cell and long distance movement. During these steps, the effective population size will decrease caused by the plant natural defense system or other plant genetic factors (Tamisier et al., 2017). Hence, although some virus could enter into the phloem of the resistant accession SC, they might not be able to accumulate and move to the following infection site to produce a systemic infection. This could also explain why the infection do not move to the SC upper leaves despite sometimes mild infection was observed in the first leaf.

During the infection assay, few SC or DHL142 plants were infected by CMV-FNY. Under normal inoculation conditions, CMV strain CMV-Ns is not able to infect *N. tabacum* cv. Xanthi plants. However, the *N. tabacum* cv. Xanthi plants were systemically infected by CMV-Ns when inoculated using a highly concentrated purified virion as inoculum (Salánki et al., 2007). Hence, we hypothesize there might be also a threshold that could affect the resistance capacity of SC. Our hypothesis was confirmed by increasing the CMV-FNY amount via co-inoculation of CMV-FNY and ZYMV, which produces a the synergism between these two viruses (Wang et al., 2004). After increasing CMV-FNY amount, all the SC plants were infected with detectable CMV-FNY accumulation in systemic leaves. Therefore, we can conclude that the resistant line SC could also be infected by non-infectious CMV after increasing virus input. In nature, though such virus concentration is not possible, we should keep in mind that mixed infections between CMV and other viruses could probably lead to an increase of infection severity (Mascia et al., 2010; Takeshita et al., 2012) or even break the resistance (Butterbach et al., 2014) as the case of CMV-FNY in SC.

4. CMV virulence determinants

The systemic infection of plant viruses is determined by the interaction between plant host factors and viral particles. Nearly all the CMV proteins 1a, 2a, 2b, 3a (MP), CP and satellite RNAs have been reported as the virulence factors (for a review see (Mochizuki and Ohki, 2012)). Some of the amino acids and nucleotide changes reported were involved in changing the severity of the infection symptoms, whereas other changes were able to break resistance (Table D-1). Chimeric viruses have been successfully used as a tool to genetically determine the

virulence of CMV against resistance genes (Kang et al., 2012; Guiu‐Aragonés et al., 2015). The use of pseudo recombinants between CMV-FNY and CMV-LS, allowed to map cmv1 dependent determinants of virulence in RNA3. The chimaeras exchanging independently 5'UTR, 3'UTR, Intergenic region, MP or CP of RNA3 demonstrated that the MP was the factor responsible for overcoming cmv1 resistance (Guiu‐Aragonés et al., 2015).

Table D-1. Amino acids and nucleic acids in CMV genes involved in virulence (Updated from (Mochizuki and Ohki, 2012))

Gene	Strain	Original symptom	Substitution or deletion	Resulting symptom	Plant species	Reference
1a	Rs (I)	Mosaic	R461C	Necrosis	*Nicotiana glutinosa*	(Divéki et al., 2004)
2a	Fny (IA)	Chlorotic spot	I267T	Mosaic	Squash	(Choi et al., 2005)
	Fny (IA)	Mosaic	aa 777–858 deletion	Attenuated	*N. glutinosa*	(Du et al., 2008)
2b	Fny (IA)	Mosaic	aa 95–100 deletion	Chlorosis	*N. tabacum*	(Lewsey et al., 2009)
	HL (IB)	Necrosis	aa 71–111 deletion	Attenuated	*A. thaliana*	(Inaba et al., 2011)
3a	Fny (IA)	Mosaic	N51K and I240F	No cycling	*N. tabacum*	(Gal-On et al., 1996)
	Fny (IA)	Mosaic	I168T	Chlorosis	Squash	(Choi et al., 2005)
	LS (II)	No infection	SNNLL64-68HGRIA, R81C, G171T and A195I	Systemic mosaic	*Cucumis.melo*	(Guiu-Aragonés et al., 2015)
CP	Fny (IA)	Mosaic	D192K	Systemic necrosis	N. tabacum	(Liu et al., 2002)
			L194K	Yellow mosaic, necrotic flecks		
sat RNA	Y-sat	Chlorosis	Mutations in nt 177–199	Attenuated	*Nicotiana* species	(Shimura et al., 2011)

In our study, we aim to determine the viral factor(s) responsible(s) for breaking *cmv1/cmvqw3.1/cmvqw10.1* resistance. CMV-FNY could break *cmv1/cmvqw3.1/cmvqw10.1* resistance while CMV-M6 could not. The nucleotide sequence similarity of CMV-FNY and

CMV-M6 was reported to 98.5%. The melon line 20-91-15 (*cmv1/cmvqw3.1/cmvqw10.1*) was interrogated using pseudo recombinants between CMV-M6 and CMV-FNY to map the determinant factors. Among the obtained pseudo recombinants, F1F2M3 was unable to infect the melon line harboring *cmv1/cmvqw3.1/cmvqw10.1*, which indicated that the virulence factor responsible for overcoming *cmv1/cmvqw3.1/cmvqw10.1*-mediated resistance is not in RNA3. RNA 3 encodes MP and CP, which are identical in M6 and FNY and therefore, could not be the determinant in this case. However, the results also exclude the untranslated sequences of this RNA as determinants of virulence for *cmvqw3.1/cmvqw10.*l.

The protein 1a contains putative methyltransferase and helicase motifs and has been described as virulence factor in some studies. The amino acid changes at position 461 of 1a protein play roles in inducing necrosis (R461C) (Divéki et al., 2004), replication inhibition (C461E, C461P and C461N) and systemic symptom development (C461K, C461R) in some *Nicotiana* species (Salánki et al., 2007). In pepper, *Cmr1* gene could inhibit the systemic infection of CMV-FNY but not CMV-P1. Six amino acids substitution in the helicase domain of 1a protein determines the virulence of CMV-P1 against theresistance *Cmr1* gene (Kang et al., 2012). In our case, the helicase domain might also be the virulence determinant in overcoming *cmv1/cmvqw3.1/cmvqw10.1* resistance. During the process of producing pseudo recombinants between CMV-M6 and CMV-FNY, a binary vector pCR1(+) (Seo et al., 2009) was used to produce CMV-FNY RNA1. However, all the pseudo recombinants, even in the combination F1F2F3, which is FNY, failed to produce infection in the melon line 20-91-15. After sequencing the binary vector pCR1(+), a T to C point mutation was found at position 2568 compared with the sequence of CMV-FNY RNA1. This point mutation alters the amino acid from Met (ATG) to Thr (ACG) at position 825 in 1a protein, which is predicted as a deleterious change by online software PROVEAN (Protein Variation Effect Analyzer) (http://provean.jcvi.org/seq_submit.php). This deleterious change might change the secondary or tertiary structure of CMV 1a. If the structure of CMV 1a is changed, the interaction between CMV 1a and 2a protein as well as with other plant host factors might also be affected. CMV replicase consists of CMV 1a, 2a and a plant host factor, which in together are involved in CMV replication (Hayes and Buck, 1990). .

Other amino acid residues in CMV 1a were also reported as virulence factors involved in cell-to-cell movement or systemic symptom development. *Cmr1* confers resistance to CMV-P0 and

CMV-FNY in pepper (Kang et al., 2010), but not to CMV-P1. Amino acid residues at positions 865, 896, 957, and 980 in the helicase domain of CMV-P1 1a protein were identified as responsible for overcoming *Cmr1*-mediated resistance (Kang et al., 2012). This difference between CMV-FNY and CMV-P1 in helicase domain affected the virus cell-to-cell movement and also was involved in virus replication (Kang et al., 2012). Therefore, the point mutation at amino acid position 825 of 1a protein could act in our system as the virulence factor overcoming *cmv1/cmvqw3.1/cmvqw10.1* resistance. Experiments are being carried out to generate a pCR1+ construct with a restored T at position 2568 to check this possibility. If the restored construct is able to overcome the resistance given by the QTLs, it is likely that the helicase domain of 1a could be the determinant of virulence. However, as we still lack the information about whether the recombinant F1M2M3 could infect melon lines harboring *cmv1/cmvqw3.1/cmvqw10.1*, we could not exclude the possibility of CMV-FNY 2a,2b or UTRs being the determinants. CMV 2a was previously reported as virulence factor involved in the CMV replication and cell-to-cell movement (Choi et al., 2005) or induction of CMV infection (Du et al., 2008). The CMV 2b protein is an RNA silencing suppressor that plays roles in CMV accumulation and virulence (Du et al., 2008; Xu et al., 2013; Du et al., 2014; Dong et al., 2016).

In our production of pseudo recombinants between CMV-M6 and CMV-FNY, only three out of six recombinants were obtained. None of the recombinants containing CMV-M6 RNA1 could be obtained in our process, which might be caused by lack of function of the *in vitro* transcribed CMV-M6 RNA1. To our knowledge, the RNA1 of many CMV strains was unstable as clone and prone to recombine. Hence, some recombination might have also occurred in the M6 RNA1 construct during its propagation. This will be confirmed by sequencing the construct. In this study, we also tried to obtain the pseudo recombinants between CMV-FNY and CMV-LS, however, we could only get three of them. Guiu-Aragonés et al., (2015) failed to obtain all possible recombinants between CMV-FNY and CMV-LS, generating only four out of six possible recombinants, since F1L2F3 and L1F2F3 were not obtained (Guiu‐Aragonés et al., 2015). In our case, F1L2F3 was obtained but finally it was found less infective in the infection assay, which resulted in only one out of three PS plants infected. We also found that the infection of melon plants with recombinants, even F1F2F3, showed most of the time only mild infection using infected *N. benthamiana* as source of sap. We tried to inoculate squash plants first with the sap of recombinants from *N. benthamiana* and then inoculate melon plants with sap from squash.

We found that the infected squash had high infection efficiency (100%) and more severe symptoms compared with the infection using sap from infected *N. benthamiana*. Thereafter, although in most cases, more virus passages are not recommended, in this case, using infected squash to infect melon plants for the determination of virulence might be an option.

5. Arms race co-evolution between plants and CMV

Natural biodiversity is a driver for host-pathogen co-evolution (Karasov et al., 2014). Elucidating and understanding this correlation between crops and pathogens would help for using genetic tools to modify crops to gain resistance against diseases (Rausher, 2001). In crops the plant-pathogen co-evolution has been described for many systems. For example, between cereals and *Blumeria graminis* (Wyand and Brown, 2003), flax and flax rust (Ravensdale et al., 2011), different crop plants and *Potato virus Y* (PVY) (for a review see (Quenouille et al., 2013)). PVY is an economically important plant pathogen that could cause severe infection in plenty of crop species. PVY is divided into PVY-0, PVY-1 and PVY1.2 subgroups according to their infectivity in pepper plants (Kyle and Palloix, 1997). A few resistant genes *pvr2 (*Ruffel et al., 2002), *Pvr4* (Caranta et al., 1996) and some other QTLs (Quenouille et al., 2014; Tamisier et al., 2017) have been described in pepper conferring resistance to different PVY pathotypes. The recessive gene *pvr2*, encoding the eukaryotic translation initiation factor 4E (eIF4E) gene, confers resistance to PVY-0 and PVY-1 pathotypes (Ruffel et al., 2002). However, different amino acid changes in the genome-linked viral protein (VPg) allow PVY to overcome *pvr2*-mediated resistance (Moury et al., 2004; Ayme et al., 2006; Ayme et al., 2007). Dominant *Pvr4* gene was reported as a broad spectrum resistance gene to nearly all PVY pathotypes and has being used for long time in pepper breeding. Some molecular markers linked to *Pvr4* were also developed for the breeding programs (Arnedo-Andrés et al., 2002; Devran et al., 2015). On the viral part, a nucleotide change (A8424G) in the NIb protein (RNA-dependent RNA polymerase) of PVY was sufficient for PVY to overcome *Pvr4*-provided resistance (Janzac et al., 2010). However, the combination of major resistance genes with some minor QTLs was proposed to provide rationale resistance, which could be a valuable tool being used in breeding (Quenouille et al., 2014).

The arms race co-evolution between CMV and crops also exists. CMV could be classified into subgroup I and subgroup II (Palukaitis et al., 1992). . Generally, subgroup I strains are more

aggressive than subgroup II strains. Subgroup I strains produce severe mosaic or stunt infection and subgroup II strains showed only mild mosaic or even symptomless infection (Mochizuki and Ohki, 2012). Co-evolution of CMV virulence factors and resistance genes has been described in different crop species. In pepper, a single dominant gene *Cmr1* was confers resistance to CMV-P0, CMV-Korean and CMV-FNY. *Cmr1* prevents virus systemic infection by inhibiting virus cell-to-cell movement from the epidermal cell layer to mesophyll cells (Kang et al., 2010). After *Cmr1* had been used in a breeding program for more than 20 years, another CMV strain, CMV-P1, able to break *Cmr1* conferred resistance, emerged (Lee et al., 2006). Four amino acid changes in the helicase domain of CMV-P1 1a protein were sufficient for overcoming *Cmr1* resistance (Kang et al., 2012). However, an Indian *C. annuum* landrace "Lam32" was found to resist CMV-P1 infection and this resistance was controlled by a single recessive resistance gene *cmr2*, which had a broad spectrum resistance, including resistance to CMV-P0, CMV-Korean and CMV-FNY (Choi et al., 2018). In melon, the accession SC is resistant to CMV (Karchi et al., 1975) but with strain-specific resistance (Díaz et al., 2003). The single recessive resistance gene *cmv1* confers resistance to CMV subgroup II strains (Essafi et al., 2009). *Cmv1* works as a gatekeeper in the BS cells, the susceptible allele *CMV1* being used by CMV-LS to be transported to the phloem, and the resistant allele, *cmv1*, not allowing such transport and affecting the virus long-distance movement (Guiu‐Aragonés et al., 2016). However, *cmv1* mediated resistance could be broken by CMV-M6 and CMV-FNY, being the MP the virulence factor involved. Therefore, *cmv1* resistant allele is only able to restrict the virus in the BS cells if MP LS is present, but MP M6 is able to use it for its transport to the phloem (Guiu‐Aragonés et al., 2015). Other two plant factors, *cmvqw3.1* and *cmvqw10.1* were needed working together with *cmv1* to confer resistance to CMV-M6 (Guiu-Aragonés et al., 2014). However, the subgroup I strain CMV-FNY must carry a new determinant of virulence that enables it to overcome the resistance determined by *cmv1/cmvqw3.1/cmvqw10.1*, although these QTLs are able to delay the virus and decrease CMV-FNY accumulation (Results, part III).

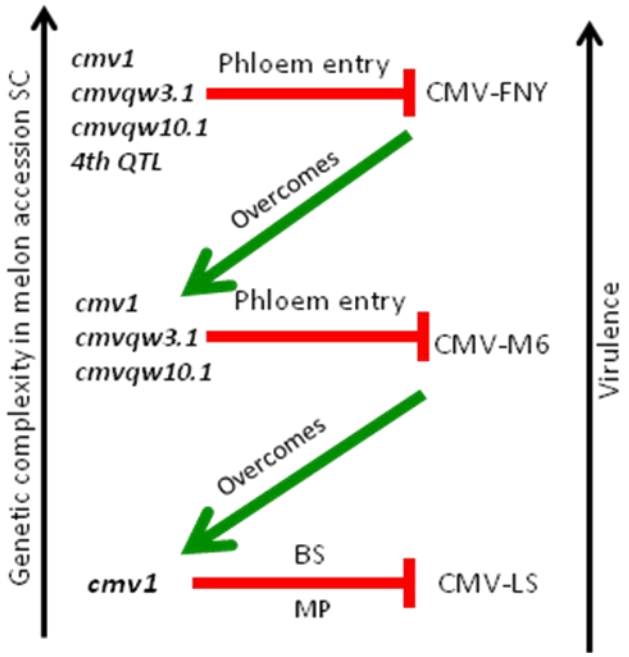

Figure D1-1. Arms race between melon SC and CMV.

MP, Movement Protein; BS, Bundle Sheath cells.

According to our results, *cmvqw3.1 and cmvqw10* act in the same step than *cmv1*, either impairing or stopping viral phloem entry, suggesting a new layer of resistance added to the same mechanism. However, at least another QTL is present in SC to provide full resistance to FNY. Whether or not this new QTL would be a new layer of resistance to prevent FNY phloem entry, remains to be seen. However, still, the CMV "Song" strains can overcome SC resistance. Therefore, they must have other determinants of virulence that enable them to overcome all the resistance layers built by SC.

Conclusions

1. A screening for resistance to the strain CMV-FNY was performed in a DHL population made between PS and SC. Two lines, DHL142 and DHL69 showed resistance to this CMV strain, which demonstrates the existence of a fourth QTL in the resistant parental accession SC.

2. The use of several F_2 populations made from the crosses DHL142 x DHL2012, DHL142 x 20-90-15 and DHL69 x DHL2012 failed to detect QTLs of small effect. Only several putative minor QTLs for resistance to CMV-FNY in LG II, LG IX, LG X and LG XII were found. However, they were not consistently detected using different phenotyping data or in different F_2 populations.

3. The complexity of the phenotyping coupled to the use of F_2 populations, preventing biological replicates, could be the cause of the failure of the QTL detection method.

4. The ILs 5-123 (*cmv1/cmvqw3.1*), 20-28-62 (*cmv1/cmvqw10.1*) and 20-91-15 (*cmv1/cmvqw3.1/cmvqw10.1*) were produced via marker assisted selection. The re-sequencing of these three ILs revealed that the SC introgressions were larger than expected, and some unintended heterozygous and homozygous SC contaminations were observed.

5. Only IL 20-91-15 was resistant to CMV-M6 and all the ILs were susceptible to CMV-FNY, therefore ILs were suitable for the characterization of the resistance conferred by all QTL combinations.

6. A delay of the systemic infection of CMV-FNY, compared with the susceptible melon line PS, was observed in the ILs 5-123, 20-28-62 and 20-91-15, indicating that the resistance QTL combinations are able to delay the movement of CMV-FNY.

7. The delay of infection correlates with a decrease in the amount of virus in the petiole of the inoculated leaf.

8. The combinations of QTLs for resistance to CMV-FNY in lines 5-123, 20-28-62, 20-91-15 participate in restricting the phloem entry, rather than in restricting the viral movement within the phloem.

9. An increase in CMV-FNY accumulation, mediated by a co-infection with ZYMV, allows CMV-FNY to break the resistance mediated by all QTLs in SC, suggesting the existence of a threshold of virus amount beyond which the resistance can be overcome.

10. Among the pseudo recombinants generated between CMV-FNY and CMV-M6, the recombinant F1F2M3 could infect the IL 20-91-15, indicating that the virulence determinants against the resistance conferred by *cmv1/cmvqw3.1/cmvqw10.1* did not map in RNA3.

Bibliography

Bibliography

Ahlquist P, Dasgupta R, Kaesberg P (1981) Near identity of 3′ RNA secondary structure in bromoviruses and cucumber mosaic virus. Cell **23:** 183-189

Ali A, Kobayashi M (2010) Seed transmission of Cucumber mosaic virus in pepper. Journal of virological methods **163:** 234-237

Alonso-Prados J, Fraile A, Garcia-Arenal F (1997) Impact of cucumber mosaic virus and watermelon mosaic virus 2 infection on melon production in Central Spain. Journal of Plant Pathology**:** 131-134

Anbinder I, Reuveni M, Azari R, Paran I, Nahon S, Shlomo H, Chen L, Lapidot M, Levin I (2009) Molecular dissection of Tomato leaf curl virus resistance in tomato line TY172 derived from Solanum peruvianum. Theoretical and Applied Genetics **119:** 519-530

Anderson P, Morales F (1994) The Emergence of New Plant Diseases: The Case of Insect‐transmitted Plant Viruses. Annals of the New York Academy of Sciences **740:** 181-194

Andreev IA, Hyon Kim S, Kalinina NO, Rakitina DV, Fitzgerald AG, Palukaitis P, Taliansky ME (2004) Molecular interactions between a plant virus movement protein and RNA: force spectroscopy investigation. J Mol Biol **339:** 1041-1047

Arazi T, Slutsky SG, Shiboleth YM, Wang Y, Rubinstein M, Barak S, Yang J, Gal-On A (2001) Engineering zucchini yellow mosaic potyvirus as a non-pathogenic vector for expression of heterologous proteins in cucurbits. Journal of biotechnology **87:** 67-82

Argyris JM, Ruiz-Herrera A, Madriz-Masis P, Sanseverino W, Morata J, Pujol M, Ramos-Onsins SE, Garcia-Mas J (2015) Use of targeted SNP selection for an improved anchoring of the melon (Cucumis melo L.) scaffold genome assembly. Bmc Genomics **16:** 4

Arnedo-Andrés M, Gil-Ortega R, Luis-Arteaga M, Hormaza J (2002) Development of RAPD and SCAR markers linked to the Pvr4 locus for resistance to PVY in pepper (Capsicum annuum L.). Theoretical and Applied Genetics **105:** 1067-1074

Ayme V, Petit-Pierre J, Souche S, Palloix A, Moury B (2007) Molecular dissection of the potato virus Y VPg virulence factor reveals complex adaptations to the pvr2 resistance allelic series in pepper. Journal of General Virology **88:** 1594-1601

Ayme V, Souche S, Caranta C, Jacquemond M, Chadœuf J, Palloix A, Moury B (2006) Different mutations in the genome-linked protein VPg of Potato virus Y confer virulence on the pvr23 resistance in pepper. Molecular plant-microbe interactions **19:** 557-563

Azadi P, Otang NV, Supaporn H, Khan RS, Chin DP, Nakamura I, Mii M (2011) Increased resistance to cucumber mosaic virus (CMV) in Lilium transformed with a defective CMV replicase gene. Biotechnology letters **33:** 1249-1255

Blanca J, Esteras C, Ziarsolo P, Pérez D, Collado C, de Pablos RR, Ballester A, Roig C, Cañizares J, Picó B (2012) Transcriptome sequencing for SNP discovery across Cucumis melo. BMC genomics **13:** 280

Boissot N, Thomas S, Sauvion N, Marchal C, Pavis C, Dogimont C (2010) Mapping and validation of QTLs for resistance to aphids and whiteflies in melon. Theoretical and Applied Genetics **121:** 9-20

Bos L, Maat D (1974) A strain of cucumber mosaic virus, seed-transmitted in beans. Netherlands Journal of Plant Pathology **80:** 113-123

Branham SE, Levi A, Katawczik M, Fei Z, Wechter WP (2018) Construction of a genome-anchored, high-density genetic map for melon (Cucumis melo L.) and identification of Fusarium oxysporum f. sp. melonis race 1 resistance QTL. Theoretical and Applied Genetics **131:** 829-837

Brotman Y, Normantovich M, Goldenberg Z, Zvirin Z, Kovalski I, Stovbun N, Doniger T, Bolger AM, Troadec C, Bendahmane A (2013) Dual resistance of melon to Fusarium oxysporum races 0 and 2 and to Papaya ring-spot virus is controlled by a pair of head-to-head-oriented NB-LRR genes of unusual architecture. Molecular plant **6:** 235-238

Brotman Y, Silberstein L, Kovalski I, Klingler J, Thompson G, Katzir N, Perl-Treves R (2000) Linkage groups of Cucumis melo, including resistance gene homologues and known genes. *In* VII Eucarpia Meeting on Cucurbit Genetics and Breeding 510, pp 441-448

Brouwer D, Clair DS (2004) Fine mapping of three quantitative trait loci for late blight resistance in tomato using near isogenic lines (NILs) and sub-NILs. Theoretical and Applied Genetics **108:** 628-638

Bibliopraphy

Bubici G, Carluccio AV, Stavolone L, Cillo F (2017) Prosystemin overexpression induces transcriptional modifications of defense-related and receptor-like kinase genes and reduces the susceptibility to Cucumber mosaic virus and its satellite RNAs in transgenic tomato plants. PloS one **12:** e0171902

Buerstmayr H, Lemmens M, Hartl L, Doldi L, Steiner B, Stierschneider M, Ruckenbauer P (2002) Molecular mapping of QTLs for Fusarium head blight resistance in spring wheat. I. Resistance to fungal spread (Type II resistance). Theoretical and Applied Genetics **104:** 84-91

Buerstmayr H, Steiner B, Hartl L, Griesser M, Angerer N, Lengauer D, Miedaner T, Schneider B, Lemmens M (2003) Molecular mapping of QTLs for Fusarium head blight resistance in spring wheat. II. Resistance to fungal penetration and spread. Theoretical and Applied Genetics **107:** 503-508

Butterbach P, Verlaan MG, Dullemans A, Lohuis D, Visser RG, Bai Y, Kormelink R (2014) Tomato yellow leaf curl virus resistance by Ty-1 involves increased cytosine methylation of viral genomes and is compromised by cucumber mosaic virus infection. Proceedings of the National Academy of Sciences **111:** 12942-12947

Canto T, Prior DA, Hellwald K-H, Oparka KJ, Palukaitis P (1997) Characterization of Cucumber mosaic virus. Virology **237:** 237-248

Caranta C, Palloix A, Gebre-Selassie K, Lefebvre V, Moury B, Daubeze A (1996) A complementation of two genes originating from susceptible Capsicum annuum lines confers a new and complete resistance to pepper veinal mottle virus. Phytopathology **86:** 739-743

Caranta C, Pflieger S, Lefebvre V, Daubeze A, Thabuis A, Palloix A (2002) QTLs involved in the restriction of cucumber mosaic virus (CMV) long-distance movement in pepper. Theoretical and Applied Genetics **104:** 586-591

Carr JP, Gal-On A, Palukaitis P, Zaitlin M (1994) Replicase-mediated resistance to cucumber mosaic virus in transgenic plants involves suppression of both virus replication in the inoculated leaves and long-distance movement. Virology **199:** 439-447

Cha-um S, Srianan B, Pichakum A, Kirdmanee C (2009) An efficient procedure for embryogenic callus induction and double haploid plant regeneration through anther culture of Thai aromatic rice (Oryza sativa L. subsp. indica). In Vitro Cellular & Developmental Biology-Plant **45:** 171-179

Chang C-W, Wang Y-H, Tung C-W (2017) Genome-wide single nucleotide polymorphism discovery and the construction of a high-density genetic map for melon (Cucumis melo L.) using genotyping-by-sequencing. Frontiers in plant science **8:** 125

Chaturvedi S, Seo J-K, Rao A (2016) Functionality of host proteins in Cucumber mosaic virus replication: GAPDH is obligatory to promote interaction between replication-associated proteins. Virology **494:** 47-55

Chen JQ, Rahbé Y, Delobel B, Sauvion N, Guillaud J, Febvay G (1997) Melon resistance to the aphid Aphis gossypii: behavioural analysis and chemical correlations with nitrogenous compounds. Entomologia Experimentalis et Applicata **85:** 33-44

Cheng P, Gedling CR, Patil G, Vuong TD, Shannon JG, Dorrance AE, Nguyen HT (2017) Genetic mapping and haplotype analysis of a locus for quantitative resistance to Fusarium graminearum in soybean accession PI 567516C. Theoretical and Applied Genetics **130:** 999-1010

Chikh-Rouhou H, González-Torres R, Oumouloud A, Alvarez JM (2011) Inheritance of race 1.2 Fusarium wilt resistance in four melon cultivars. Euphytica **182:** 177

Choi S, Lee J-H, Kang W-H, Kim J, Huy HN, Park S-W, Son E-H, Kwon J-K, Kang B-C (2018) Identification of Cucumber mosaic resistance 2 (cmr2) that confers resistance to a new Cucumber mosaic virus isolate P1 (CMV-P1) in pepper (Capsicum spp). Frontiers in Plant Science **9:** 1106

Choi SK, Palukaitis P, Min BE, Lee MY, Choi JK, Ryu KH (2005) Cucumber mosaic virus 2a polymerase and 3a movement proteins independently affect both virus movement and the timing of symptom development in zucchini squash. Journal of general virology **86:** 1213-1222

Cillo F, Roberts IM, Palukaitis P (2002) In situ localization and tissue distribution of the replication-associated proteins of Cucumber mosaic virus in tobacco and cucumber. Journal of virology **76:** 10654-10664

Clark LJ, Price AH, Steele KA, Whalley WR (2008) Evidence from near-isogenic lines that root penetration increases with root diameter and bending stiffness in rice. Functional Plant Biology **35:** 1163-1171

Claveria E, Garcia-Mas J, Dolcet-Sanjuan R (2005) Optimization of cucumber doubled haploid line production using in vitro rescue of in vivo induced parthenogenic embryos. Journal of the American Society for Horticultural Science **130:** 555-560

Bibliopraphy

Cockerton HM, Vickerstaff RJ, Karlström A, Wilson F, Sobczyk M, He JQ, Sargent DJ, Passey AJ, McLeary KJ, Pakozdi K (2018) Identification of powdery mildew resistance QTL in strawberry (Fragaria× ananassa). Theoretical and Applied Genetics **131:** 1995-2007

Cuozzo M, O'Connell KM, Kaniewski W, Fang R-X, Chua N-H, Tumer NE (1988) Viral protection in transgenic tobacco plants expressing the cucumber mosaic virus coat protein or its antisense RNA. Nature Biotechnology **6:** 549

Daryono B, Somowiyarjo S, Natsuaki K (2003) New source of resistance to Cucumber mosaic virus in melon. SABRAO Journal of Breeding and Genetics **35:** 19-26

Dashti NH, Ali NY, Cherian VM, Montasser MS (2012) Application of plant growth-promoting rhizobacteria (PGPR) in combination with a mild strain of Cucumber mosaic virus (CMV) associated with viral satellite RNAs to enhance growth and protection against a virulent strain of CMV in tomato. Canadian journal of plant pathology **34:** 177-186

De Wispelaere M, Rao A (2009) Production of cucumber mosaic virus RNA5 and its role in recombination. Virology **384:** 179-191

Deleu W, Esteras C, Roig C, González-To M, Fernández-Silva I, Gonzalez-Ibeas D, Blanca J, Aranda MA, Arús P, Nuez F (2009) A set of EST-SNPs for map saturation and cultivar identification in melon. BMC Plant Biology **9:** 90

Devran Z, Kahveci E, Özkaynak E, Studholme DJ, Tör M (2015) Development of molecular markers tightly linked to Pvr4 gene in pepper using next-generation sequencing. Molecular Breeding **35:** 101

Díaz A, Martín-Hernández AM, Dolcet-Sanjuan R, Garcés-Claver A, Álvarez JM, Garcia-Mas J, Picó B, Monforte AJ (2017) Quantitative Trait Loci analysis of melon (Cucumis melo L.) domestication-related traits. Theoretical and Applied Genetics **130:** 1837-1856

Diaz JA, Mallor C, Soria C, Camero R, Garzo E, Fereres A, Alvarez JM, Gómez-Guillamón ML, Luis-Arteaga M, Moriones E (2003) Potential sources of resistance for melon to nonpersistently aphid-borne viruses. Plant Disease **87:** 960-964

Díaz JA, Mallor C, Soria C, Camero R, Garzo E, Fereres A, Alvarez JM, Gómez-Guillamón ML, Luis-Arteaga M, Moriones E (2003) Potential sources of resistance for melon to nonpersistently aphid-borne viruses. Plant Disease **87:** 960-964

Ding B, Li Q, Nguyen L, Palukaitis P, Lucas WJ (1995) Cucumber mosaic virus 3a protein potentiates cell-to-cell trafficking of CMV RNA in tobacco plants. Virology **207:** 345-353

Dintinger JA, Salgon S, Reynaud B (2014) QTL mapping of a partial resistance to the corn delphacid‐transmitted viruses in Lepidopteran‐resistant maize line Mp 705. Plant breeding **133:** 19-27

Divéki Z, Salánki K, Balázs E (2004) The necrotic pathotype of the Cucumber mosaic virus (CMV) Ns strain is solely determined by amino acid 461 of the 1a protein. Molecular plant-microbe interactions **17:** 837-845

Dogimont C, Leconte L, Perin C, Thabuis A, Lecoq H, Pitrat M (2000) Identification of QTLs contributing to resistance to different strains of cucumber mosaic cucumovirus in melon. *In* VII Eucarpia Meeting on Cucurbit Genetics and Breeding 510, pp 391-398

Dong K, Wang Y, Zhang Z, Chai LX, Tong X, Xu J, Li D, Wang XB (2016) Two amino acids near the N‐terminus of Cucumber mosaic virus 2b play critical roles in the suppression of RNA silencing and viral infectivity. Molecular plant pathology **17:** 173-183

Du Z, Chen A, Chen W, Liao Q, Zhang H, Bao Y, Roossinck MJ, Carr JP (2014) Nuclear-cytoplasmic partitioning of the Cucumber mosaic virus 2b protein determines the balance between its roles as a virulence determinant and RNA silencing suppressor. Journal of virology**:** JVI. 00284-00214

Du Z, Chen F, Zhao Z, Liao Q, Palukaitis P, Chen J (2008) The 2b protein and the C-terminus of the 2a protein of cucumber mosaic virus subgroup I strains both play a role in viral RNA accumulation and induction of symptoms. Virology **380:** 363-370

Dubey VK, Chandrasekhar K, Srivastava A, Aminuddin, Singh VP, Dhar K, Arora PK (2015) Expression of coat protein gene of Cucumber mosaic virus (CMV-subgroup IA) Gladiolus isolate in Nicotiana tabacum. Journal of plant interactions **10:** 296-304

Eckes P, Rosahl S, Schell J, Willmitzer L (1986) Isolation and characterization of a light-inducible, organ-specific gene from potato and analysis of its expression after tagging and transfer into tobacco and potato shoots. Molecular and General Genetics MGG **205:** 14-22

Bibliopraphy

Eduardo I, Arús P, Monforte AJ (2005) Development of a genomic library of near isogenic lines (NILs) in melon (Cucumis melo L.) from the exotic accession PI161375. Theoretical and applied genetics **112:** 139-148

Eduardo I, Arús P, Monforte AJ, Obando J, Fernández-Trujillo JP, Martínez JA, Alarcón AL, Álvarez JM, van der Knaap E (2007) Estimating the genetic architecture of fruit quality traits in melon using a genomic library of near isogenic lines. Journal of the American Society for Horticultural Science **132:** 80-89

Edwardson J, Christie R (1991) CRC handbook of viruses infecting legumes, p 293–319. *In*. CRC Press, Boca Raton, FL

Elena SF, Sanjuán R (2007) Virus evolution: insights from an experimental approach. Annu. Rev. Ecol. Evol. Syst. **38:** 27-52

Elsharkawy M, Shimizu M, Takahashi H, Hyakumachi M (2012) Induction of systemic resistance against Cucumber mosaic virus by Penicillium simplicissimum GP17‐2 in Arabidopsis and tobacco. Plant Pathology **61:** 964-976

Elsharkawy MM, Shimizu M, Takahashi H, Ozaki K, Hyakumachi M (2013) Induction of systemic resistance against Cucumber mosaic virus in Arabidopsis thaliana by Trichoderma asperellum SKT-1. The plant pathology journal **29:** 193

Epinat C, Pitrat M, Bertrand F (1992) Genetic analysis of resistance of five melon lines to powdery mildews. Euphytica **65:** 135-144

Essafi A, Díaz-Pendón JA, Moriones E, Monforte AJ, Garcia-Mas J, Martín-Hernández AM (2009) Dissection of the oligogenic resistance to Cucumber mosaic virus in the melon accession PI 161375. Theoretical and applied genetics **118:** 275-284

Esteras C, Formisano G, Roig C, Díaz A, Blanca J, Garcia-Mas J, Gómez-Guillamón ML, López-Sesé AI, Lázaro A, Monforte AJ (2013) SNP genotyping in melons: genetic variation, population structure, and linkage disequilibrium. Theoretical and Applied Genetics **126:** 1285-1303

Eun MH, Han J-H, Yoon JB, Lee J (2016) QTL mapping of resistance to the Cucumber mosaic virus P1 strain in pepper using a genotyping-by-sequencing analysis. Horticulture, Environment, and Biotechnology **57:** 589-597

Fernandez-Silva I, Eduardo I, Blanca J, Esteras C, Pico B, Nuez F, Arus P, Garcia-Mas J, Monforte AJ (2008) Bin mapping of genomic and EST-derived SSRs in melon (Cucumis melo L.). Theoretical and Applied Genetics **118:** 139-150

Fernandez-Silva I, Moreno E, Essafi A, Fergany M, Garcia-Mas J, Martín-Hernandez AM, Álvarez JM, Monforte AJ (2010) Shaping melons: agronomic and genetic characterization of QTLs that modify melon fruit morphology. Theoretical and applied genetics **121:** 931-940

Friedmann M, Lapidot M, Cohen S, Pilowsky M (1998) A novel source of resistance to tomato yellow leaf curl virus exhibiting a symptomless reaction to viral infection. Journal of the American Society for Horticultural Science **123:** 1004-1007

Fukino N, Ohara T, Monforte AJ, Sugiyama M, Sakata Y, Kunihisa M, Matsumoto S (2008) Identification of QTLs for resistance to powdery mildew and SSR markers diagnostic for powdery mildew resistance genes in melon (Cucumis melo L.). Theoretical and Applied Genetics **118:** 165-175

Gal-On A, Kaplan I, Roossinck MJ, Palukaitis P (1994) The kinetics of infection of zucchini squash by cucumber mosaic virus indicate a function for RNA 1 in virus movement. Virology **205:** 280-289

Gal-On A, Kaplan IB, Palukaitis P (1996) Characterization of cucumber mosaic virus: II. Identification of movement protein sequences that influence its accumulation and systemic infection in tobacco. Virology **226:** 354-361

Galpaz N, Gonda I, Shem‐Tov D, Barad O, Tzuri G, Lev S, Fei Z, Xu Y, Mao L, Jiao C (2018) Deciphering genetic factors that determine melon fruit‐quality traits using RNA‐Seq‐based high‐resolution QTL and eQTL mapping. The Plant Journal **94:** 169-191

Garcıa-Arenal F, Palukaitis P (2008) Cucumber mosaic virus. Desk encyclopedia of plant and fungal virology**:** 171-176

Garcia-Mas J, Benjak A, Sanseverino W, Bourgeois M, Mir G, González VM, Hénaff E, Câmara F, Cozzuto L, Lowy E (2012) The genome of melon (Cucumis melo L.). Proceedings of the National Academy of Sciences **109:** 11872-11877

Bibliopraphy

Garcia-Mas J, Oliver M, Gomez-Paniagua H, De Vicente M (2000) Comparing AFLP, RAPD and RFLP markers for measuring genetic diversity in melon. Theoretical and Applied Genetics **101:** 860-864

Gera A, Loebenstein G, Raccah B (1979) Protein coats of two strains of cucumber mosaic virus affect transmission by Aphis gossypii. Phytopathology **69:** 396-399

Giner A, Pascual L, Bourgeois M, Gyetvai G, Rios P, Picó B, Troadec C, Bendahmane A, Garcia-Mas J, Martín-Hernández AM (2017) A mutation in the melon Vacuolar Protein Sorting 41prevents systemic infection of Cucumber mosaic virus. Scientific reports **7:** 10471

Gonzalo M, Oliver M, Garcia-Mas J, Monfort A, Dolcet-Sanjuan R, Katzir N, Arus P, Monforte A (2005) Simple-sequence repeat markers used in merging linkage maps of melon (Cucumis melo L.). Theoretical and Applied Genetics **110:** 802-811

Guiu-Aragonés C (2014) Study of Cucumber mosaic virus infection in the resistant melon accession PI 161375.

Guiu-Aragonés C, Monforte AJ, Saladié M, Corrêa RX, Garcia-Mas J, Martín-Hernández AM (2014) The complex resistance to cucumber mosaic cucumovirus (CMV) in the melon accession PI161375 is governed by one gene and at least two quantitative trait loci. Molecular breeding **34:** 351-362

Guiu‐Aragonés C, Díaz‐Pendón JA, Martín‐Hernández AM (2015) Four sequence positions of the movement protein of Cucumber mosaic virus determine the virulence against cmv1‐mediated resistance in melon. Molecular plant pathology **16:** 675-684

Guiu‐Aragonés C, Sánchez‐Pina MA, Díaz‐Pendón JA, Peña EJ, Heinlein M, Martín‐Hernández AM (2016) cmv1 is a gate for Cucumber mosaic virus transport from bundle sheath cells to phloem in melon. Molecular plant pathology **17:** 973-984

Guo G, Wang S, Liu J, Pan B, Diao W, Ge W, Gao C, Snyder JC (2017) Rapid identification of QTLs underlying resistance to Cucumber mosaic virus in pepper (Capsicum frutescens). Theoretical and Applied Genetics **130:** 41-52

Gutiérrez L, Germán S, Pereyra S, Hayes PM, Pérez CA, Capettini F, Locatelli A, Berberian NM, Falconi EE, Estrada R (2015) Multi-environment multi-QTL association mapping identifies disease resistance QTL in barley germplasm from Latin America. Theoretical and applied genetics **128:** 501-516

Habili N, Symons RH (1989) Evolutionary relationship between luteoviruses and other RNA plant viruses based on sequence motifs in their putative RNA polymerases and nucleic acid helicases. Nucleic acids research **17:** 9543-9555

Hales D, Tomiuk J, Wöhrmann K, Sunnucks P (1997) Evolutionary and genetic aspects of aphid biology: a review. European Journal of Entomology **94:** 1-55

Harel-Beja R, Tzuri G, Portnoy V, Lotan-Pompan M, Lev S, Cohen S, Dai N, Yeselson L, Meir A, Libhaber S (2010) A genetic map of melon highly enriched with fruit quality QTLs and EST markers, including sugar and carotenoid metabolism genes. Theoretical and applied genetics **121:** 511-533

Harrison BD, Mayo MA, Baulcombe DC (1987) Virus resistance in transgenic plants that express cucumber mosaic virus satellite RNA. Nature **328:** 799

Hayes RJ, Buck KW (1990) Complete replication of a eukaryotic virus RNA in vitro by a purified RNA-dependent RNA polymerase. Cell **63:** 363-368

Hipper C, Brault V, Ziegler-Graff V, Revers F (2013) Viral and cellular factors involved in phloem transport of plant viruses. Frontiers in plant science **4:** 154

Hobbs H, Eastburn D, D'Arcy C, Kindhart J, Masiunas J, Voegtlin D, Weinzierl R, McCoppin N (2000) Solanaceous weeds as possible sources of Cucumber mosaic virus in southern Illinois for aphid transmission to pepper. Plant disease **84:** 1221-1224

Hong JS, Ohnishi S, Masuta C, Choi JK, Ryu KH (2007) Infection of soybean by cucumber mosaic virus as determined by viral movement protein. Arch Virol **152:** 321-328

Hu Z, Deng G, Mou H, Xu Y, Chen L, Yang J, Zhang M (2017) A re-sequencing-based ultra-dense genetic map reveals a gummy stem blight resistance-associated gene in Cucumis melo. DNA Research **25:** 1-10

Huang Z, He G, Shu L, Li X, Zhang Q (2001) Identification and mapping of two brown planthopper resistance genes in rice. Theoretical and Applied Genetics **102:** 929-934

Huynh B-L, Matthews WC, Ehlers JD, Lucas MR, Santos JR, Ndeve A, Close TJ, Roberts PA (2016) A major QTL corresponding to the Rk locus for resistance to root-knot nematodes in cowpea (Vigna unguiculata L. Walp.). Theoretical and Applied Genetics **129:** 87-95

Bibliopraphy

Hyodo K, Okuno T (2014) Host factors used by positive-strand RNA plant viruses for genome replication. Journal of general plant pathology **80:** 123-135

Inaba J-i, Kim BM, Shimura H, Masuta C (2011) Virus-induced necrosis is a consequence of direct protein–protein interaction between a viral RNA silencing suppressor and a host catalase. Plant physiology**:** pp. 111.180042

Janzac B, Montarry J, Palloix A, Navaud O, Moury B (2010) A point mutation in the polymerase of Potato virus Y confers virulence toward the Pvr4 resistance of pepper and a high competitiveness cost in susceptible cultivar. Molecular plant-microbe interactions **23:** 823-830

Jeffrey C (1980) A review of the Cucurbitaceae. Botanical Journal of the Linnean society **81:** 233-247

Ji L-H, Ding S-W (2001) The suppressor of transgene RNA silencing encoded by Cucumber mosaic virus interferes with salicylic acid-mediated virus resistance. Molecular Plant-Microbe Interactions **14:** 715-724

Jiang G-H, He Y-Q, Xu C-G, Li X-H, Zhang Q (2004) The genetic basis of stay-green in rice analyzed in a population of doubled haploid lines derived from an indica by japonica cross. Theoretical and Applied Genetics **108:** 688-698

Joobeur T, King JJ, Nolin SJ, Thomas CE, Dean RA (2004) The fusarium wilt resistance locus Fom‐2 of melon contains a single resistance gene with complex features. The Plant Journal **39:** 283-297

Kang W-H, Hoang NH, Yang H-B, Kwon J-K, Jo S-H, Seo J-K, Kim K-H, Choi D, Kang B-C (2010) Molecular mapping and characterization of a single dominant gene controlling CMV resistance in peppers (Capsicum annuum L.). Theoretical and applied genetics **120:** 1587-1596

Kang W-H, Seo J-K, Chung BN, Kim K-H, Kang B-C (2012) Helicase domain encoded by Cucumber mosaic virus RNA1 determines systemic infection of Cmr1 in pepper. PloS one **7:** e43136

Kaper J, Tousignant M (1977) Cucumber mosaic virus-associated RNA 5: I. Role of host plant and helper strain in determining amount of associated RNA 5 with virions. Virology **80:** 186-195

Kaplan IB, Shintaku MH, Li Q, Zhang L, Marsh LE, Palukaitis P (1995) Complementation of virus movement in transgenic tobacco expressing the cucumber mosaic virus 3a gene. Virology **209:** 188-199

Karasov TL, Horton MW, Bergelson J (2014) Genomic variability as a driver of plant–pathogen coevolution? Current opinion in plant biology **18:** 24-30

Karchi Z, Cohen S, Govers A (1975) Inheritance of resistance to cucumber mosaic virus in melons. Phytopathology

Keurentjes JJ, Bentsink L, Alonso-Blanco C, Hanhart CJ, Blankestijn-De Vries H, Effgen S, Vreugdenhil D, Koornneef M (2006) Development of a near isogenic line population of Arabidopsis thaliana and comparison of mapping power with a recombinant inbred line population. Genetics

Kim H-T, Park J-I, Robin AHK, Ishikawa T, Kuzuya M, Horii M, Yashiro K, Nou I-S (2016) Identification of a new race and development of DNA markers associated with powdery mildew in melon. Plant Breeding and Biotechnology **4:** 225-233

Kim MJ, Huh SU, Ham B-K, Paek K-H (2008) A novel methyltransferase methylates Cucumber mosaic virus 1a protein and promotes systemic spread. Journal of virology **82:** 4823-4833

Kim MJ, Kim HR, Paek K-H (2006) Arabidopsis tonoplast proteins TIP1 and TIP2 interact with the cucumber mosaic virus 1a replication protein. Journal of general virology **87:** 3425-3431

Kim S, Lee S, Kim B-D, Paek K-H (1997) Satellite-RNA-mediated resistance to cucumber mosaic virus in transgenic plants of hot pepper (Capsicum annuum cv. Golden Tower). Plant Cell Reports **16:** 825-830

Kim SH, Palukaitis P, Park YI (2002) Phosphorylation of cucumber mosaic virus RNA polymerase 2a protein inhibits formation of replicase complex. The EMBO journal **21:** 2292-2300

Kitomi Y, Kanno N, Kawai S, Mizubayashi T, Fukuoka S, Uga Y (2015) QTLs underlying natural variation of root growth angle among rice cultivars with the same functional allele of DEEPER ROOTING 1. Rice **8:** 16

Klingler J, Kovalski I, Silberstein L, Thompson GA, Perl-Treves R (2001) Mapping of cotton-melon aphid resistance in melon. Journal of the American Society for Horticultural Science **126:** 56-63

Kobori T, Miyagawa M, Nishioka K, Satoshi TO, Osaki T (2002) Amino acid 129 of Cucumber mosaic virus coat protein determines local symptom expression and systemic movement in Tetragonia expansa, Momordica charantia and Physalis floridana. Journal of general plant pathology **68:** 81-88

Kowalski SP, Lan T-H, Feldmann KA, Paterson AH (1994) QTL mapping of naturally-occurring variation in flowering time of Arabidopsis thaliana. Molecular and General Genetics MGG **245:** 548-555

KT S (2016) Genetics of Resistance to Downy Mildew in Muskmelon (Cucumis Melo L.).

Bibliopraphy

Kumar D, Kumar R, Hyun TK, Kim J-Y (2015) Cell-to-cell movement of viruses via plasmodesmata. Journal of plant research **128:** 37-47

Kumar K, Sarao PS, Bhatia D, Neelam K, Kaur A, Mangat GS, Brar DS, Singh K (2017) High-resolution genetic mapping of a novel brown planthopper resistance locus, Bph34 in Oryza sativa L. X Oryza nivara (Sharma & Shastry) derived interspecific F 2 population. Theoretical and Applied Genetics**:** 1-9

Kyle M, Palloix A (1997) Proposed revision of nomenclature for potyvirusresistance genes in Capsicum. Euphytica **97:** 183-188

Lee M-Y, Lee J-H, Ahn H-I, Yoon J-Y, Her N-H, Choi J-K, Choi G-S, Kim D-S, Harn C-H, Ryu K-H (2006) Identification and sequence analysis of RNA3 of a resistance-breaking Cucumber mosaic virus isolate on Capsicum annuum. The Plant Pathology Journal **22:** 265-270

Lewsey M, Surette M, Robertson FC, Ziebell H, Choi SH, Ryu KH, Canto T, Palukaitis P, Payne T, Walsh JA (2009) The role of the Cucumber mosaic virus 2b protein in viral movement and symptom induction. Molecular plant-microbe interactions **22:** 642-654

Li Z, Jakkula L, Hussey R, Tamulonis J, Boerma H (2001) SSR mapping and confirmation of the QTL from PI96354 conditioning soybean resistance to southern root-knot nematode. Theoretical and Applied Genetics **103:** 1167-1173

Liu S, He X, Park G, Josefsson C, Perry KL (2002) A conserved capsid protein surface domain of Cucumber mosaic virus is essential for efficient aphid vector transmission. Journal of virology **76:** 9756-9762

López-Sesé A, Staub J, Gómez-Guillamón M (2003) Genetic analysis of Spanish melon (Cucumis melo L.) germplasm using a standardized molecular-marker array and geographically diverse reference accessions. Theoretical and Applied Genetics **108:** 41-52

Lotfi M, Alan A, Henning M, Jahn M, Earle E (2003) Production of haploid and doubled haploid plants of melon (Cucumis melo L.) for use in breeding for multiple virus resistance. Plant Cell Reports **21:** 1121-1128

Luan F, Delannay I, Staub JE (2008) Chinese melon (Cucumis melo L.) diversity analyses provide strategies for germplasm curation, genetic improvement, and evidentiary support of domestication patterns. Euphytica **164:** 445-461

Lucy AP, Guo HS, Li WX, Ding SW (2000) Suppression of post‐transcriptional gene silencing by a plant viral protein localized in the nucleus. The EMBO Journal **19:** 1672-1680

Martin GB, Williams J, Tanksley SD (1991) Rapid identification of markers linked to a Pseudomonas resistance gene in tomato by using random primers and near-isogenic lines. Proceedings of the National Academy of Sciences **88:** 2336-2340

Mascia T, Cillo F, Fanelli V, Finetti-Sialer MM, De Stradis A, Palukaitis P, Gallitelli D (2010) Characterization of the interactions between Cucumber mosaic virus and Potato virus Y in mixed infections in tomato. Molecular plant-microbe interactions **23:** 1514-1524

McCormick S (2017) Discovery of new QTLs underlying hybrid fertility and reproductive isolation in rice. The Plant Journal **92:** 347-348

McCreight JD, Pitrat M, Thomas C, Kishaba A, Bohn G (1987) Powdery mildew resistance genes in muskmelon. J. Amer. Soc. Hort. Sci **112:** 156-160

Melchinger AE, Piepho H-P, Utz HF, Muminović J, Wegenast T, Törjék O, Altmann T, Kusterer B (2007) Genetic basis of heterosis for growth-related traits in Arabidopsis investigated by testcross progenies of near-isogenic lines reveals a significant role of epistasis. Genetics **177:** 1827-1837

Mliki A, Staub JE, Zhangyong S, Ghorbel A (2001) Genetic diversity in melon (Cucumis melo L.): anevaluation of African germplasm. Genetic resources and crop evolution **48:** 587-597

Mochizuki T, Ohki ST (2012) Cucumber mosaic virus: viral genes as virulence determinants. Molecular plant pathology **13:** 217-225

Monforte A, Garcia‐Mas J, Arús P (2003) Genetic variability in melon based on microsatellite variation. Plant breeding **122:** 153-157

Monforte A, Oliver M, Gonzalo M, Alvarez J, Dolcet-Sanjuan R, Arus P (2004) Identification of quantitative trait loci involved in fruit quality traits in melon (Cucumis melo L.). Theoretical and Applied Genetics **108:** 750-758

Moon JY, Park JM (2016) Cross-talk in viral defense signaling in plants. Frontiers in microbiology **7:** 2068

Morales M, Orjeda G, Nieto C, Van Leeuwen H, Monfort A, Charpentier M, Caboche M, Arús P, Puigdomènech P, Aranda MA (2005) A physical map covering the nsv locus that confers resistance to Melon necrotic spot virus in melon (Cucumis melo L.). Theoretical and applied genetics **111:** 914-922

Moreno E, Obando JM, Dos-Santos N, Fernández-Trujillo JP, Monforte AJ, Garcia-Mas J (2008) Candidate genes and QTLs for fruit ripening and softening in melon. Theoretical and Applied Genetics **116:** 589-602

Moury B, Morel C, Johansen E, Guilbaud L, Souche S, Ayme V, Caranta C, Palloix A, Jacquemond M (2004) Mutations in Potato virus Y genome-linked protein determine virulence toward recessive resistances in Capsicum annuum and Lycopersicon hirsutum. Molecular Plant-Microbe Interactions **17:** 322-329

Nakajima M, Hayakawa T, Nakamura I, Suzuki M (1993) Protection against cucumber mosaic virus (CMV) strains O and Y and chrysanthemum mild mottle virus in transgenic tobacco plants expressing CMV-O coat protein. Journal of general virology **74:** 319-322

Nakata E, Staub JE, López-Sesé AI, Katzir N (2005) Genetic diversity of Japanese melon cultivars (Cucumis melo L.) as assessed by random amplified polymorphic DNA and simple sequence repeat markers. Genetic Resources and Crop Evolution **52:** 405-419

Natarajan S, Kim H-T, Thamilarasan SK, Veerappan K, Park J-I, Nou I-S (2016) Whole genome re-sequencing and characterization of powdery mildew disease-associated allelic variation in melon. PloS one **11:** e0157524

Nimmakayala P, Tomason YR, Abburi VL, Alvarado A, Saminathan T, Vajja VG, Salazar G, Panicker GK, Levi A, Wechter WP (2016) Genome-wide differentiation of various melon horticultural groups for use in GWAS for fruit firmness and construction of a high resolution genetic map. Frontiers in plant science **7:** 1437

Ning X, Wang X, Gao X, Zhang Z, Zhang L, Yan W, Li G (2014) Inheritances and location of powdery mildew resistance gene in melon Edisto47. Euphytica **195:** 345-353

Niones JM (2004) Five mapping of the salinity tolerance gene on chromosome 1 of rice (Oryza sativa L.) using near-isogenic lines.

Nitta N, Takanami Y, Kuwata S, Kubo S (1988) Inoculation with RNAs 1 and 2 of cucumber mosaic virus induces viral RNA replicase activity in tobacco mesophyll protoplasts. Journal of general virology **69:** 2695-2700

Nono‐Womdim R, Palloix A, Gébré‐Selassié K, Marchoux G (1993) Partial resistance of bell pepper to cucumber mosaic virus movement within plants: field evaluation of its efficiency in southern France. Journal of Phytopathology **137:** 125-132

Ntui VO, Kong K, Azadi P, Khan RS, Chin DP, Igawa T, Mii M, Nakamura I (2014) RNAi-mediated resistance to cucumber mosaic virus (CMV) in genetically engineered tomato. American Journal of Plant Sciences **5:** 554

Obando-Ulloa JM, Eduardo I, Monforte AJ, Fernández-Trujillo JP (2009) Identification of QTLs related to sugar and organic acid composition in melon using near-isogenic lines. Scientia horticulturae **121:** 425-433

Obando-Ulloa JM, Ruiz J, Monforte AJ, Fernández-Trujillo JP (2010) Aroma profile of a collection of near-isogenic lines of melon (Cucumis melo L.). Food chemistry **118:** 815-822

Obando J, Fernández-Trujillo JP, Martinez JA, Alarcón AL, Eduardo I, Arús P, Monforte AJ (2008) Identification of melon fruit quality quantitative trait loci using near-isogenic lines. Journal of the American Society for Horticultural Science **133:** 139-151

Palomares-Rius FJ, Viruel MA, Yuste-Lisbona FJ, López-Sesé AI, Gómez-Guillamón ML (2011) Simple sequence repeat markers linked to QTL for resistance to Watermelon mosaic virus in melon. Theoretical and applied genetics **123:** 1207

Palukaitis P, Garcia-Arenal F (2003) Cucumoviruses. Adv Virus Res **62:** 241-323

Palukaitis P, Roossinck MJ, Dietzgen RG, Francki RI (1992) Cucumber mosaic virus. *In* Advances in virus research, Vol 41. Elsevier, pp 281-348

Pavan S, Marcotrigiano AR, Ciani E, Mazzeo R, Zonno V, Ruggieri V, Lotti C, Ricciardi L (2017) Genotyping-by-sequencing of a melon (Cucumis melo L.) germplasm collection from a secondary center of diversity highlights patterns of genetic variation and genomic features of different gene pools. BMC genomics **18:** 59

Perchepied L, Bardin M, Dogimont C, Pitrat M (2005) Relationship between loci conferring downy mildew and powdery mildew resistance in melon assessed by quantitative trait loci mapping. Phytopathology **95:** 556-565

Perchepied L, Dogimont C, Pitrat M (2005) Strain-specific and recessive QTLs involved in the control of partial resistance to Fusarium oxysporum f. sp. melonis race 1.2 in a recombinant inbred line population of melon. Theoretical and applied genetics **111:** 65-74

Perchepied L, Pitrat M (2004) Polygenic inheritance of partial resistance to Fusarium oxysporum f. sp. melonis race 1.2 in melon. Phytopathology **94:** 1331-1336

Pitrat M (2008) Handbook of Crop Breeding Vol I. Vegetables.

Pitrat M, Lecoq H (1980) Inheritance of resistance to cucumber mosaic virus transmission by Aphis gossypii in Cucumis melo. Phytopathology **70:** 958-961

Pitrat M, Lecoq H (1984) Inheritance of zucchini yellow mosaic virus resistance in Cucumis melo L. Euphytica **33:** 57-61

Quenouille J, Paulhiac E, Moury B, Palloix A (2014) Quantitative trait loci from the host genetic background modulate the durability of a resistance gene: a rational basis for sustainable resistance breeding in plants. Heredity **112:** 579

Quenouille J, Vassilakos N, Moury B (2013) P otato virus Y: a major crop pathogen that has provided major insights into the evolution of viral pathogenicity. Molecular plant pathology **14:** 439-452

Rabanal FA, Nizhynska V, Mandáková T, Novikova PY, Lysak MA, Mott R, Nordborg M (2017) Unstable inheritance of 45S rRNA genes in Arabidopsis thaliana. G3: Genes, Genomes, Genetics**:** g3. 117.040204

Raccah B, Gal‐On A, Eastop V (1985) The role of flying aphid vectors in the transmission of cucumber mosaic virus and potato virus Y to peppers in Israel. Annals of applied Biology **106:** 451-460

Rausher MD (2001) Co-evolution and plant resistance to natural enemies. Nature **411:** 857

Ravensdale M, Nemri A, Thrall PH, Ellis JG, Dodds PN (2011) Co‐evolutionary interactions between host resistance and pathogen effector genes in flax rust disease. Molecular plant pathology **12:** 93-102

Rawat N, Pumphrey MO, Liu S, Zhang X, Tiwari VK, Ando K, Trick HN, Bockus WW, Akhunov E, Anderson JA (2016) Wheat Fhb1 encodes a chimeric lectin with agglutinin domains and a pore-forming toxin-like domain conferring resistance to Fusarium head blight. Nature genetics **48:** 1576

Requena A, Simón-Buela L, Salcedo G, García-Arenal F (2006) Potential involvement of a cucumber homolog of phloem protein 1 in the long-distance movement of Cucumber mosaic virus particles. Molecular plant-microbe interactions **19:** 734-746

Rietveld K, Pleij C, Bosch L (1983) Three‐dimensional models of the tRNA‐like 3′ termini of some plant viral RNAs. The EMBO journal **2:** 1079-1085

Ríos P, Argyris J, Vegas J, Leida C, Kenigswald M, Tzuri G, Troadec C, Bendahmane A, Katzir N, Picó B (2017) ETHQV 6.3 is involved in melon climacteric fruit ripening and is encoded by a NAC domain transcription factor. The Plant Journal **91:** 671-683

Risser G (1973) Etude de l'heredite de la resistance du melon (Cucumis melo) aux races 1 et 2 de Fusarium oxysporum f. melonis. *In* Annales de l'Amélioration des Plantes,

Risser G, Banihashemi Z, Davis D (1976) A proposed nomenclature of Fusarium oxysporum f. sp. melonis races and resistance genes in Cucumis melo [Muskmelon, fungal diseases]. Phytopathology (USA)

Rizzo TM, Palukaitis P (1990) Construction of full-length cDNA clones of cucumber mosaic virus RNAs 1, 2 and 3: generation of infectious RNA transcripts. Molecular and General Genetics MGG **222:** 249-256

Roberts A, Oparka K (2003) Plasmodesmata and the control of symplastic transport. Plant, Cell & Environment **26:** 103-124

Rodríguez-Moreno L, González VM, Benjak A, Martí MC, Puigdomènech P, Aranda MA, Garcia-Mas J (2011) Determination of the melon chloroplast and mitochondrial genome sequences reveals that the largest reported mitochondrial genome in plants contains a significant amount of DNA having a nuclear origin. BMC genomics **12:** 424

Roossinck MJ (2001) Cucumber mosaic virus, a model for RNA virus evolution. Molecular Plant Pathology **2:** 59-63

Roossinck MJ, Palukaitis P (1990) Rapid induction and severity of symptoms in zucchini squash (Cucurbita pepo) map to RNA 1 of cucumber mosaic virus. Mol. Plant-Microbe Interact **3:** 188-192

Roossinck MJ, Zhang L, Hellwald K-H (1999) Rearrangements in the 5′ nontranslated region and phylogenetic analyses of cucumber mosaic virus RNA 3 indicate radial evolution of three subgroups. Journal of virology **73:** 6752-6758

Ruffel S, Dussault MH, Palloix A, Moury B, Bendahmane A, Robaglia C, Caranta C (2002) A natural recessive resistance gene against potato virus Y in pepper corresponds to the eukaryotic initiation factor 4E (eIF4E). The Plant Journal **32:** 1067-1075

Bibliopraphy

Ruggieri V, Alexiou KG, Morata J, Argyris J, Pujol M, Yano R, Nonaka S, Ezura H, Latrasse D, Boualem A (2018) An improved assembly and annotation of the melon (Cucumis melo L.) reference genome. Scientific reports **8:** 8088

Sáez C, Esteras C, Martínez C, Ferriol M, Dhillon NP, López C, Picó B (2017) Resistance to tomato leaf curl New Delhi virus in melon is controlled by a major QTL located in chromosome 11. Plant cell reports **36:** 1571-1584

Saito Y, Komari T, Masuta C, Hayashi Y, Kumashiro T, Takanami Y (1992) Cucumber mosaic virus-tolerant transgenic tomato plants expressing a satellite RNA. Theoretical and Applied Genetics **83:** 679-683

Saladié M, Cañizares J, Phillips MA, Rodriguez-Concepcion M, Larrigaudière C, Gibon Y, Stitt M, Lunn JE, Garcia-Mas J (2015) Comparative transcriptional profiling analysis of developing melon (Cucumis melo L.) fruit from climacteric and non-climacteric varieties. BMC genomics **16:** 440

Salanki K, Gellert A, Huppert E, Naray-Szabo G, Balazs E (2004) Compatibility of the movement protein and the coat protein of cucumoviruses is required for cell-to-cell movement. J Gen Virol **85:** 1039-1048

Salánki K, Gellért Á, Náray-Szabó G, Balázs E (2007) Modeling-based characterization of the elicitor function of amino acid 461 of Cucumber mosaic virus 1a protein in the hypersensitive response. Virology **358:** 109-118

Salánki K, Kiss L, Gellért Á, Balázs E (2011) Identification a coat protein region of cucumber mosaic virus (CMV) essential for long-distance movement in cucumber. Archives of virology **156:** 2279-2283

Sallam A, Arbaoui M, El-Esawi M, Abshire N, Martsch R (2016) Identification and verification of QTL associated with frost tolerance using linkage mapping and GWAS in winter faba bean. Frontiers in plant science **7:** 1098

Seo J-K, Kwon S-J, Choi H-S, Kim K-H (2009) Evidence for alternate states of Cucumber mosaic virus replicase assembly in positive-and negative-strand RNA synthesis. Virology **383:** 248-260

Serres-Giardi L, Dogimont C (2012) How microsatellite diversity helps to understand the domestication history of melon. *In* Sari N, Solmaz I, Aras V (eds) Cucurbitaceae 2012. Proceedings of the Xth EUCARPIA Meeting on Genetics and Breeding of Cucurbitaceae, Antalya (TR), pp 15-18

Shamasbi FV, Dehestani A, Golkari S (2014) AFLP based genetic diversity assessment among Cucumis melo var. agrestis genotypes in Southern Caspian coastline. Int. J. Biosci **4:** 54-61

Shaner G, Finney R (1977) The effect of nitrogen fertilization on the expression of slow-mildewing resistance in Knox wheat. Phytopathology **67:** 1051-1056

Shi L, Yang Y, Xie Q, Miao H, Bo K, Song Z, Wang Y, Xie B, Zhang S, Gu X (2018) Inheritance and QTL mapping of cucumber mosaic virus resistance in cucumber (Cucumis Sativus L.). PloS one **13:** e0200571

Shimura H, Pantaleo V, Ishihara T, Myojo N, Inaba J-i, Sueda K, Burgyán J, Masuta C (2011) A viral satellite RNA induces yellow symptoms on tobacco by targeting a gene involved in chlorophyll biosynthesis using the RNA silencing machinery. PLoS pathogens **7:** e1002021

Song GC, Choi HK, Ryu C-M (2013) The folate precursor para-aminobenzoic acid elicits induced resistance against Cucumber mosaic virus and Xanthomonas axonopodis. Annals of botany **111:** 925-934

Soyk S, Müller NA, Park SJ, Schmalenbach I, Jiang K, Hayama R, Zhang L, Van Eck J, Jiménez-Gómez JM, Lippman ZB (2017) Variation in the flowering gene SELF PRUNING 5G promotes day-neutrality and early yield in tomato. Nature genetics **49:** 162

Stam P (1993) Construction of integrated genetic linkage maps by means of a new computer package: Join Map. The plant journal **3:** 739-744

Stepansky A, Kovalski I, Perl-Treves R (1999) Intraspecific classification of melons (Cucumis melo L.) in view of their phenotypic and molecular variation. Plant Systematics and Evolution **217:** 313-332

Su S, Liu Z, Chen C, Zhang Y, Wang X, Zhu L, Miao L, Wang X-C, Yuan M (2010) Cucumber mosaic virus movement protein severs actin filaments to increase the plasmodesmal size exclusion limit in tobacco. The Plant Cell**:** tpc. 108.064212

Sugawara T, Trifonova EA, Kochetov AV, Kanayama Y (2016) Expression of an extracellular ribonuclease gene increases resistance to Cucumber mosaic virus in tobacco. BMC plant biology **16:** 246

Symons RH (1975) Cucumber mosaic virus RNA contains 7-methyl guanosine at the 5′ -terminus of all four RNA species. Molecular biology reports **2:** 277-285

Bibliopraphy

Takahashi H, Miller J, Nozaki Y, Sukamto, Takeda M, Shah J, Hase S, Ikegami M, Ehara Y, Dinesh‐Kumar S (2002) RCY1, an Arabidopsis thaliana RPP8/HRT family resistance gene, conferring resistance to cucumber mosaic virus requires salicylic acid, ethylene and a novel signal transduction mechanism. The Plant Journal **32:** 655-667

Takahashi H, Suzuki M, Natsuaki K, Shigyo T, Hino K, Teraoka T, Hosokawa D, Ehara Y (2001) Mapping the virus and host genes involved in the resistance response in cucumber mosaic virus-infected Arabidopsis thaliana. Plant and cell physiology **42:** 340-347

Takahashi H, Tian A, Miyashita S, Kanayama Y, Ando S, Kormelink R (2018) Survey of the response of 82 domestic landraces of Zea mays to cucumber mosaic virus (CMV) reveals geographical region‐related resistance to CMV in Japan. Plant Pathology

Takeshita M, Koizumi E, Noguchi M, Sueda K, Shimura H, Ishikawa N, Matsuura H, Ohshima K, Natsuaki T, Kuwata S (2012) Infection dynamics in viral spread and interference under the synergism between Cucumber mosaic virus and Turnip mosaic virus. Molecular plant-microbe interactions **25:** 18-27

Tamisier L, Rousseau E, Barraillé S, Nemouchi G, Szadkowski M, Mailleret L, Grognard F, Fabre F, Moury B, Palloix A (2017) Quantitative trait loci in pepper control the effective population size of two RNA viruses at inoculation. Journal of General Virology **98:** 1923-1931

Thompson JR, Buratti E, de Wispelaere M, Tepfer M (2008) Structural and functional characterization of the 5′ region of subgenomic RNA5 of cucumber mosaic virus. Journal of general virology **89:** 1729-1738

Tomlinson J, CARTER AL (1970) Studies on the seed transmission of cucumber mosaic virus in chickweed (Stellaria media) in relation to the ecology of the virus. Annals of Applied Biology **66:** 381-386

Tricoll DM, Carney KJ, Russell PF, McMaster JR, Groff DW, Hadden KC, Himmel PT, Hubbard JP, Boeshore ML, Quemada HD (1995) Field evaluation of transgenic squash containing single or multiple virus coat protein gene constructs for resistance to cucumber mosaic virus, watermelon mosaic virus 2, and zucchini yellow mosaic virus. Nature Biotechnology **13:** 1458

van Berloo R (2008) GGT 2.0: versatile software for visualization and analysis of genetic data. Journal of Heredity **99:** 232-236

VanOoijen J, Maliepard CM (1996) version 3.0: Software for the calculation of QTL positions on genetic maps. Centre for Plant Breeding and Reproduction Research, Wageningen

Vaquero C, Turner A, Demangeat G, Sanz A, Serra M, Roberts K, Garcia-Luque I (1994) The 3a protein from cucumber mosaic virus increases the gating capacity of plasmodesmata in transgenic tobacco plants. Journal of general virology **75:** 3193-3197

Vegas J, Garcia-Mas J, Monforte AJ (2013) Interaction between QTLs induces an advance in ethylene biosynthesis during melon fruit ripening. Theoretical and applied genetics **126:** 1531-1544

Wang A (2015) Dissecting the molecular network of virus-plant interactions: the complex roles of host factors. Annual review of phytopathology **53:** 45-66

Wang H, Paulo J, Kruijer W, Boer M, Jansen H, Tikunov Y, Usadel B, Van Heusden S, Bovy A, Van Eeuwijk F (2015) Genotype–phenotype modeling considering intermediate level of biological variation: a case study involving sensory traits, metabolites and QTLs in ripe tomatoes. Molecular BioSystems **11:** 3101-3110

Wang R, Du Z, Bai Z, Liang Z (2017) The interaction between endogenous 30S ribosomal subunit protein S11 and Cucumber mosaic virus LS2b protein affects viral replication, infection and gene silencing suppressor activity. PloS one **12:** e0182459

Wang Y-H, Thomas C, Dean R (1997) A genetic map of melon (Cucumis melo L.) based on amplified fragment length polymorphism (AFLP) markers. Theoretical and applied genetics **95:** 791-798

Wang Y, Lee K, Gaba V, Wong S, Palukaitis P, Gal-On A (2004) Breakage of resistance to Cucumber mosaic virus by co-infection with Zucchini yellow mosaic virus: enhancement of CMV accumulation independent of symptom expression. Archives of virology **149:** 379-396

Waterhouse PM, Wang M-B, Lough T (2001) Gene silencing as an adaptive defence against viruses. Nature **411:** 834

Wintermantel WM, Banerjee N, Oliver JC, Paolillo DJ, Zaitlin M (1997) Cucumber mosaic virus is restricted from entering minor veins in transgenic tobacco exhibiting replicase-mediated resistance. Virology **231:** 248-257

Bibliopraphy

Wong S-M, Thio SS-C, Shintaku MH, Palukaitis P (1999) The rate of cell-to-cell movement in squash of cucumber mosaic virus is affected by sequences of the capsid protein. Molecular plant-microbe interactions **12:** 628-632

Wyand RA, Brown JK (2003) Genetic and forma specialis diversity in Blumeria graminis of cereals and its implications for host‐pathogen co‐evolution. Molecular Plant Pathology **4:** 187-198

Xie X, Song M-H, Jin F, Ahn S-N, Suh J-P, Hwang H-G, McCouch S (2006) Fine mapping of a grain weight quantitative trait locus on rice chromosome 8 using near-isogenic lines derived from a cross between Oryza sativa and Oryza rufipogon. Theoretical and Applied Genetics **113:** 885-894

Xu A, Zhao Z, Chen W, Zhang H, Liao Q, Chen J, Carr JP, Du Z (2013) Self‐interaction of the cucumber mosaic virus 2b protein plays a vital role in the suppression of RNA silencing and the induction of viral symptoms. Molecular plant pathology **14:** 803-812

Yang Y, Kim KS, Anderson EJ (1997) Seed transmission of cucumber mosaic virus in spinach. Phytopathology **87:** 924-931

Yoshii M, Nishikiori M, Tomita K, Yoshioka N, Kozuka R, Naito S, Ishikawa M (2004) The Arabidopsis cucumovirus multiplication 1 and 2 loci encode translation initiation factors 4E and 4G. Journal of Virology **78:** 6102-6111

Yuste-Lisbona FJ, Capel C, Sarria E, Torreblanca R, Gómez-Guillamón ML, Capel J, Lozano R, López-Sesé AI (2011) Genetic linkage map of melon (Cucumis melo L.) and localization of a major QTL for powdery mildew resistance. Molecular breeding **27:** 181-192

Zhang C, Ren Y, Guo S, Zhang H, Gong G, Du Y, Xu Y (2013) Application of comparative genomics in developing markers tightly linked to the Pm-2F gene for powdery mildew resistance in melon (Cucumis melo L.). Euphytica **190:** 157-168

Zhang Y, Luo L, Xu C, Zhang Q, Xing Y (2006) Quantitative trait loci for panicle size, heading date and plant height co-segregating in trait-performance derived near-isogenic lines of rice (Oryza sativa). Theoretical and applied genetics **113:** 361-368

Zhao F, Li Y, Chen L, Zhu L, Ren H, Lin H, Xi D (2016) Temperature dependent defence of Nicotiana tabacum against Cucumber mosaic virus and recovery occurs with the formation of dark green islands. Journal of Plant Biology **59:** 293-301